

ISSN 1881-7831 Online ISSN 1881-784X

DD & T

Drug Discoveries & Therapeutics

Volume 11, Number 2
April, 2017



www.ddtjournal.com

DD & T

Drug Discoveries & Therapeutics



ISSN: 1881-7831
Online ISSN: 1881-784X
CODEN: DDTRBX
Issues/Year: 6
Language: English
Publisher: IACMHR Co., Ltd.

Drug Discoveries & Therapeutics is one of a series of peer-reviewed journals of the International Research and Cooperation Association for Bio & Socio-Sciences Advancement (IRCA-BSSA) Group and is published bimonthly by the International Advancement Center for Medicine & Health Research Co., Ltd. (IACMHR Co., Ltd.) and supported by the IRCA-BSSA and Shandong University China-Japan Cooperation Center for Drug Discovery & Screening (SDU-DDSC).

Drug Discoveries & Therapeutics publishes contributions in all fields of pharmaceutical and therapeutic research such as medicinal chemistry, pharmacology, pharmaceutical analysis, pharmaceuticals, pharmaceutical administration, and experimental and clinical studies of effects, mechanisms, or uses of various treatments. Studies in drug-related fields such as biology, biochemistry, physiology, microbiology, and immunology are also within the scope of this journal.

Drug Discoveries & Therapeutics publishes Original Articles, Brief Reports, Reviews, Policy Forum articles, Case Reports, News, and Letters on all aspects of the field of pharmaceutical research. All contributions should seek to promote international collaboration in pharmaceutical science.

Editorial Board

Editor-in-Chief:

Kazuhisa SEKIMIZU
The University of Tokyo, Tokyo, Japan

Co-Editors-in-Chief:

Xishan HAO
Tianjin Medical University, Tianjin, China
Munehiro NAKATA
Tokai University, Hiratsuka, Japan

Chief Director & Executive Editor:

Wei TANG
The University of Tokyo, Tokyo, Japan

Senior Editors:

Guanhua DU
Chinese Academy of Medical Science and Peking Union Medical College, Beijing, China
Xiao-Kang LI
National Research Institute for Child Health and Development, Tokyo, Japan
Masahiro MURAKAMI
Osaka Ohtani University, Osaka, Japan
Yutaka ORIHARA
The University of Tokyo, Tokyo, Japan
Tomofumi SANTA
The University of Tokyo, Tokyo, Japan
Hongbin SUN
China Pharmaceutical University, Nanjing, China

Fengshan WANG
Shandong University, Ji'nan, China

Managing Editor:

Hiroshi HAMAMOTO
The University of Tokyo, Tokyo, Japan

Web Editor:

Yu CHEN
The University of Tokyo, Tokyo, Japan

Proofreaders:

Curtis BENTLEY
Roswell, GA, USA
Thomas R. LEBON
Los Angeles, CA, USA

Editorial and Head Office:

Pearl City Koishikawa 603,
2-4-5 Kasuga, Bunkyo-ku,
Tokyo 112-0003, Japan
Tel.: +81-3-5840-9697
Fax: +81-3-5840-9698
E-mail: office@ddtjournal.com

Drug Discoveries & Therapeutics

Editorial and Head Office

Pearl City Koishikawa 603, 2-4-5 Kasuga, Bunkyo-ku,
Tokyo 112-0003, Japan

Tel: +81-3-5840-9697, Fax: +81-3-5840-9698
E-mail: office@ddtjournal.com
URL: www.ddtjournal.com

Editorial Board Members

Alex ALMASAN <i>(Cleveland, OH)</i>	Rodney J. Y. HO <i>(Seattle, WA)</i>	Xingyuan MA <i>(Shanghai)</i>	Yuhong XU <i>(Shanghai)</i>
John K. BUOLAMWINI <i>(Memphis, TN)</i>	Hsing-Pang HSIEH <i>(Zhunan, Miaoli)</i>	Ken-ichi MAFUNE <i>(Tokyo)</i>	Bing YAN <i>(Ji'nan, Shandong)</i>
Jianping CAO <i>(Shanghai)</i>	Yongzhou HU <i>(Hangzhou, Zhejiang)</i>	Sridhar MANI <i>(Bronx, NY)</i>	Yun YEN <i>(Duarte, CA)</i>
Shousong CAO <i>(Buffalo, NY)</i>	Yu HUANG <i>(Hong Kong)</i>	Tohru MIZUSHIMA <i>(Tokyo)</i>	Yasuko YOKOTA <i>(Tokyo)</i>
Jang-Yang CHANG <i>(Tainan)</i>	Hans E. JUNGINGER <i>(Marburg, Hesse)</i>	Abdulla M. MOLOKHIA <i>(Alexandria)</i>	Takako YOKOZAWA <i>(Toyama, Toyama)</i>
Fen-Er CHEN <i>(Shanghai)</i>	Amrit B. KARMARKAR <i>(Karad, Maharashtra)</i>	Yoshinobu NAKANISHI <i>(Kanazawa, Ishikawa)</i>	Rongmin YU <i>(Guangzhou, Guangdong)</i>
Zhe-Sheng CHEN <i>(Queens, NY)</i>	Toshiaki KATADA <i>(Tokyo)</i>	Weisan PAN <i>(Shenyang, Liaoning)</i>	Guangxi ZHAI <i>(Ji'nan, Shandong)</i>
Zilin CHEN <i>(Wuhan, Hubei)</i>	Gagan KAUSHAL <i>(Philadelphia, PA)</i>	Rakesh P. PATEL <i>(Mehsana, Gujarat)</i>	Liangren ZHANG <i>(Beijing)</i>
Shaofeng DUAN <i>(Lawrence, KS)</i>	Ibrahim S. KHATTAB <i>(Kuwait)</i>	Shivanand P. PUTHLI <i>(Mumbai, Maharashtra)</i>	Lining ZHANG <i>(Ji'nan, Shandong)</i>
Chandradhar DWIVEDI <i>(Brookings, SD)</i>	Shiroh KISHIOKA <i>(Wakayama, Wakayama)</i>	Shafi qur RAHMAN <i>(Brookings, SD)</i>	Na ZHANG <i>(Ji'nan, Shandong)</i>
Mohamed F. EL-MILIGI <i>(6th of October City)</i>	Robert Kam-Ming KO <i>(Hong Kong)</i>	Adel SAKR <i>(Cairo)</i>	Ruiwen ZHANG <i>(Amarillo, TX)</i>
Hao FANG <i>(Ji'nan, Shandong)</i>	Nobuyuki KOBAYASHI <i>(Nagasaki, Nagasaki)</i>	Gary K. SCHWARTZ <i>(New York, NY)</i>	Xiu-Mei ZHANG <i>(Ji'nan, Shandong)</i>
Marcus L. FORREST <i>(Lawrence, KS)</i>	Norihiro KOKUDO <i>(Tokyo, Japan)</i>	Yuemao SHEN <i>(Ji'nan, Shandong)</i>	Yongxiang ZHANG <i>(Beijing)</i>
Takeshi FUKUSHIMA <i>(Funabashi, Chiba)</i>	Toshiro KONISHI <i>(Tokyo)</i>	Brahma N. SINGH <i>(New York, NY)</i>	
Harald HAMACHER <i>(Tübingen, Baden-Württemberg)</i>	Chun-Guang LI <i>(Melbourne)</i>	Tianqiang SONG <i>(Tianjin)</i>	<i>(As of February 2017)</i>
Kenji HAMASE <i>(Fukuoka, Fukuoka)</i>	Minyong LI <i>(Ji'nan, Shandong)</i>	Sanjay K. SRIVASTAVA <i>(Amarillo, TX)</i>	
Junqing HAN <i>(Ji'nan, Shandong)</i>	Xun LI <i>(Ji'nan, Shandong)</i>	Chandan M. THOMAS <i>(Bradenton, FL)</i>	
Xiaojiang HAO <i>(Kunming, Yunnan)</i>	Jikai LIU <i>(Kunming, Yunnan)</i>	Murat TURKOGLU <i>(Istanbul)</i>	
Kiyoshi HASEGAWA <i>(Tokyo)</i>	Xinyong LIU <i>(Ji'nan, Shandong)</i>	Hui WANG <i>(Shanghai)</i>	
Waseem HASSAN <i>(Rio de Janeiro)</i>	Yuxiu LIU <i>(Nanjing, Jiangsu)</i>	Quanxing WANG <i>(Shanghai)</i>	
Langchong HE <i>(Xi'an, Shaanxi)</i>	Hongxiang LOU <i>(Jinan, Shandong)</i>	Stephen G. WARD <i>(Bath)</i>	

Original Articles

- 54 -63 **Structural characterization and biological activities of a novel polysaccharide from *Phyllanthus emblica*.**
Zihan Zeng, Wenjie Lv, Yongshuai Jing, Zhiyan Chen, Liyan Song, Ting Liu, Rongmin Yu
- 64 -89 **Influence of clove oil and eugenol on muscle contraction of silkworm (*Bombyx mori*).**
Kantaporn Kheawfu, Surachai Pikulkaew, Hiroshi Hamamoto, Kazuhisa Sekimizu, Siriporn Okonogi
- 70 -77 **Biological activities and antibacterial biomarker of *Sesbania grandiflora* bark extract.**
Pimporn Anantaworasakul, Hiroshi Hamamoto, Kazuhisa Sekimizu, Siriporn Okonogi
- 78 -83 **Genomic analysis of vancomycin-resistant *Staphylococcus aureus* VRS3b and its comparison with other VRSA isolates.**
Suresh Panthee, Hiroshi Hamamoto, Atmika Paudel, Kazuhisa Sekimizu
- 84 - 90 **Investigation of antiaromatase activity using hepatic microsomes of Nile tilapia (*Oreochromis niloticus*).**
Tanongsak Sassa-deepaeng, Wasana Chaisri, Surachai Pikulkaew, Siriporn Okonogi
- 91 - 97 **Ultrastructural and physico-chemical characterization of saliva during menstrual cycle in perspective of ovulation in human.**
Ganesan Saibaba, Mahalingam Srinivasan, Archunan Priya Aarthy, Velliyangiri Silambarasan, Govindaraju Archunan
- 98 - 103 **Comparison of three acute stress models for simulating the pathophysiology of stress-related mucosal disease.**
Bhagawati Saxena, Sanjay Singh

Brief Reports

- 104 - 109 **1,2,3-Triazolyl esterization of PAK1-blocking propolis ingredients, artepillin C (ARC) and caffeic acid (CA), for boosting their anticancer/anti-PAK1 activities along with cell-permeability.**
Hideaki Takahashi, Binh Cao Quan Nguyen, Yoshihiro Uto, Md Shahinozzaman, Shinkichi Tawata, Hiroshi Maruta

CONTENTS

(Continued)

- 110 - 114 **Frondoside A from sea cucumber and nymphaeols from Okinawa propolis: Natural anti-cancer agents that selectively inhibit PAK1 *in vitro*.**
Binh Cao Quan Nguyen, Kazuki Yoshimura, Shigenori Kumazawa, Shinkichi Tawata, Hiroshi Maruta

Case Report

- 115 - 117 **Levetiracetam and topiramate poisoning: Two overdoses on those drugs with no lasting effects.**
Moaziz Sarfaraz, Syeda Rana Hasan

Guide for Authors

Copyright

Structural characterization and biological activities of a novel polysaccharide from *Phyllanthus emblica*

Zihan Zeng^{1,*}, Wenjie Lv^{2,*}, Yongshuai Jing², Zhiyan Chen³, Liyan Song^{2,3}, Ting Liu³, Rongmin Yu^{2,**}

¹ Pharmaceutical Department, the First Affiliated Hospital of Jinan University, Guangzhou, Guangdong Province, China;

² Biotechnological Institute of Chinese Materia Medica, Jinan University, Guangzhou, Guangdong Province, China;

³ Department of Pharmacology, Jinan University, Guangzhou, Guangdong Province, China.

Summary

A novel water-soluble polysaccharide named PEPW80-1, with a molecular mass of 4.7 kDa, was isolated from the pulp tissues of *Phyllanthus emblica*, and purified by sephadex G-100 column and sephacryl S-300 HR chromatography. The structural features of PEPW80-1 were investigated by a combination of acid hydrolysis, periodate oxidation-Smith degradation, methylation analysis, gas chromatography-mass spectrometry, scanning electron microscope, Fourier transform infrared spectroscopy, and nuclear magnetic resonance spectroscopy. The results showed that PEPW80-1 had a specific optical rotation of $[\alpha]_D^{25} = +113^\circ$ (c = 0.5 mg/mL) and its backbone composed of (1,3)-linked- β -L-rhamnose and (1,3,6)-linkage- β -D-galactose, with two branch chains of (1,4)-linked- α -D-galactose and (1,6)-linked- β -D-galactose and terminated with 1- α -L-arabinose. The antioxidant assays showed that PEPW80-1 possess 2,2-diphenyl-1-picrylhydrazyl radical-scavenging activity and hydroxyl radical-scavenging activity, enhancing reductive power. The results of immunomodulatory assays *in vitro* showed that PEPW80-1 could promote the proliferation of mouse splenocytes. Those proposed that PEPW80-1 might be developed as a potential value-added product with the activities of immunomodulator and free-radical inhibitors.

Keywords: *Phyllanthus emblica*, polysaccharide, structure characterization, antioxidant activities, immunomodulatory activity

1. Introduction

In recent years, polysaccharides extracted from plants, animals and microorganisms have attracted increasing attention due to their unique biological activities (1), such as antioxidant activity (2), hepatoprotective activity (3), antitumor activity (4), immunomodulatory activity (5) and interferon-inducing activity (6). Many studies have demonstrated that botanical polysaccharides have the potential to activate cells

involved in innate immunity (7). Interestingly, the botanical polysaccharides have also been proven to possess high antioxidant activities (8). Literature also indicates that the herbal antioxidants concurrently exhibit significantly immunomodulatory activities (9). It is therefore of great interest to investigate immunomodulatory effects of herbal polysaccharides that exhibit antioxidant activity with low toxicity.

Oxidation is essential to many organisms for the production of energy to fuel biological processes. However, reactive oxygen species are often over-produced under pathological conditions, resulting in oxidative stress (10). There are many kinds of reactive oxygen species (ROS), such as hydrogen peroxide (H₂O₂), hydroxyl radical and singlet oxygen (11). Although ROS at physiological concentration may be required for normal cell function, excessive amount of ROS can damage cellular components such as lipids, proteins and DNA. Many diseases such as cancer, cardiovascular

Released online in J-STAGE as advance publication April 25, 2017.

*These authors contributed equally to this works.

**Address correspondence to:

Dr. Rongmin Yu, Biotechnological Institute of Chinese Materia Medica, Jinan University, Guangzhou 510632, Guangdong Province, China.

E-mail: tyrm@jnu.edu.cn

diseases, rheumatoid arthritis, and atherosclerosis are believed to be related to the production of excessive amounts of ROS in the body (12). The free radical theory of aging suggests that the damage produced by the interactions of such free radicals with cellular macromolecules results in cellular senescence and aging. Although almost all organisms possess antioxidant and repair systems to protect them against oxidative damage, these systems are insufficient to prevent the damage entirely (13).

There is increasing evidence that many kinds of polysaccharides isolated from plants, fungi and bacteria are associated with immunostimulatory properties without significant side effects (14). The spleen combines the innate and adaptive immune system in a uniquely organized way, which has been the most important organ for antibacterial and antifungal immune reactivity. Therefore, the spleen has been an ideal tissue in immune research (15).

Phyllanthus emblica is extensively distributed in subtropical and tropical areas of China, India, Indonesia, and Malaysia and well known by consumers for its unique taste. The fruit of *P. emblica*, which has been used widely for thousands of years in Chinese and Indian traditional medicinal systems (16), was reported to have lipid-lowering (17) and hypoglycemic activities (18). It acts as not only an important constituent of many hepatoprotective formulations available (19), but also an antimicrobial (20,21), anticancer (22,23) and antiinflammatory agent (24,25), improving metal-induced clastogenic effects (26).

In the present study, we report for the first time the extraction, purification, structural characterization and ultrastructure of PEPW80-1 from the pulp tissues of *P. emblica* and evaluate its antioxidant and immunomodulatory activities *in vitro*.

2. Materials and Methods

2.1. Materials and reagents

Kunming mice (male, 8-12 weeks old, 18.0-20.0 g, License No. SCXK, 2011-0029) were purchased from Experimental Animal Center of Sun Yat-sen University, Guangzhou, Guangdong province, China. All mice were kept at the animal facilities under specific pathogen-free condition until used. Sterile food and water were supplied.

The fresh fruits of *P. emblica*, at the commercially mature stage, were purchased from Jieyang, Guangdong province, China. The material was identified by Professor R.M. Yu, College of Pharmacy, Jinan University, China. The fruit was dried at 55°C, and the pulp tissues were carefully removed from the seeds.

Diethylaminoethyl (DEAE) cellulose-52 was obtained from Whatman Ltd. (England). Sephadex G-100 and Sephacryl S-300 HR was purchased from Amersham

Biosciences (Swenden). Ascorbic acid (vitamin C, Vc), H₂O₂, ferrous sulfate (FeSO₄), and sulfate acid (H₂SO₄) were obtained from Guangzhou Chemical Reagent Co., Guangzhou, Guangdong province, China. All other reagents were obtained from Sigma Chemical Co. (USA) and all reagents were of analytical grade. Dimethylsulfoxide (DMSO), 3-(4,5-dimethylthiazol-2-yl)-2,5-diphenyltetrazolium- bromide (MTT), trypan, concanavalin A (Con A), penicillin G and streptomycin were obtained from Sigma Chemical Co. (St. Louis, MO, USA).

2.2. Preparation and isolation of polysaccharides

Preparation of the crude polysaccharide (PEPW80) from *P. emblica* was performed by water extraction and ethanol precipitation (27). *P. emblica* powder was extracted with 95% ethanol and then with distilled water for 2 h at 80°C three times. The water extracts were combined, filtered, concentrated, and then precipitated by addition of four-fold-volume of 95% ethanol. The precipitate was collected by centrifugation and dissolved by distilled water. The solution was deproteinated by a combination of papain enzymolysis and Sevag method, then dialyzed against tap water and distilled water, each for 48 h and lyophilized to obtain PEPW80. The obtained polysaccharide was applied to DEAE-52 cellulose column (1.6 × 50 cm) equilibrated with distilled water. The polysaccharide was fractionated and eluted at 0.7 mL/min of distilled water and sodium chloride (NaCl) solutions (0-0.8 mol/L), respectively. The main fractions were combined according to the total carbohydrate content quantified by the phenol-sulfuric acid method. Then one of fractions PEPW80-b was further fractionated with size-exclusion chromatography on a sephadex G-100 column (1.6 × 50 cm) and eluted at the flow rate of 0.3 mL/min with deionized water. The fraction was collected, concentrated, dialyzed and lyophilized to obtain a purified polysaccharide (PEPW80-1). The PEPW80-1 was then stored in bottle desiccators at room temperature for further study.

2.3. Measurement of molecular weight of PEPW80-1

Molecular weight of PEPW80-1 was determined by gel permeation chromatography on a column of sephacryl S-300 HR (2.6 × 80 cm) with water as the eluant at a flow rate of 0.3 mL/min. The column was calibrated with glucose, standard T-series dextran and blue dextran, respectively. Elution volume of polysaccharide was plotted in the same graph, and then the molecular weight of PEPW80-1 was determined.

2.4. Analysis of monosaccharide composition

PEPW80-1 (5.0 mg) was hydrolyzed with 2.0 M trifluoroacetic acid (TFA, 10 mL) at 100°C in a reaction

tube for 6 h. Excess acid was removed by evaporation on water bath at 60°C and co-distilled with methanol after the hydrolysis was completed. The hydrolysate (1.0 mg) was dissolved in pure water (1.0 mL) and used for the ion chromatographic analysis by high performance anion exchange chromatography-pulsed amperometric detector (HPAEC-PAD) on the Dionex ICS-2500 system, eluted with a mixture of water and 200 mM sodium hydroxide (NaOH) in the volume ratio of 92:8 (28).

2.5. Partial acid hydrolysis of PEPW80-1

Fractions 1 and 2 were hydrolyzed with 2 M TFA, after excess TFA in the fraction was removed by codistillation with methanol (1 mL × 3), and fraction 3 was tested by HPAEC-PAD, respectively (Figure 1).

2.6. Periodate oxidation–Smith degradation

The periodate oxidation analysis was performed as described in reference (29). The sample (25 mg) was dissolved in 0.015 M sodium periodate (NaIO₄) (25 mL) and the solution was kept at 4°C in dark. The A₂₂₃ nm of the reaction solution was measured every 6 h with a spectrophotometer. After the oxidation reaction was completed (96 h), the excess NaIO₄ was decomposed with ethylene glycol (1 mL). The amount of NaIO₄ consumption was calculated according to the decrease in absorbance at 223 nm. Formic acid production was determined by titration with 0.01 M NaOH. The reaction mixture was dialyzed against tap water and then distilled

water, each for 48 h. After dialysis, the retentate was freeze-dried, hydrolyzed with 2 M TFA (1 mL) at 120°C for 2 h, reduced by sodium borohydride (NaBH₄), acetylated with pyridine (0.5 mL) and acetic anhydride (0.5 mL) at 90°C for 1 h and then analyzed for sugar composition by gas chromatography (GC). GC was performed on a Shimadzu GC-14C instrument equipped with a hydrogen flame ionization detector and an Rtx-2330 column (0.32 mm × 15 m, i.d. 0.2 μm).

2.7. Fourier transform infrared spectrophotometer (FT-IR) analysis

FT-IR spectrum of the sample was determined using a Fourier transform infrared spectrophotometer (Nexus 5DXC FT-IR, Thermo Nicolet, America). The sample was grounded with spectroscopic grade potassium bromide (KBr) powder and then pressed into a 1 mm pellet for FT-IR measurement in the frequency range of 4,000-400 cm⁻¹ (27).

2.8. NuclearMagneticResonance (NMR) analysis

The freeze-dried polysaccharide was kept over phosphoric anhydride (P₂O₅) in vacuum for several days. The deuterium-exchanged polysaccharides (30 mg) were put in a 5-mm NMR tube and dissolved in 0.5 mL 99.96% deuterium oxide (D₂O). ¹³C NMR spectrum was recorded with a Bruker AM 500 MHz spectrometer (Bruker, Rheinstetten, Germany), operating frequencies 100.61 MHz for ¹³C NMR at 30°C. Chemical shift was

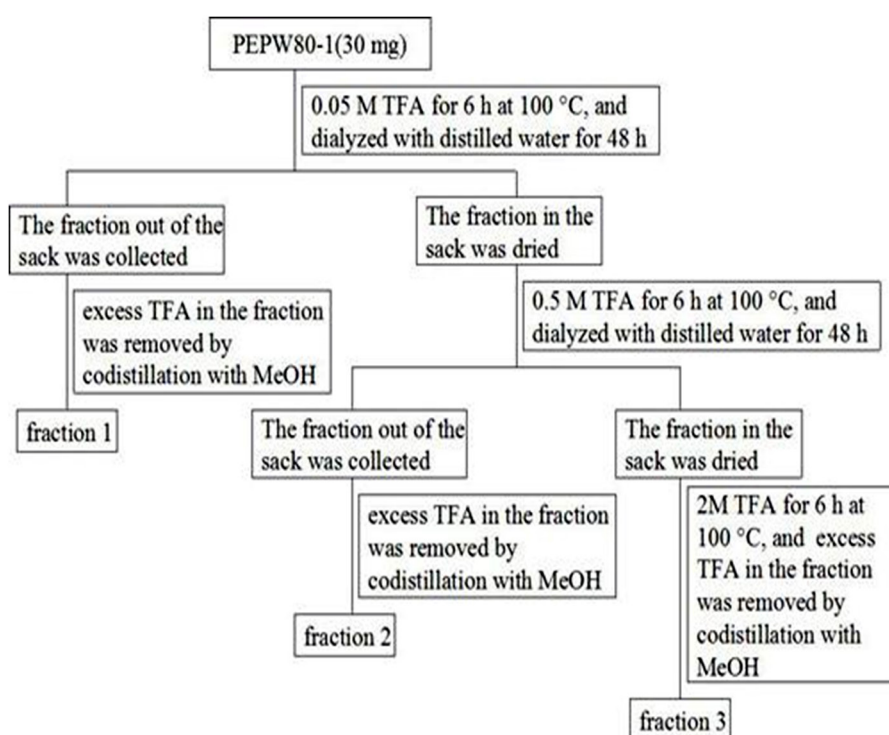


Figure 1. Procedure of partial acid hydrolysis of PEPW80-1.

expressed in ppm. Tetramethyl-silane was used as an internal standard.

2.9. Scanning electron microscopy analysis

Specimen was glued on specimen stubs using silver conducting tape and coated with gold-palladium using a sputter coater (BAL-TEC SCD 500, Liechtenstein). Scanning electron micrographs were obtained using an environmental scanning electron microscopy (SEM) (XL 30 ESEM, Philips, Holland) with the parameters HJ: 20 kV, resolution ratio: 3.4 nm, and spot: 4.

2.10. Determination of antioxidant activities in vitro of PEPW80-1

2.10.1. DPPH radical-scavenging assay

2,2-Diphenyl-1-picrylhydrazyl (DPPH) radical scavenging activity was measured using the method with slight modification (28). The solution of DPPH radical (0.1 mM) in methanol was prepared and 1.0 mL of this solution was added to 3.0 mL of the polysaccharide of different concentrations (0.1-3.2 mg/mL) in water. The mixture was shaken and incubated at 25°C for 30 min in the dark, and then the absorbance was measured at 517 nm against a blank (water instead of test sample and DPPH radical solution). Lower absorbance of the reaction mixture indicates higher free-radical scavenging activity. The percent scavenging activity was calculated by the following formula:

$$\text{Scavenging rate (\%)} = [1 - (A_1 - A_2)/A_0] \times 100$$

where A_0 is the absorbance of the control (water instead of test sample solution), A_1 is the absorbance of the sample. A_2 is the absorbance of the sample under identical conditions as A_1 and with water instead of DPPH radical solution.

2.10.2. Hydroxyl radical-scavenging (HOSC) assay

Hydroxyl radicals were generated using an innovative method (30). Sodium phosphate buffer (3 mL, 150 mM, pH 7.4), which contained 10 mM ferrous sulfate (FeSO_4), 2 mM sodium salicylate, 6 mM H_2O_2 , and different concentrations (0.1-3.2 mg/mL) of polysaccharide, were incubated at 37°C for 1 h. The absorbance was detected at 510 nm, and Vc was used as a positive control. The percent scavenging activity of hydroxyl radicals was calculated as follows:

$$\text{Scavenging rate (\%)} = [(A_s - A_0)/(A - A_0)] \times 100$$

where A_s is the absorbance in the presence of the sample, A_0 is the absorbance of the control in the absence of the sample, and A is the absorbance without the sample and Fenton reaction system.

2.10.3. Ferric-reducing antioxidant power

Ferric-reducing antioxidant power (FRAP) potential of PEPW80-1 was determined according to the modified method by Nakajima (31). Different concentrations (0.1-3.2 mg/mL) of PEPW80-1 was mixed with 2.5 mL of 0.2 M phosphate buffered saline (PBS) (pH 6.6) and 2.5 mL of 1% potassium ferricyanide ($\text{K}_3[\text{Fe}(\text{CN})_6]$). The mixture was incubated at 50°C for 20 min. Aliquots (2.5 mL) of 10% trichloroacetic acid were added to the mixture, which was then centrifuged for 10 min at 1,500× g. The upper layer of solution (2.5 mL) was mixed with 2.5 mL of distilled water and 0.5 mL of 0.1% FeCl_3 , and the absorbance was measured at 700 nm using UV-vis spectrophotometer (UV-2450, Shmadzu, Japan).

2.11. Measurement of immunomodulatory activity

2.11.1. Cells and animals

Splenocytes were prepared from mice as described by Kim (6). The cells were freed of red blood cells by treatment with lysis buffer (0.15 M ammonium chloride (NH_4Cl), 0.01 M potassium bicarbonate (KHCO_3), and 0.1 mM sodium ethylene diamine tetracetate (Na_2EDTA), pH 7.4). To remove adherent cells such as macrophages, splenocytes were incubated for 2 h in Petri dishes at a concentration of 5×10^6 cells/mL. The suspended cell populations were collected and used as the splenocytes populations.

2.11.2. Splenocytes proliferation

The splenocytes proliferation was assessed by using MTT-based colorimetric assay as previously described (32). An aliquot of 100 μL of splenocytes was seeded into 96-well flat bottom microtitre plates, thereafter the polysaccharide (final concentration 25, 50, 100, 200 and 400 $\mu\text{g}/\text{mL}$) was added, giving a final volume of 200 μL . Con A was used for reference purposes at a final concentration of 10 $\mu\text{g}/\text{mL}$. After incubation at 37°C in a humid atmosphere with 5% carbon dioxide (CO_2) for 48 h, 50 μL of MTT solution (1 mg/mL) was added to each well and incubated for another 6 h. The plate was centrifuged on 1,000× g for 5 min and the supernate was discard, and then 150 μL DMSO was added per well. Absorbance at 570 nm was measured on a microplate reader (Multiskan Spectrum, Thermo Scientific Instruments).

2.12. Statistical Analysis

All experiments were repeated three times. Results are presented as the mean \pm the standard error of the mean (SEM). Comparison of the data was performed using the single-factor analysis of variance (ANOVA) test. Significance was defined as a p value of < 0.05 .

3. Results

3.1. Fractionation of PEPW80-1

Two fractions consecutively eluted by 0-0.8 mol/L NaCl through an anion-exchange column were respectively coded as PEPW80-a and PEPW80-b. The yield of PEPW80-a and PEPW80-b respectively accounted for 5.08% and 56.02% of the crude polysaccharide extract, while the ratio of their peak areas was 3.07:35.02, indicating that PEPW80-b was the major component. PEPW80-b was further purified on a Sephadex G-100 (GE Health Care Biosciences AB, Uppsala, Sweden) gel filtration column (600 × 16 mm), and then the collected fraction was checked by sephacryl S-300 HR column which showed a single, symmetric, and sharp peak, named PEPW80-1, indicating near-homogeneity, with purity of 98.4% (data not shown). Surface and clear shape of refined polysaccharides could be observed with SEM. SEM analysis of the membrane sample provides a qualitative indication of the nature of polysaccharides. As shown in the Figure 2, the amber-colored loose powder PEPW80-1 was smooth and regular. In addition, PEPW80-1 contained no protein and nucleic acid, as evidenced by the lack of absorbance near 260 and 280 nm.

3.2. Structural elucidation of PEPW80-1

PEPW80-1 was consisted of rhamnose, arabinose and galactose (3.02:1.00:4.23). Its initial structural features were analyzed by partial acid hydrolysis, methylation, FT-IR and ^{13}C NMR.

The average molecular weight of the PEPW80-1 was determined to be 4.7 kDa by gel permeation chromatography (GPC) technique on a Sephacryl S-300 HR column. Calibration was performed with dextran molecular weight standards. In the FT-IR spectrum of PEPW80-1, the strong band at $3,425.4\text{ cm}^{-1}$ was attributed to the hydroxyl stretching vibration of the polysaccharide, and that at $2,926.6\text{ cm}^{-1}$ was due to the C-H stretching vibration absorption. The absence of any bands at $1,735.0\text{ cm}^{-1}$ confirmed that there was no uronic acidic in this fraction. The band around $1,624.7\text{ cm}^{-1}$ was due to the bound water. The absorption band at 890.0 cm^{-1} indicated that PEPW80-1 contained a β -type glycosidic linkage in its structure and the characteristic bands at $1,000.0$ - $1,100.0\text{ cm}^{-1}$ suggested the presence of pyranose form of the glucosyl residue.

The analysis results of fractions 1 and 2 showed that the branched structure of PEPW80-1 was composed of galactose and terminated with arabinose, and that of fraction 3 indicated that rhamnose, galactose could be the backbone of the structure of PEPW80-1. The periodate oxidized products were fully hydrolyzed and analyzed by GC after 2M TFA hydrolysis. The results showed that there were galactose, rhamnose in

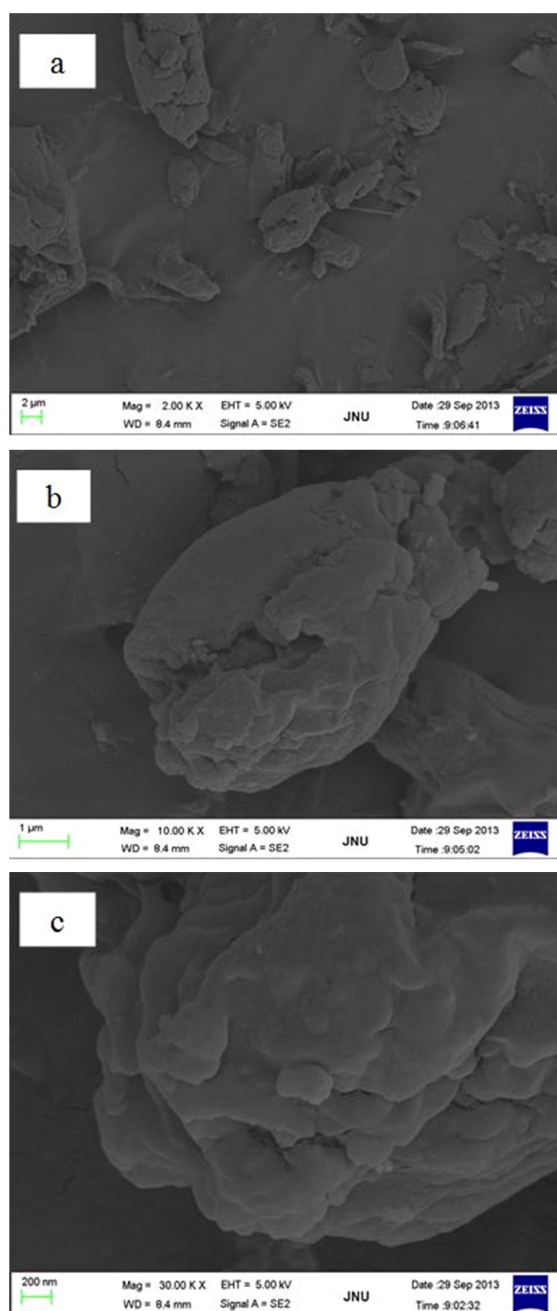


Figure 2. PEPW80-1 of imaged by SEM. a: 2.00 KX, b: 10.00 KX, c: 30.00 KX.

the oxidation products. The presence of rhamnose and galactose indicated that some residues of rhamnose and galactose were 1,3-, 1,2,3-, 1,2,4-, 1,3,4-, 1,3,6- or 1,2,3,4-linked, which cannot be oxidized. At the same time, a part of galactose were 1,4- and 1,6-linkage, which might be oxidized to produce erythritol and glycerol.

NMR spectroscopy has been the most powerful technique for the structure analysis of carbohydrates (33). The data (δ , ppm) of ^{13}C NMR of PEPW80-1 was shown in Figure 3, and five signals appeared in the anomeric region, suggesting the presence of five different linkage patterns. The data of ^{13}C NMR

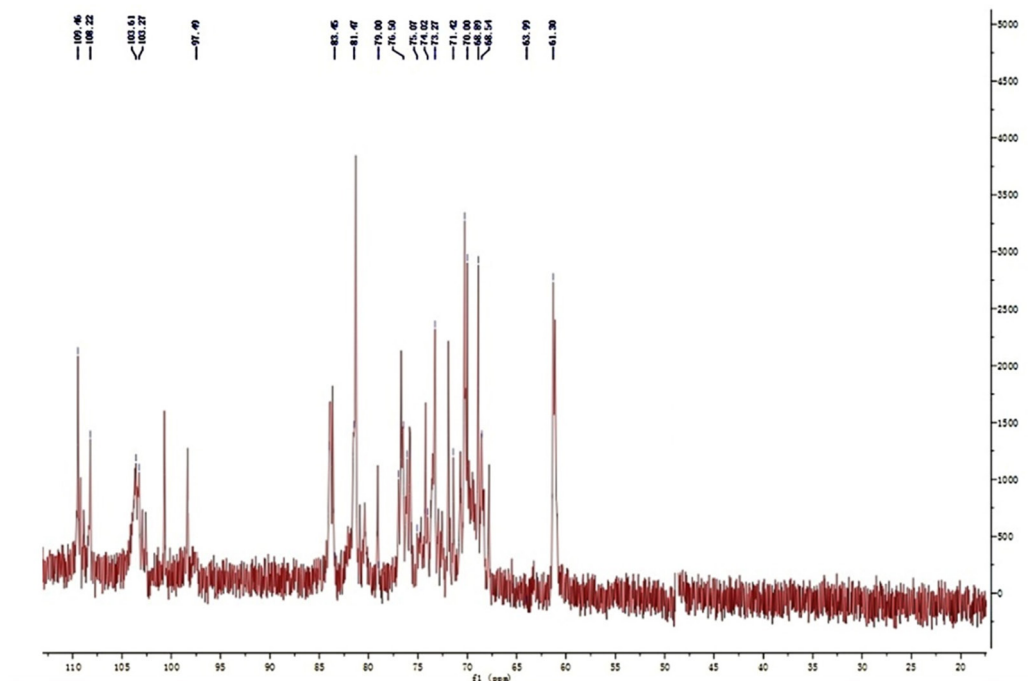


Figure 3. ^{13}C -NMR spectrum of PEPW80-1.

Table 1. Assignment of ^{13}C NMR chemical shifts of PEPW80-1

Sugar residue	Chemical shifts (ppm)						
	C1	C2	C3	C4	C5	C6	CH ₃
α -L-Araf(1 \rightarrow	109.2	81.5	76.5	83.8	64.0		
\rightarrow 3)- β -L-Rhap(1 \rightarrow	108.3	78.9	83.8	76.7	74.1		16.4
\rightarrow 6)- β -D-Galp(1 \rightarrow	103.7	74.1	76.1	71.4	75.1	64.0	
\rightarrow 3,6)- β -D-Galp(1 \rightarrow	103.3	73.2	77.0	69.9	76.7	68.8	
\rightarrow 4)- α -D-Galp(1 \rightarrow	97.21	70.3	69.8	78.9	68.8	61.3	

identified the signals as 1,6- β -D-galactopyranose (δ 103.7), 1,3,6- β -D-galactopyranose (δ 103.3), 1,3- β -L-rhamnopyranose (δ 108.3), 1,4- α -D-galactopyranose (δ 97.2) and 1- α -L-arabino-furanose (δ 109.2) terminal residues. The result also proposed that the backbone was composed of 1,3,6- β -D-galactopyranose and 1,3- β -L-rhamnopyranose residues, with two branch chains of (1,4)-linked- α -D-galactose and (1,6)-linked- β -D-galactose and terminated with 1- α -L-arabinose (34-35,28). The assignment of the carbon atom signals was shown in Table 1.

According to above elucidation, PEPW80-1 could be proposed as a heteropolysaccharide, with a backbone of 1,3- β -L-rhamnose and 1,3,6- β -D-galactose, two branch chains of 1,6- β -D-galactose and 1,4- α -D-galactose based on the experimental results. The terminal residue was 1- α -L-arabinose. On the basis of above discussion, the structure of PEPW80-1 might be assigned as Figure 4.

3.3. Methylation analysis by GC-MS

Methylation analysis by GC-MS was used to provide

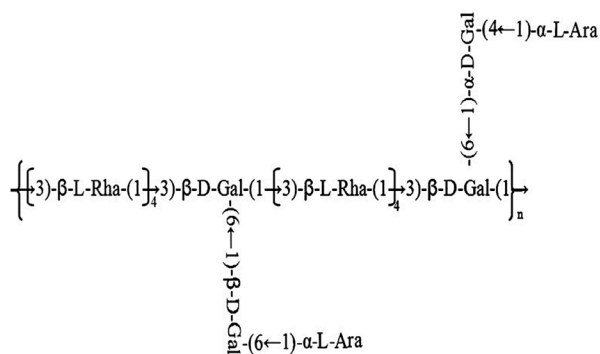
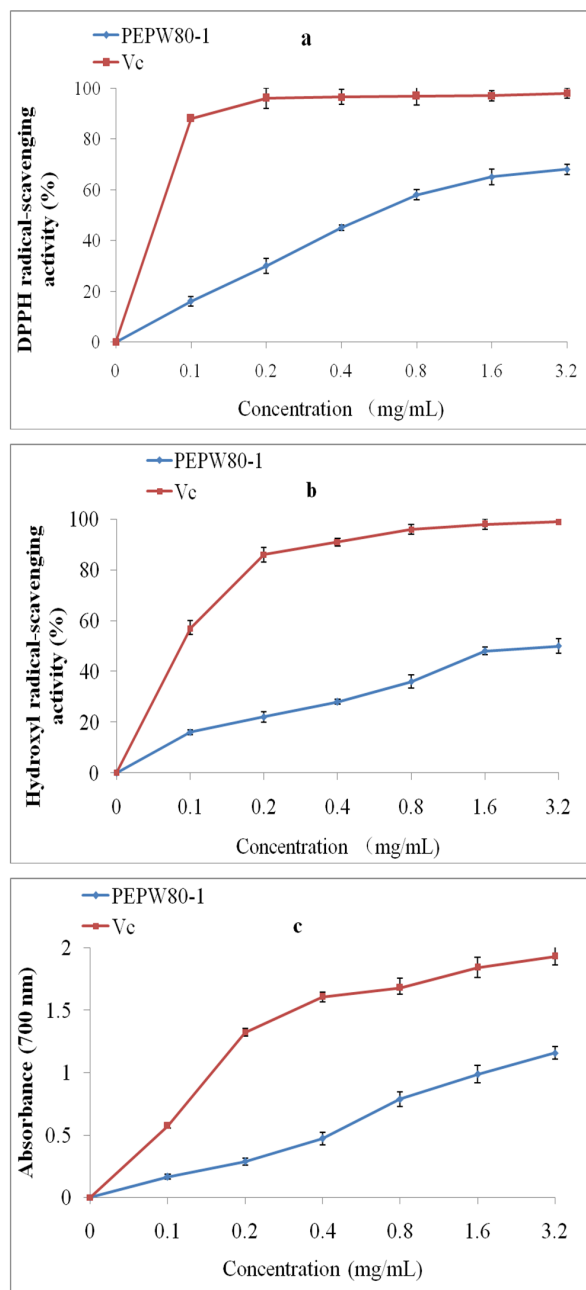


Figure 4. The proposed structure of PEPW80-1.

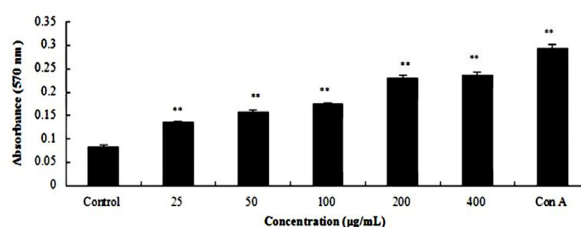
more structural information for PEPW80-1. The results shown as 2,4-Me₂-Rha, 2,3,6-Me₃-Gal, 4,6-Me₂-Gal, 2,3,4-Me₃-Gal, 2,3,4-Me₃-Ara in a molar ratio of 4.03:1.07:1.05:1.00:1.15 (Table 2). Therefore, it suggested that the repeating unit of PEPW80-1 consisted of 1,3-linked galactose, 1,4,6-linked galactose, 1,6-linked galactose, 1,3-linked rhamnose and 1-linked glucose.

Table 2. Glycosidic linkage composition of methylated PEPW80-1

Methylation sugar	Molar ratio	Mass fragments (m/z)	Linkage type
2,3,6-Me ₃ -Gal	1.07	43, 59, 72, 118, 233	1→4
2,4-Me ₂ -Gal	1.05	43,86, 117, 129, 189	1→3,6
2,3,4-Me ₃ -Gal	1.00	43, 71, 101, 129, 161, 189, 233	1→6
2,3,4-Me ₃ -Ara	1.15	43, 45, 71, 87, 101, 117, 129, 161	1→
2,4-Me ₂ -Rha	4.03	43, 59, 69, 75, 85, 99, 101, 117, 129	1→3

**Figure 5. Antioxidant activities of PEPW80-1. a:** DPPH radical-scavenging activity, **b:** Hydroxyl radical-scavenging activity, **c:** Ferric-reducing activity. Values are means \pm SD of three separate experiments.

The molar ratio of these residues agreed overall with the monosaccharide composition of PEPW80-1 described above.

**Figure 6. Effects of PEPW80-1 promoted splenocyte proliferation.** Values are means \pm SD of three separate determinations.

3.4. Antioxidant activity of PEPW80-1

3.4.1. Scavenging activity to the DPPH radical

As shown in Figure 5a, the results of scavenging activity to the DPPH radical indicated that PEPW80-1 showed obvious scavenging activity on DPPH radical in a concentration-dependent manner at relatively low concentration (0.0-0.8 mg/mL). The maximum value of PEPW80-1 reached 69.2% that of Vc. The IC₅₀ values of PEPW80-1 was 0.5 mg/mL.

3.4.2. Scavenging effects on hydroxyl radicals

Removing hydroxyl radical is important for the protection of living systems. The results of hydroxyl radical scavenging (HOSC) activities of the PEPW80-1 and Vc were given in Figure 5b. The scavenging effect of PEPW80-1 was enhanced significantly with the increase of sample concentration ranging from 0 to 1.6 mg/mL. After that, the scavenging activity increased slowly with the increase of sample concentration. The IC₅₀ value of PEPW80-1 was 2.0 mg/mL. The maximum value of PEPW80-1 reached 51.7% that of Vc.

3.4.3. Ferric-reducing antioxidant power (FRAP)

The antioxidant capacity of PEPW80-1 was shown in Figure 5c and compared with Vc. The reducing capacity ascended with increasing concentration from 0 to 1.6 mg/mL. The maximum value of PEPW80-1 reached 57.8% that of Vc.

3.4.4. In vitro immunomodulatory activity of PEPW80-1

MTT assay was used to evaluate splenocyte proliferation

induced by Con A or PEPW80-1 *in vitro*. Spleen cells increased with the increase of sample concentration, and the polysaccharide significantly promoted the proliferation of splenocytes. At a lower concentration (25 µg/mL) PEPW80-1 could significantly enhance induced lymphocyte proliferation ($p < 0.01$) as compared with that of the normal control group (Figure 6).

4. Discussion

Polysaccharides, consisting 10 or/over 10 monosaccharides joined by glycosidic linkages, are considered as active compounds in plants and animals (36-38). Nowadays, many studies demonstrated that botanical polysaccharides had antioxidant activity (2) and immunomodulatory activity (5). As there was no study in polysaccharides of *P. emblica*, it attracted our interest to know if it had any polysaccharide with biological activities. PEPW80-1 was isolated and characterized from the pulp tissues of *P. emblica*, which contained rhamnose, arabinose and galactose (3.02:1.00:4.23).

Although antioxidant activity was usually associated with low molecular weight compounds such as phenols and carotenoids, increasing evidence indicated that polysaccharides from different sources might also possess strong antioxidant properties without concerns of cytotoxicity and could be developed as novel dietary antioxidants (39). Therefore, the DPPH radical, HOSC and FRAP assays were further evaluated for PEPW80-1.

It is well accepted that DPPH radical scavenging by antioxidants is due to their hydrogen-donating ability. The method of scavenging DPPH radical is based on the reduction of DPPH radical ethanol solution in the presence of a hydrogen-donating antioxidant, resulting in the formation of the non-radical form DPPH-H. DPPH radical is a stable radical and could accept an electron or hydrogen radical to become a stable diamagnetic molecule. Therefore, the antioxidant activity of a substance might be expressed as its ability in scavenging the DPPH radical. The results of DPPH radical scavenging test showed that the maximum value of PEPW80-1 reached 69.2% that of Vc and the IC₅₀ values of PEPW80-1 was 0.5 mg/mL. PEPW80-1 had greater DPPH radical scavenging ability than polysaccharide from *Panax japonicus* (40) with a value IC₅₀ of 3.0 mg/mL. These results indicated that the PEPW80-1 could act as an electron or hydrogen donor to scavenge DPPH radical.

Hydroxyl radical can easily cross cell membranes, readily react with most biomolecules including carbohydrates, proteins, lipids, and DNA in cells, and cause tissue damage or cell death (41). The IC₅₀ value of PEPW80-1 was 2.0 mg/mL, which was less than the polysaccharide from *Panax japonicus* (5 mg/mL) (40). The maximum value of PEPW80-1 reached 51.7% that of Vc. The antioxidant mechanism might be due to the supply of hydrogen by the polysaccharide, which

combines with radicals and forms a stable radical to terminate the radical chain reaction. The other possibility is that polysaccharide could combine with the radical ions which are necessary for radical chain reaction, and the reaction is terminated.

The FRAP assay treats the antioxidants contained in the samples as reductants in a redox linked colorimetric reaction, and the value reflects the reducing power of antioxidants. It has been reported that there was a direct correlation between antioxidant activity and reducing capacity (42). The antioxidant potential of PEPW80-1 was estimated by its ability to reduce the ferric complex to the ferrous complex. The maximum value of PEPW80-1 reached 57.8% that of Vc. It suggested that PEPW80-1 was electron donors and could react with free radicals to convert them into more stable products and terminate the radical chain reactions. Our experimental results demonstrated that there might be a direct correlation between antioxidant activity and reducing capacity.

Immunoregulation was one of the basic functions associated with polysaccharides (43). The spleen is the body's largest immune organ, capable of producing a large number of lymphocytes. Splenocyte proliferation is a crucial event in the activation cascade of both cellular and humoral immune responses. Immunomodulatory effect of the PEPW80-1 was investigated, and the results showed that PEPW80-1 could significantly induce lymphocyte proliferation at a low concentration (25 µg/mL), which is greater than the polysaccharides from the swollen culms of *Zizania latifolia* (200 and 400 µg/mL) (44).

Acknowledgements

The authors thank Dr. Dongbo Yu of The University of Chicago, Illinois, USA, for proofreading our manuscript.

References

1. Forabosco A, Bruno G, Sparapano L, Liut G, Marino D, Delben F. Pullulans produced by strains of *Cryphonectria parasitica*-I. Production and characterisation of the exopolysaccharides. *Carbohydr Polym.* 2006; 63:535-544.
2. Qiao DL, Ke CL, Hu B, Luo JG, Ye H, Sun Y, Yan XY, Zeng XX. Antioxidant activities of polysaccharides from *Hyriopsis cumingii*. *Carbohydr Polym.* 2009; 78:199-204.
3. Liu Q, Zhu M, Geng X, Wang H, Ng TB. Characterization of polysaccharides with antioxidant and hepatoprotective activities from the edible mushroom *Oudemansiella radicata*. *Molecules.* 2017; 22:234.
4. Chen RZ, Meng FL, Liu ZQ, Chen RP, Zhang M. Antitumor activities of different fractions of polysaccharide purified from *Ornithogalum caudatum* Ait. *Carbohydr Polym.* 2010; 80:845-851.
5. Sun YG, Wang SS, Li TB, Li X, Jiao LL, Zhang LP. Purification, structure and immunobiological activity of a new water-soluble polysaccharide from the mycelium

- of *Polyporus albicans* (Imaz.) Teng. Bioresour Technol. 2008; 99:900-904.
6. Kim HM, Oh GT, Hong DH, Hyun BH, Cha YN, Yoo BS, Han SB. Facilitation of apoptosis by autologous serum and related immunosuppression in the splenocyte culture. Immunopharmacology. 1996; 34:39-50.
 7. Jeong SC, Koyyalamudi SR, Jeong YT, Song CH, Pang G. Macrophage immunomodulating and antitumor activities of polysaccharides isolated from *Agaricus bisporus* white button mushrooms. J Med Food. 2012; 15:58-65.
 8. Sun LQ, Wang CH, Shi QJ, Ma CH. Preparation of different molecular weight polysaccharides from *Porphyridium cruentum* and their antioxidant activities. Int J Biol Macromol. 2009; 45:42-47.
 9. Chandrashekar PM, Prashanth KV, Venkatesh YP. Isolation, structural elucidation and immunomodulatory activity of fructans from aged garlic extract. Phytochemistry. 2011; 72:255-264.
 10. Wang CC, Chang SC, Stephen Inbaraj B, Chen BH. Isolation of carotenoids, flavonoids and polysaccharides from *Lycium barbarum* L. and evaluation of antioxidant activity. Food Chem. 2010; 120:184-192.
 11. Hu T, Liu D, Chen Y, Wu J, Wang S. Antioxidant activity of sulfated polysaccharide fractions extracted from *Undaria pinnatifida* in vitro. Int J Biol Macromol. 2010; 46:193-198.
 12. Liu W, Wang H, Yao W, Gao X, Yu L. Effects of sulfation on the physicochemical and functional properties of a water-insoluble polysaccharide preparation from *Ganoderma lucidum*. J Agric Food Chem. 2010; 58:3336-3341.
 13. Tseng Y, Yang J, Mau J. Antioxidant properties of polysaccharides from *Ganoderma tsugae*. Food Chem. 2008; 107:732-738.
 14. Schepetkin IA, Quinn MT. Botanical polysaccharides: macrophage immunomodulation and therapeutic potential. Int Immunopharmacol. 2006; 6:317-333.
 15. Mebius RE, Kraal G. Structure and function of the spleen. Nat Rev Immunol. 2005; 5:606-616.
 16. Zhang YJ, Tanaka T, Iwamoto Y, Yang CR, Kouno I. Phyllaemblic acid, a novel highly oxygenated norbisabolane from the roots of *Phyllanthus emblica*. Tetrahedron Lett. 2000; 41:1781-1784.
 17. Anila L, Vijayalakshmi NR. Beneficial effects of flavonoids from *Sesamum indicum*, *Emblica officinalis* and *Momordica charantia*. Phytother Res. 2000; 14:592-595.
 18. Abesundara KJ, Matsui T, Matsumoto K. Alpha-glucosidase inhibitory activity of some Sri Lanka plant extracts, one of which, *Cassia auriculata*, exerts a strong anti-hyperglycemic effect in rats comparable to the therapeutic drug acarbose. J Agric Food Chem. 2004; 52:2541-2545.
 19. Panda S, Kar A. Fruit extract of *Emblica officinalis* ameliorates hyperthyroidism and hepatic lipid peroxidation in mice. Pharmazie. 2003; 58:753-755.
 20. Godbole SH, Pendse GS. Antibacterial property of some plants. Indian J Pharmacy. 1960; 22:39-42.
 21. Rani P, Khullar N. Antimicrobial evaluation of some medicinal plants for their anti-enteric potential against multi-drug resistant *Salmonella typhi*. Phytother Res. 2004; 18:670-673.
 22. Jeena KJ, Kuttan R. Antitumour activity of *Emblica officinalis*. J Ethnopharmacol. 2001; 75:65-69.
 23. Zhang YJ, Nagao T, Tanaka T, Yang CR, Okabe H, Kouno I. Antiproliferative activity of the main constituents from *Phyllanthus emblica*. Biol Pharm Bull. 2004; 27:251-255.
 24. Perianayagam JB, Sharma SK, Joseph A, Christina AJ. Evaluation of anti-pyretic and analgesic activity of *Emblica officinalis* Gaertn. J Ethnopharmacol. 2004; 95:83-85.
 25. Wang CC, Yuan JR, Wang CF, Yang N, Chen J, Liu D, Song J, Feng L, Tan XB, Jia XB. Anti-inflammatory effects of *Phyllanthus emblica* L on benzopyrene-induced precancerous lung lesion by regulating the IL-1 β /miR-101/Lin28B signaling pathway. Integr Cancer Ther. 2016. DOI: 10.1177/1534735416659358.
 26. Biswas S, Talukder G, Sharma A. Protection against cytotoxic effects of arsenic by dietary supplementation with crude extract of *Emblica officinalis* fruit. Phytother Res. 1999; 13:513-516.
 27. Luo A, He X, Zhou S, Fan Y, Luo AS, Chun Z. Purification, composition analysis and antioxidant activity of the polysaccharides from *Dendrobium nobile* Lindl. Carbohydr Polym. 2010; 79:1014-1019.
 28. Yuan F, Yu RM, Yin Y, Shen JR, Dong QF, Zhong L, Song LY. Structure characterization and antioxidant activity of a novel polysaccharide isolated from *Ginkgo biloba*. Int J Biol Macromol. 2010; 46:436-439.
 29. Chaplin FM, Kennedy JF. Carbohydrate analysis: A practical approach (2nd ed.). London: IRL Press, 1994; pp. 81-95.
 30. Smirnoff N, Cumbes QJ. Hydroxyl radical scavenging activity of compatible solutes. Phytochemistry. 1989; 28:1057-1060.
 31. Nakajima Y, Sato Y, Konishi T. Antioxidant small phenolic ingredients in *Inonotus obliquus* (persoon) Pilat (Chaga). Chem Pharm Bull. 2007; 55:1222-1226.
 32. Zhang YL, Lu XY, Zhang YN, Qin LG, Zhang JB. Sulfated modification and immunomodulatory activity of water-soluble polysaccharides derived from fresh Chinese persimmon fruit. Int J Biol Macromol. 2010; 46:67-71.
 33. Niu YG, Yan W, Lv JL, Yao WB, Yu LL. Characterization of a novel polysaccharide from tetraploid *Gynostemma pentaphyllum* Makino. J Agric Food Chem. 2013; 61:4882-4889.
 34. Hu XQ, Huang YY, Dong QF, Song LY, Yuan F, Yu RM. Structure characterization and antioxidant activity of a novel polysaccharide isolated from pulp tissues of *Litchi chinensis*. J Agric Food Chem. 2011; 59:11548-11552.
 35. Hua DH, Zhang DZ, Huang B, Yi P, Yan CY. Structural characterization and DPPH \cdot radical scavenging activity of a polysaccharide from *Guava* fruits. Carbohydr Polym. 2014; 103:143-147.
 36. Wang J, Hu S, Nie S, Yu Q, Xie M. Reviews on mechanisms of in vitro antioxidant activity of polysaccharides. Oxid Med Cell Longev. 2016; 2016:5692852.
 37. Mellal M, Jaffrin MY, Ding LH, Delattre C, Michaud P, Courtois J. Separation of oligoglucuronans of low degrees of polymerization by using a high shear rotating disk filtration module. Sep Purif Technol. 2008; 60:22-29.
 38. Delattre C, Michaud P, Hamze K, Courtois B, Courtois J, Vijayalakshmi MA. Purification of oligouronides using hollow-fiber membrane functionalized with L-histidine. J Chromatogr A. 2005; 1099:121-126.
 39. Chen GT, Ma XM, Liu ST, Liao YL, Zhao GQ. Isolation, purification and antioxidant activities of polysaccharides from *Grifola frondosa*. Carbohydr Polym. 2012; 89:61-66.
 40. Yang XL, Wang RF, Zhang XP, Zhu WJ, Tang J, Liu JF,

- Chen P, Zhang DM, Ye WC, Zheng YL. Polysaccharides from *Panax japonicus* C.A. Meyer and their antioxidant activities. *Carbohydr Polym.* 2014; 101:386-391.
41. Yuan JF, Zhang ZQ, Fan ZC, Yang JX. Antioxidant effects and cytotoxicity of three purified polysaccharides from *Ligusticum chuanxiong* Hort. *Carbohydr Polym.* 2008; 74:822-827.
42. Amarowicz R, Pegg RB, Rahimi-Moghaddam P, Barl B, Weil JA. Free-radical scavenging capacity and antioxidant activity of selected plant species from the *Canadian prairies*. *Food Chem.* 2004; 84:551-562.
43. Su Z, Dai Z, Yang J. Research progress on immunologic mechanism of polysaccharide. *J Yunnan Agric Univ.* 2006; 21:205-209.
44. Wang M, Zhu P, Zhao S, Nie C, Wang N, Du X, Zhou Y. Characterization, antioxidant activity and immunomodulatory activity of polysaccharides from the swollen culms of *Zizania latifolia*. *Int J Biol Macromol.* 2017; 95:809-817.

(Received February 12, 2017; Revised April 11, 2017; Accepted April 18, 2017)

Influence of clove oil and eugenol on muscle contraction of silkworm (*Bombyx mori*)

Kantaporn Kheawfu¹, Surachai Pikulkaew^{2,*}, Hiroshi Hamamoto^{3,4}, Kazuhisa Sekimizu^{3,4}, Siriporn Okonogi^{5,6,*}

¹Nanoscience and Nanotechnology Program, The Graduate School, Chiang Mai University, Chiang Mai, Thailand;

²Department of Food Animal Clinic, Faculty of Veterinary Medicine, Chiang Mai University, Chiang Mai, Thailand;

³Laboratory of Microbiology, Graduate School of Pharmaceutical Sciences, The University of Tokyo, Tokyo, Japan;

⁴Teikyo University Institute of Medical Mycology, Tokyo, Japan;

⁵Department of Pharmaceutical Sciences, Faculty of Pharmacy, Chiang Mai University, Chiang Mai, Thailand;

⁶Research Center of Pharmaceutical Nanotechnology, Chiang Mai University, Chiang Mai, Thailand.

Summary

Clove oil is used in fish anesthesia and expected to have a mechanism *via* glutamic receptor. The present study explores the activities of clove oil and its major compound, eugenol, in comparison with L-glutamic acid on glutamic receptor of silkworm muscle and fish anesthesia. It was found that clove oil and eugenol had similar effects to L-glutamic acid on inhibition of silkworm muscle contraction after treated with D-glutamic acid and kainic acid. Anesthetic activity of the test samples was investigated in goldfish. The results demonstrated that L-glutamic acid at 20 and 40 mM could induce the fish to stage 3 of anesthesia that the fish exhibited total loss of equilibrium and muscle tone, whereas clove oil and eugenol at 60 ppm could induce the fish to stage 4 of anesthesia that the reflex activity of the fish was lost. These results suggest that clove oil and eugenol have similar functional activities and mechanism to L-glutamic acid on muscle contraction and fish anesthesia.

Keywords: Clove oil, eugenol, glutamic acid, kainic acid, silkworm

1. Introduction

Clove oil, an essential oil obtained from buds of clove tree (*Syzygium aromaticum*), has been traditionally used as topical anesthetic for toothaches, headaches, joint pain. It is also used as an alternative fish anesthetic (1,2), according to its ease of obtaining and inexpensiveness as well as safety for both fish and human (3).

The major component of clove oil is eugenol, which is about 90-97% of total oil. Both clove oil

and eugenol have been used to anesthetize rainbow trout (*Oncorhynchus mykiss*) (4), red pacu (*Piaractus brachypomus*) (5), beluga (*Huso huso*) (6), Nile tilapia (*Oreochromis niloticus*) (7), and flowerhorn fish (*Amphilophus labiatus* × *Amphilophus trimaculatus*) (8). Furthermore, eugenol can be used in other aquatic animals such as Indian shrimp (*Fenneropenaeus indicus*) (9), whiteleg shrimp (*Litopenaeus vannamei*) (10), and the amphibians as African clawed frog (*Xenopus laevis*) (11), as well as mammals like rat and mouse (12,13).

Even both compounds are widely used for anesthesia of aquatic animals, the anesthetic mechanism pathway of clove oil or eugenol is unclear in fish, but a hypothesis is expectedly *via* gamma-aminobutyric acid (GABA) and glutamate receptors (14). Invertebrate animal models are preferable choice for drug-screening and used instead of vertebrates. They offer a great potential for cost-effective due to culture conditions fulfill the requirements for large-scale screens, less ethical concern, and fundamental biological mechanisms of invertebrates correlate with mammals (15). In case of signal transmission, the receptor of invertebrate

Released online in J-STAGE as advance publication April 30, 2017.

*Address correspondence to:

Dr. Siriporn Okonogi, Department of Pharmaceutical Sciences, Faculty of Pharmacy, Chiang Mai University, Chiang Mai, Thailand.

E-mail: okng2000@gmail.com

Dr. Surachai Pikulkaew, Department of Food Animal Clinic, Faculty of Veterinary Medicine, Chiang Mai University, Chiang Mai, Thailand.

E-mail: surapikulkaew@gmail.com

animals such as cricket (*Gryllus domestica*) and fruit fly (*Drosophila melanogaster*) on presynaptic nerve terminals or muscle membranes have a similar pharmacological profile as 5-HT like receptor subtype (16,17). Furthermore, silkworm (*Bombyx mori*) was discovered that the neurotransmitters of glutamic acid functions acted on their neuromuscular junction. D-glutamic acid and kainic acid as glutamate receptor agonists could induce muscle contraction in silkworm after injected into hemolymph, meanwhile, L-glutamic acid presented as antagonist to the activities of D-glutamic acid and kainic acid. Hence, after injection these glutamate receptor agonists, muscle contraction would be inhibited by injection of L-glutamic acid (18).

It was suspected whether the mechanism of action of clove oil as anesthetic agent was involved in glutamic acid functions. We hypothesized that clove oil and eugenol might have anesthetic activity as glutamate receptor antagonist, and should inhibit muscle contraction induced by both D-glutamic acid and kainic acid.

2. Materials and Methods

2.1. Materials

Clove oil was purchased from Thai-China Flavours & Fragrances Industry (Nonthaburi, Thailand). Eugenol was from Sigma-Aldrich (Steinheim, Germany). L-glutamic acid, D-glutamic acid, sodium hydroxide, and ethanol were from Wako Pure Chemical Industries (Osaka, Japan). Kainic acid was from Abcam (Cambridge, UK). Saline was from Otsuka Pharmaceutical (Tokyo, Japan).

2.2. Silkworm larvae muscle contraction assay

The assay was performed according to the method previously described by Sekimizu *et al.* (18). The 5th instar larval stage silkworms, body weight of 4-6 g, were prepared and their heads were cut off with scissors, then peritrophic membranes and silk glands were removed. Each specimen was tied with strings and attached with load of 29-30 g. The test samples of this study, included 20-80 mM L-glutamic acid, 0.9-90% ethanol (as vehicle), clove oil containing 6-600 mM eugenol (namely 6-600 mM clove oil), and 6-600 mM pure eugenol, were dispersed in saline and filled in a 1-mL syringe attached to a 27-gauge needle (Terumo, Tokyo, Japan). Then, the test samples (50 μ L) were injected into the silkworm specimens, followed by an injection of 40 mM D-glutamic acid or 0.2 mM kainic acid (50 μ L). The intensity of muscle contraction was expressed as the contraction value calculated by the following equation; $(x - y)/x$. Where x and y are the maximum length (mm) of each individual specimen before and after injection, respectively.

2.3. Fish anesthetic experiment

Twenty-four goldfish (*Carassius auratus*) with an average length of 3.97 ± 0.33 cm were stocked separately in 20-L tank and supplied with running and aerated water for 1 week under control conditions. The fish were not fed for 24 h prior to testing.

For the determination of the anesthetic activity, 8 fish were netted and transferred individually to 8 plastic experimental tanks filled with 2 L of water from a similar source. Clove oil and eugenol were diluted with ethanol to obtain the desired concentrations. The fish were placed into each tank containing 60 ppm clove oil, 60 ppm (or 0.36 mM) eugenol, 540 ppm ethanol (as a vehicle control), and 0.4, 4, 20, and 40 mM L-glutamic acid. The tank without any test sample was used as a control tank. Induction time, recovery time, and mortality were estimated, as described by Iversen *et al.* and Iwama *et al.* (19,20). The induction time is the period from the moment a fish is exposed to the samples until it exhibits anesthesia which can be divided based on fish behavior into 4 stages as followings; no reaction to external stimuli (stage 1), partial loss equilibrium (stage 2), total loss equilibrium and muscle tone (stage 3), and loss of reflex activity (stage 4). After 10-sec stay in stage 4, the fish were transferred into the identical tank without any anesthetic agent and were observed to determine recovery time or mortality. The recovery time is the time that an anesthetized fish takes in order to regain full equilibrium from the moment it is placed in a recovery tank. The recovery is divided into 3 stages as followings; fish begin to have opercular movement (stage 1), recovery of equilibrium and body movement (stage 2), and full recovery similar to pre-anesthesia (stage 3). The recovery and induction times were recorded for each fish individually. After recovery, the fish were transferred into the maintenance tanks (20 L) and the adverse effects were observed for one week. Each sample was tested in triplicate.

2.4. Statistical analysis

Statistical evaluation of anesthetic induction and recovery times in fish experiment was performed by one-way ANOVA (Bonferroni test). Data were presented as mean \pm SD. The value of $p < 0.05$ was considered to indicate significant differences.

3. Results

3.1. Effect of eugenol on D-glutamic acid-induced muscle contraction in silkworm

We re-examined the inhibitory effect of L-glutamic acid on D-glutamic acid followed the established silkworm muscle contraction experiment. D-glutamic acid is an amino acid existed in silkworm hemolymph and

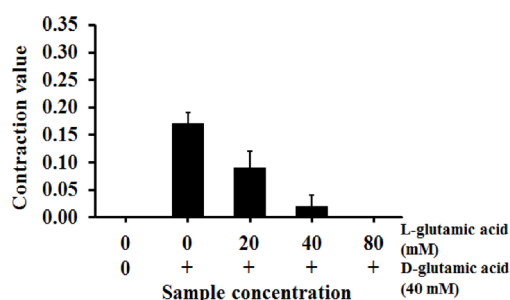


Figure 1. The effect of L-glutamic acid on D-glutamic acid induced silkworm muscle contraction ($n \geq 2$).

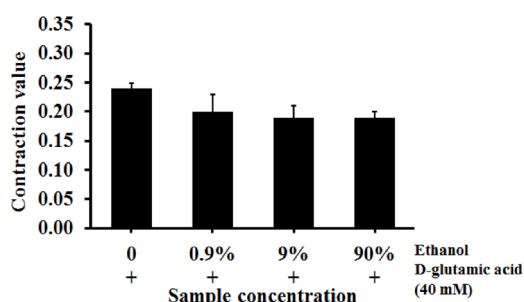


Figure 2. The effect of ethanol on D-glutamic acid induced muscle contraction in silkworm ($n \geq 2$).

thought to regulate the muscle contraction in silkworm. A single injection of D-glutamic acid in decapitated silkworm caused muscle contraction with a contraction value of 0.25 within 1 min. After 3 min of this contraction, slightly muscle relaxation was observed and fully relaxation was found in 30 min. Pre-injection with L-glutamic acid showed inhibition on the D-glutamic acid induced muscle contraction as shown in Figure 1, as previously reported (18).

We next examined the action of ethanol, which was used to dissolve clove oil and eugenol to the desired concentrations before dispersing in water for fish anesthesia. The ethanol did not show any effect on D-glutamic acid induced muscle contraction, as presented in Figure 2. Pretreatment of the muscle specimen with clove oil and eugenol showed inhibition of the muscle contraction induced by D-glutamic acid, similar to the pretreatment with L-glutamic acid. However, there was some difference in this inhibitory effect. Silkworm larvae injected with clove oil and eugenol followed by D-glutamic acid firstly showed a short spasmodic contraction for about 2 sec with a contraction value of 0.18 and then fully muscle relaxation was observed. In contrast, L-glutamic acid suddenly showed the inhibitory effect on D-glutamic acid induced muscle contraction, so that the entire muscle relaxation in silkworm larvae was observed. However, after 10 min, the inhibitory activity of L-glutamic acid was disappeared and some slight muscle contraction was observed. Figure 3 showed that the inhibitory activity of clove oil and eugenol on D-glutamic acid induced muscle contraction was dose

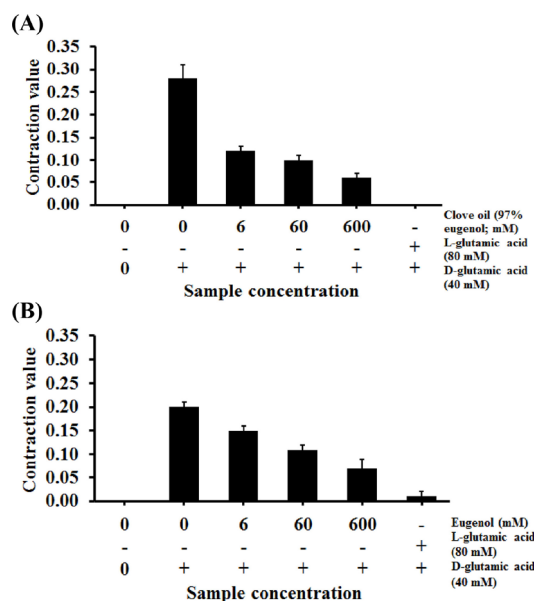


Figure 3. Contraction value of silkworm injected with clove oil (A) and eugenol (B) followed by D-glutamic acid ($n = 2$).

dependent. From these results, percent inhibition of 6-600 mM clove oil and eugenol could be calculated and it was found to be 57-79% and 25-65%, respectively. It is concluded that clove oil and eugenol possessed inhibitory effect on D-glutamic acid-induced muscle contraction.

3.2. Effect of eugenol on kainic acid-induced muscle contraction in silkworm

Kainic acid, a glutamate receptor agonist, can also induce muscle contraction of decapitated silkworm. Its activity is stronger than D-glutamic acid. A single injection of kainic acid in decapitated silkworm caused muscle contraction with a contraction value of 0.27 within 1 min. After 5-10 min of this contraction, slightly muscle relaxation was observed and fully relaxation was found in 30 min. Ethanol displayed no effect on the contraction by kainic acid. Prior injection of clove oil and eugenol into silkworm larvae inhibited muscle contraction induced by kainic acid in dose-dependent manner, similar to that induced by D-glutamic acid. However, the inhibitory action resulted from clove oil and eugenol on muscle contraction induced by kainic acid was lower than that induced by D-glutamic acid. This might be due to the stronger activity of kainic acid than D-glutamic acid. Silkworm larvae injected with clove oil and eugenol followed by kainic acid firstly showed a slight spasmodic contraction for about 5-10 sec with a contraction value of 0.15 and then fully muscle relaxation was gradually observed. The results in Figure 4 confirmed that clove oil and eugenol inhibited muscle contraction induced by kainic acid. The inhibition was found to be 37-70% and 24-59%, respectively, slightly lower than that induced by D-glutamic acid. From this experiment, it could

be concluded that clove oil and eugenol possessed the inhibitory effect on kainic acid-induced muscle contraction.

3.3. Fish anesthetic effect of L-glutamic acid

Clove oil and eugenol at 60 ppm induced goldfish anesthesia to stage 4 of anesthetic induction within 6 min, and the fish recovered within 10 min. L-glutamic acid at 20 and 40 mM also induced goldfish anesthesia but to stage 3 within 35 and 25 min, respectively, and the

fish could not recover but died. The goldfish received 20 and 40 mM L-glutamic acid significantly showed longer induction and shorter recovery times than those received clove oil and eugenol. Moreover, the fish which received L-glutamic acid at these concentrations were anesthetized to only stage 3, whereas those received clove oil and eugenol could be anesthetized to stage 4 of anesthesia. The recovery behavior was also different. The anesthetized fish which received L-glutamic acid could recover to only stage 2 and then died after that, whereas those received clove oil and eugenol could fully recover to stage 3. Furthermore, it was found that L-glutamic acid at a concentration of 4 mM could induce anesthetic effect in goldfish within 5 min but only to stage 1, after that the fish fully recovered, as exhibited in Figure 5. The obtained results indicated that L-glutamic acid has slight anesthetic effect on fish.

4. Discussion

This study demonstrates that clove oil and its main component, eugenol, can inhibit muscle contraction induced by D-glutamic acid and kainic acid in silkworm larvae, similar to the inhibitory effect of L-glutamic acid. Eugenol has been reported to inhibit the nociceptive response caused by glutamate, α -amino-3-hydroxy-5-methyl-4-isoxazolepropionic acid, and kainite in mice (21). In addition, eugenol showed the inhibitory effect against acetylcholine esterase, an enzyme for hydrolysis the acetylcholine, which can induce paralysis in rice weevil (*Sitophilus oryzae*) (22).

The chemical structure of eugenol and L-glutamic acid are completely different which the eugenol is a phenylpropene, whereas L-glutamic acid is an amino acid containing amine and carboxylic acid functional groups, as seen in Figure 6. This point leads to some different results between these two compounds that the silkworm muscles after L-glutamic acid injection presented the delayed muscle contraction after relaxation by inhibiting D-glutamic acid and kainic acid action. It is possible that silkworm bodies have enzyme to degrade glutamic acid, which preferably degrades L-glutamic acid to D-glutamic

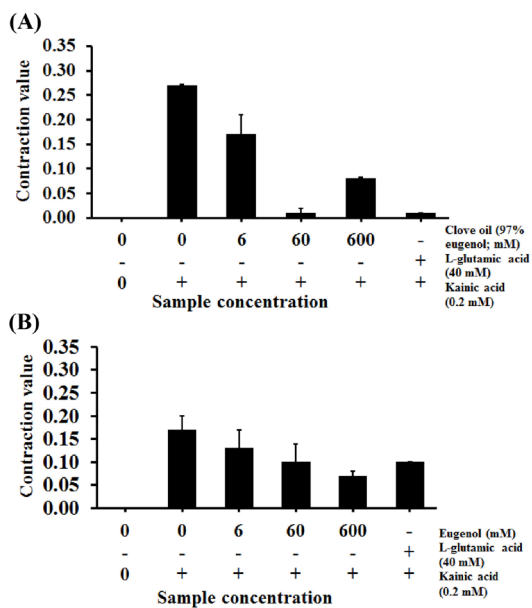


Figure 4. The effect of clove oil (A) and eugenol (B) on the kainic acid-induced silkworm muscle contraction ($n = 2$).

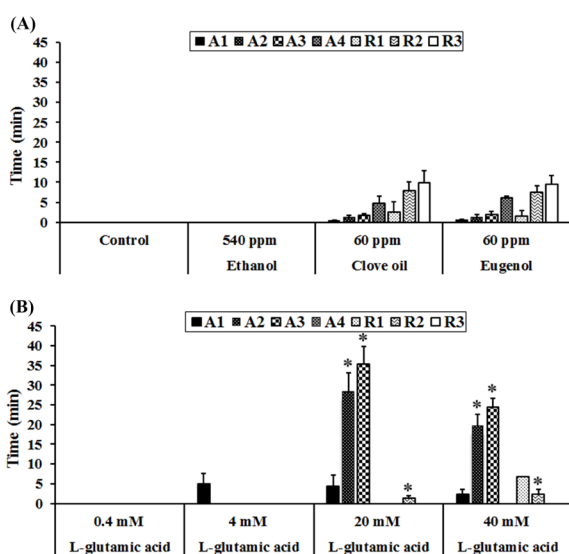


Figure 5. Anesthetic induction and recovery time of control, ethanol, clove oil and eugenol (A), L-glutamic acid (B) ($n = 3$). A1 to A4 represented the anesthetic induction stage 1 to stage 4, respectively and R1 to R3 represented the recovery at stage 1 to stage 3, respectively. $*p < 0.05$ compared to clove oil and eugenol groups.

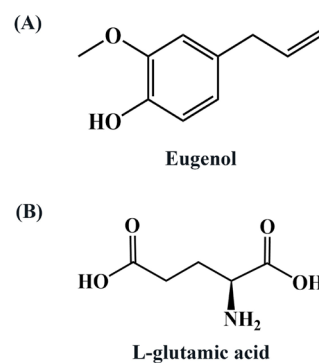


Figure 6. The chemical structure of eugenol (A) and L-glutamic acid (B).

acid. Therefore, L-glutamic acid is eliminated faster than D-glutamic acid. Then, the remained D-glutamic acid or kainic acid could show their action of muscle contraction again after L-glutamic acid elimination.

Most of insects have an open circulatory system. The body cavity is filled with hemolymph that bathes the internal organs (23). Our study demonstrates that injection of clove oil and eugenol into silkworm bodies can induce muscle relaxation, and has inhibitory effect on muscle contraction activity of kainic acid and D-glutamic acid which are agonists of glutamate receptor expressed on larval body wall muscles (18,24). The results indicate that clove oil and eugenol have some effects on silkworm glutamate receptor, supporting the effect of these compounds tested *in vitro* and *in vivo* in mice (21,25).

In contrast to silkworm, fish can receive the test samples which were dispersed in the water tank for fish *via* the expected organ like gill. The gill is an important organ for respiratory and circulating system for re-oxygenated of blood. After that the blood with active substances flows to the other organs including brain (26), and to the expected GABA subtype A receptors as predominate receptor responds for anesthetic mechanism in fish (27).

The present study firstly demonstrated that L-glutamic acid, a biological agonist excitatory neurotransmitter in the nervous system, had anesthetic effect in fish. It is possible that glutamate receptor also responded on this effect, contributed to mechanism of eugenol. In case of fish, 0.8-1 mM L-glutamic acid induced transient excitation followed by suppression on the isolated *Plotosus* electroreceptor, contrast with lower dose (0.2-0.3 mM) induced a sustained excitation (28). Meanwhile, D-glutamic acid induced fictive swimming in the isolated Lamprey spinal cords that closely matches the *in vivo* swimming pattern, analogous to isolated mammalian spinal cords (29).

However, the goldfish which received L-glutamic acid could not recover. It has been hypothesized that glutamic acid is advantaged substance in hyperammonemic conditions, ammonia was detoxified by glutamic acid and then generated glutamine in astrocyte. However, the excess of glutamine could exert osmotic effects and contribute to brain swelling (30). The prior study showed that glutamine can directly exert toxic effects on cultured astrocytes by increasing reactive oxygen species production and by inducing the mitochondrial permeability transition (31).

This is the first paper to use silkworm larvae for testing fish anesthetic agents and comparing the action of clove oil, eugenol, and L-glutamic acid in both animals. The further investigation is required to challenge with other fish anesthetic agents. It might be possible to use silkworm as model animals for screening new anesthetic agents for fish, since the use of silkworm is low cost, easy breeding, simple handle, and reproducible obtained results (32).

In conclusion, these results suggest that clove oil and eugenol have inhibitory effect on the D-glutamic acid and kainic acid-induced silkworm muscle contraction similar to L-glutamic acid effect. Moreover, L-glutamic acid induced dose dependent anesthetic effects in goldfish similar to clove oil and eugenol.

Acknowledgements

This work was supported by the Thailand Research Fund (TRF) through the Royal Golden Jubilee PhD Program (RGJ) Grant No 5.NS.CM/56/A.1. We also thank Research Center of Pharmaceutical Nanotechnology, Chiang Mai University, Thailand and Teikyo University, Japan for their support.

References

- Bunyaphatsara N. Clove oil. In: Thai Medicinal Plants (Bunyaphatsara N, Chokchaijarenporn O., eds.). Prachachon, Bangkok, Thailand, 1996; pp. 211-224.
- Woody CA, Nelson J, Ramstad K. Clove oil as an anaesthetic for adult sockeye salmon: Field trials. *J Fish Biol.* 2002; 60:340-347.
- Pirhonen J, Schreck CB. Effects of anaesthesia with MS-222, clove oil and CO₂ on feed intake and plasma cortisol in steelhead trout (*Oncorhynchus mykiss*). *Aquaculture.* 2003; 220:507-514.
- Prince A, Powell C. Clove oil as an anesthetic for invasive field procedures on adult rainbow trout. *N Am J Fish Manag.* 2000; 20:1029-1032.
- Sladky KK, Swanson CR, Stoskopf MK, Loomis MR, Lewbart GA. Comparative efficacy of tricaine methanesulfonate and clove oil for use as anesthetics in red pacu (*Piaractus brachyomus*). *Am J Vet Res.* 2001; 62:337-342.
- Hoseini SM, Ghelichpour M. Efficacy of clove solution on blood sampling and hematological study in beluga, *Huso Huso* (L.). *Fish Physiol Biochem.* 2012; 38:493-498.
- Ribeiro PAP, Miranda-Filho KC, de Melo DC, Luz RK. Efficiency of eugenol as anesthetic for the early life stages of Nile tilapia (*Oreochromis niloticus*). *An Acad Bras Ciênc.* 2015; 87:529-535.
- Tarkhani R, Imani A, Jamali H, Moghanlou, KS. Anaesthetic efficacy of eugenol on Flowerhorn (*Amphilophus labiatus* × *Amphilophus trimaculatus*). *Aquacult Res.* 2016; 47:1-9.
- Akbari S, Khoshnod MJ, Rajaian H, Afsharnasab M. The use of eugenol as an anesthetic in transportation of white Indian shrimp (*Fenneropenaeus indicus*) post larvae. *Turk J Fish Aquat Sci.* 2010; 10:423-429.
- Parodi TV, Cunha MA, Heldwein CG, de Souza DM, Martins AC, Garcia LO, Wasielesky WJ, Monserrat JM, Schmidt D, Caron BO, Heinzmann B, Baldisserotto B. The anesthetic efficacy of eugenol and the essential oils of *Lippia alba* and *Aloysia triphylla* in post-larvae and sub-adults of *Litopenaeus vannamei* (Crustacea, Penaeidae). *Comp Biochem Physiol C Toxicol Pharmacol.* 2012; 155:462-468.
- Goulet F, Vachon P, Hélie P. Evaluation of the toxicity

- of eugenol at anesthetic doses in African clawed frogs (*Xenopus laevis*). *Toxicol Pathol.* 2011; 39:471-477.
12. Sell A, Carlini E. Anesthetic action of methyleugenol and other eugenol derivatives. *Pharmacology.* 1976; 14:367-377.
 13. Guenette SA, Beaudry F, Marier JF, Vachon P. Pharmacokinetics and anesthetic activity of eugenol in male Sprague-Dawley rats. *J Vet Pharmacol Ther.* 2006; 29:265-270.
 14. Meyer RE, Fish RE. Pharmacology of injectable anesthetics, sedatives, and tranquilizers. In: *Anesthesia and Analgesia in Laboratory Animals* (Fish RE, Brown MJ, Danneman PJ, Karas AZ, eds.). Elsevier, Massachusetts, USA, 2008; pp. 59-60.
 15. Segalat L. Invertebrate animal models of diseases as screening tools in drug discovery. *ACS Chem Biol.* 2007; 2:231-236.
 16. Baines RA, Downer RG. Pharmacological characterization of a 5-hydroxytryptamine-sensitive receptor/adenylate cyclase complex in the mandibular closer muscles of the cricket, *Gryllus domestica*. *Arch Insect Biochem Physiol.* 1991; 16:153-163.
 17. Wu WH, Cooper RL. Serotonin and synaptic transmission at invertebrate neuromuscular junctions. *Exp Neurobiol.* 2012; 21:101-112.
 18. Sekimizu K, Larranaga J, Hamamoto H, Sekine M, Furuchi T, Katane M, Homma H, Matsuki N. D-glutamic acid-induced muscle contraction in the silkworm, *Bombyx mori*. *J Biochem.* 2005; 203:199-203.
 19. Iversen M, Finstad B, McKinley RS, Eliassen R. The efficacy of metomidate, clove oil, Aqui-S™ and Benzoak® as anaesthetics in Atlantic salmon (*Salmo salar* L.) smolts, and their potential stress-reducing capacity. *Aquaculture.* 2003; 221:549-566.
 20. Iwama GK, McGeer JC, Pawluk MP. The effects of five fish anaesthetics on acid-base balance, hematocrit, cortisol, and adrenaline in rainbow trout. *Can J Zool.* 1989; 67:2065-2073.
 21. Dal BW, Luiz AP, Martins DF, Mazzardo-Martins L, Santos ARS. Eugenol reduces acute pain in mice by modulating the glutamatergic and tumor necrosis factor alpha (TNF- α) pathways. *Fundam Clin Pharmacol.* 2013; 27:517-525.
 22. Lee S, Lee B, Choi W, Park B, Kim J, Campbell BC. Fumigant toxicity of volatile natural products from Korean spices and medicinal plants towards the rice weevil, *Sitophilus oryzae* (L.). *Pest Manag Sci.* 2001; 57:548-553.
 23. Miller TA, Pass G. Circulatory system. In: *Encyclopedia of Insects* (Resh VH, Cardé RT, eds.). Academic Press, Massachusetts, USA, 2009; pp. 169-173.
 24. Ishii K, Hamamoto H, Sasaki T, Ikegaya Y, Yamatsugu K, Kanai M, Shibasaki M, Sekimizu K. Pharmacologic action of oseltamivir on the nervous system. *Drug Discov Ther.* 2008; 2:24-34.
 25. Won MH, Lee JC, Kim YH, Song DK, Suh HW, Oh YS, Kim JH, Shin TK, Lee YJ, Wie MB. Postischemic hypothermia induced by eugenol protects hippocampal neurons from global ischemia in gerbils. *Neurosci Lett.* 1998; 254:101-104.
 26. Sneddon LU. Clinical anesthesia and analgesia in fish. *J Exot Pet Med.* 2012; 21:59-70.
 27. Heldwein CG, Silva LL, Gai EZ, Roman C, Parodi TV, Bürger ME, Baldisserotto B, Flores ÉM, Heinzmann BM. S-(+)-Linalool from *Lippia alba*: Sedative and anesthetic for silver catfish (*Rhamdia quelen*). *Vet Anaesth Analg.* 2014; 41:621-629.
 28. Okano K, Obara S. Effects of bath-applied L-glutamate and related chemicals on the afferent synapse of the *Plotosus* electroreceptor. *Brain Res.* 1988; 457:79-88.
 29. Jinks SL, Andrada J. Validation and insights of anesthetic action in an early vertebrate network: The isolated lamprey spinal cord. *Anesth Analg.* 2011; 113:1033-1042.
 30. Ip YK, Chew SF. Ammonia production, excretion, toxicity, and defense in fish: A review. *Front Physiol.* 2010; 1:1-20.
 31. Jayakumar AR, Rama Rao KV, Schousboe A, Norenberg MD. Glutamine-induced free radical production in cultured astrocytes. *Glia.* 2004; 46:296-301.
 32. Sekimizu N, Paudel A, Hamamoto H. Animal welfare and use of silkworm as a model animal. *Drug Discov Ther.* 2012; 6:226-229.

(Received February 18, 2017; Revised April 16, 2017; Accepted April 20, 2017)

Biological activities and antibacterial biomarker of *Sesbania grandiflora* bark extract

Pimporn Anantaworasakul¹, Hiroshi Hamamoto², Kazuhisa Sekimizu², Siriporn Okonogi^{1,*}

¹Department of Pharmaceutical Sciences, Faculty of Pharmacy, Chiang Mai University, Chiang Mai, Thailand;

²Teikyo University Institute of Medical Mycobiology, Tokyo, Japan.

Summary

In the present study, the fractionated extracts of *Sesbania grandiflora* bark were prepared and evaluated for their biological activities. The ethyl acetate fractionate (EAF) showed high antioxidant activity along with free radical scavenging and reducing mechanisms. The free radical scavenging antioxidant activity of EAF was $69.3 \pm 3.6\%$ where its Trolox equivalent antioxidant capacity was 13.6 ± 0.7 mM/mg. EAF exhibited the reducing power equivalent to ferrous sulfate at 152 ± 2 mM/mg and equivalent to gallic acid at 1.05 ± 0.01 mM/mg. In addition, EAF presented high potential on inhibition of bacterial growth with the minimum bactericidal concentration less than 1 mg/mL. Further isolation of EAF using normal-phase open column of silica gel 60, showed that the fractions eluted with the mixture of chloroform and methanol at the ratios of 4:1, 3:2, and 2:3 possessed antibacterial activity. The recovery activity of total different active fractions was 5% EAF, 20 times less than that of EAF. The chromatogram of EAF from a high-performance liquid chromatography was compared with caffeic acid, catechin, coumaric acid, ellagic acid, gallic acid, quercetin, syringin, naringic acid, trans-cinnamic acid, and vanilic acid. The result demonstrated that one major compound of EAF was gallic acid. These results suggest that the fractionated extracts of *S. grandiflora* bark contained antioxidant and antibacterial activities.

Keywords: *Sesbania grandiflora*, antioxidant activity, antibacterial activity, bark extract, HPLC fingerprint

1. Introduction

Sesbania grandiflora (L.) Pers., family Fabaceae, is commonly found in Thailand and many Asian countries. Its leaves and flowers have been reported to possess anticancer (1), antioxidant (2), anxiolytic (3), anticonvulsant (3) and antimicrobial activities (4,5). Its bark has been used as traditional medicine for treatment of inflammation (6), ulcers (7) and wound-healing (8). It is known that inflammation and oxidation are related mechanisms in the body. Excess endogenous oxidation causes an increase in the formation of the radical oxygen

species (ROS) and radical nitrogen species (RNS). The overproduction of ROS and RNS is responsible for damage at inflammatory sites (9). In addition, these reactive species play important roles in inflammation by being trigger elements or by being signaling messenger molecules which regulate the expression of key cytokines (10). Wounds are injuries that affect in an opening or breaking of the skin, and also disrupting the soft tissue. This symptom is hazard to be occurred inflammation and infection. Contraction and closure of the injury and restoration of functional status of the skin is necessary in treatment of wounds (11). Wound healing is interrelated with reactive oxygen species and bacterial infection (12). Therefore, antioxidants are necessary for prevention of tissue damage and encourage wound healing process. Furthermore, infection prevention is one of the most important to enhance wound healing (13). It was previously reported that the combination of plant extracts possessing antioxidant and antibacterial activities can efficiently enhance wound healing (14). Although S.

Released online in J-STAGE as advance publication April 30, 2017.

*Address correspondence to:

Dr. Siriporn Okonogi, Department of Pharmaceutical Sciences, Faculty of Pharmacy, Chiang Mai University, Chiang Mai, Thailand.

E-mail: okng2000@gmail.com

grandiflora has been applied for treatment in many diseases, the study deeply on which a potential extract of this plant having both antioxidant and antibacterial activities has not been reported. Our previous study reported the comparison of antibacterial activity among different parts such as leaf, branch, stem bark, and stem core of the plant. It was found that the bark of *S. grandiflora* possessed the strongest antibacterial activity against different pathogenic strains (15). Therefore, the bark of this plant was selected to use in the current study.

Using medicinal plants for treatment of many diseases is an interesting alternative way (16) as there are many phytochemical compounds which enable to relieve ailment (17). The pharmacological activities of several plants are from metabolite products existed in the plants (18). Most studies reveal that the phytochemical compounds having health promoting properties are phenolic compounds. Thus, these compounds have been widely used for treatment and management of disorders, also explored as model systems of plant research due to ubiquitous in plants of different areas (19). The phenolic compounds generally found in plant extracts are phenolic acids, flavonoids, and tannins (20,21). However, pre-clinical studies of estimating the phytochemical, toxic, and biological properties of the plant extracts are important before administrating in the clinical studies. It is very essential to know the biomarker of the extracts before establishing further efficacy scientific models in clinical trials. The identical analysis of phytochemical compounds as biomarkers of plant extracts can be primary done by comparing with standard compounds (22).

The purpose of the present study is to evaluate antioxidant and antibacterial activities of *S. grandiflora* bark extracts against pathogenic bacteria. Isolation of the most potential extract on antibacterial activity was done in order to search for the bioactive marker existing in the extract. Different standard phenolic compounds were subjected to high-performance liquid chromatography (HPLC) to obtain HPLC chromatograms for comparing with the tested extract.

2. Materials and Methods

2.1. Chemicals and reagents

Butylatedhydroxytoluene (BHT), vitamin-E (Vit-E), 6-hydroxy-2,5,7,8-tetramethylchroman-2-carboxylic acid (Trolox), 2,2-diphenyl-1-picrylhydrazil (DPPH), 2,4,6-tri(2-pyridil)-S-triazine (TPTZ), ferrous sulfate, ferric chloride, sodium chloride, sodium carbonate, dimethyl sulphoxide (DMSO), caffeic acid, catechin, coumaric acid, ellagic acid, gallic acid, quercetin, syringin, naringic acid, trans-cinnamic acid, vanilic acid, and methanol (HPLC grade) were from Sigma-Aldrich (St. Louis, MO). Muller-Hinton broth (MHB) and tryptic soy agar were from Becton Dickinson Labware

(Franklin Lakes, NJ). Vancomycin was from Shionogi & Co., Ltd. (Osaka, Japan). Gentamicin was from Sankyo Co., Ltd. (Tokyo, Japan). Organic solvents were from Merck (Darmstadt, Germany) and Wako Pure Chemical Industries (Osaka, Japan). Other chemicals were of analytical grade.

2.2. Plant material

The bark samples of *S. grandiflora* were collected from Chiang Mai province, a northern area of Thailand. The plant species was identified and the voucher specimen (No. 023207) was deposited at the Herbarium of the Faculty of Pharmacy, Chiang Mai University, Chiang Mai, Thailand.

2.3. Plant extract preparation

The bark samples of *S. grandiflora* were dried at 50°C for 48 h and ground into powder. The dried powder was sequentially macerated with organic solvents started from hexane followed by chloroform, and ethyl acetate, respectively. The maceration of each solvent was performed for 24 h × 3 cycles at room temperature. The filters from each solvent from the maceration was removed under vacuum by using rotary evaporator at 40°C. Dried fractionate extracts of hexane (HXF), chloroform (CFF), and ethyl acetate (EAF) were kept in the tight containers in the refrigerator for further studies.

2.4. Antioxidant study

2.4.1. Free radical scavenging assay

This free radical scavenging assay was done using DPPH as free radicals. The performance was according to a method previously developed (23) with some modification. Briefly, the extract was mixed with DPPH in ethanol solution. The mixture was left in dark cabinet at room temperature for 30 min. Then the absorbance of the mixture was measured spectrophotometrically at 520 nm using microplate reader. BHT and Vit-E were used as positive controls. The results were calculated and expressed as percentage of radical scavenging antioxidant activity (RSAA) and Trolox equivalent antioxidant capacity (TEAC) for 1 mg extract (24,25).

2.4.2. Reducing power assay

Reducing power of the extracts was investigated using a method to determine ferric reducing antioxidant power (FRAP) described previously (26) with some modification. Briefly, the FRAP reagent was firstly prepared by mixing 10 mM TPTZ solution with 20 mM ferric chloride and 300 mM sodium acetate buffer (pH 3.6) at a ratio of 1:1:10. The extract was added in the

FRAP reagent solution and mixed. The absorbance of the mixture was measured at 595 nm after standing 5 min by microplate reader. BHT and Vit-E were used as positive controls. The result was calculated and expressed as ferrous sulfate equivalent concentration (EC) and gallic acid equivalent concentration (GAE) for 1 mg extract (27).

2.5. Antibacterial activity study

The *in vitro* antibacterial activity of the extracts was investigated by broth micro-dilution assay in order to determine a minimum inhibitory concentration (MIC) and minimum bactericidal concentration (MBC). The extracts were dissolved in MHB containing 10% DMSO. The stock suspensions of the tested extracts were centrifuged at 14,000 rpm for 1 min for removing undissolved matters. The supernatant was collected and serially two-fold diluted with MHB. A 100-fold dilution of bacterial suspension of standard strain of *Staphylococcus aureus* ATCC 25923 at a concentration equivalent to McFarland turbidity standard No. 0.5 was added to each dilution of the extracts at the same volume. The mixtures were incubated at 37°C for 24 h. Negative controls were prepared without bacterial suspension, whereas positive controls were received bacterial suspension without the test samples. Acceptable, no bacterial growth in the negative control and complete growth, indicated by turbidity, in the positive control. Comparing with the negative and positive controls, the bacterial growth inhibition of the test samples was visually observed. The lowest concentration of the extracts which could inhibit the bacterial growth at this step was indicated as MIC. Furthermore, the tested broth which presented inhibitory action from MIC assay were taken for MBC determination by streaking on freshly prepared tryptic soy agar plates and further incubated at 37°C for 24 h. After incubating, the bacterial growth on surface of the agar plates was observed. The lowest concentration of the samples which showed no bacterial growth after this subculturing, indicating the bacteria were completely killed, was recorded as MBC. Vancomycin and gentamicin were used as control antimicrobial agents.

2.6. Isolation of the highest antibacterial extract

The fractionated extract which demonstrated the highest antibacterial activity was selected for further isolation using normal-phase column chromatography. The extract was dissolved in chloroform and subjected to an open column containing silica gel 60, then eluted with mixture of chloroform and methanol with polarity increasing by stepwise gradient of chloroform to methanol ratios of 5:0, 4:1, 3:2, 2:3, 1:4, and 0:5, respectively. Each fraction was collected from the column and removed the solvent using vacuum centrifugal evaporator. The obtained

fractions were dissolved in sterile MHB and investigated for antibacterial activity against *S. aureus* as mentioned in section 2.5.

2.7. HPLC analysis

HPLC fingerprint of the extract which demonstrated the strongest antibacterial activity and that of 10 standard phenolic compounds including caffeic acid, catechin, coumaric acid, ellagic acid, gallic acid, quercetin, syringin, naringic acid, trans-cinnamic acid, and vanilic acid was performed by HPLC using a Hypersil ODS column (4.6 i.d. × 250 mm) and gradient eluent of solvent A (1% acetic acid in water) and solvent B (methanol). The eluent gradient program started from 100% of solvent A for 1 min then turned to 70% and 40% at 10 and 20 min, respectively. After that, the eluent composition was put back to 100% of solvent A at 25 min and held on 5 min. The extract and the standard compounds were dissolved in methanol (HPLC grade) and filtered through a 0.22 µm filter membrane before injection. The HPLC condition was operated with a mobile flow rate of 1 mL/min, an injection volume of 10 µL, and running time of 30 min. The eluent was monitored with UV/VIS detector at a wavelength of 280 nm.

To confirm the major compound in the extract, the HPLC fingerprint of the extract and the standard which showed the same retention time to the extract was performed again with different eluting ratios of solvent A to solvent B; 90:10, 85:15, and 80:20, and detected at 280 nm. Isocratic conditions were performed with a flow rate of 1 mL/min, an injection volume of 10 µL, and running time of 15 min.

2.8. Statistical analysis

All experiments were performed in triplicate and the results are expressed as mean ± SD. The obtained data were analyzed statistically by SPSS statistic 17.0 software. The mean were determined for significance at $p < 0.05$ by ANOVA and Tukey's Multiple test.

3. Results

3.1. Yield and biological activities of the extracts

It was found that sequential extraction of dried *S. grandiflora* in powder by hexane, chloroform, and ethyl acetate gave different yield of extracts as shown in Table 1. The yield of CFF was the highest (1.45%) followed by that of EAF and HXF, respectively.

The antioxidant activity of *S. grandiflora* in bark extracts comparison with BHT and Vit-E as the positive controls are presented in Figure 1. Among these three different fractionated extracts; HXF, CFF, and EAF, it was obviously seen that EAF possessed the highest free

Table 1. The percentage yield and antibacterial activities expressed as MIC and MBC values of different fractionated extracts of *S. grandiflora* bark against *S. aureus* by broth dilution method

Extracts	Yield (% w/w)	MIC (mg/mL)	MBC (mg/mL)
HXF	0.23	10.00	> 10.00
CFF	1.45	2.50	2.50
EAF	0.27	0.63	0.63

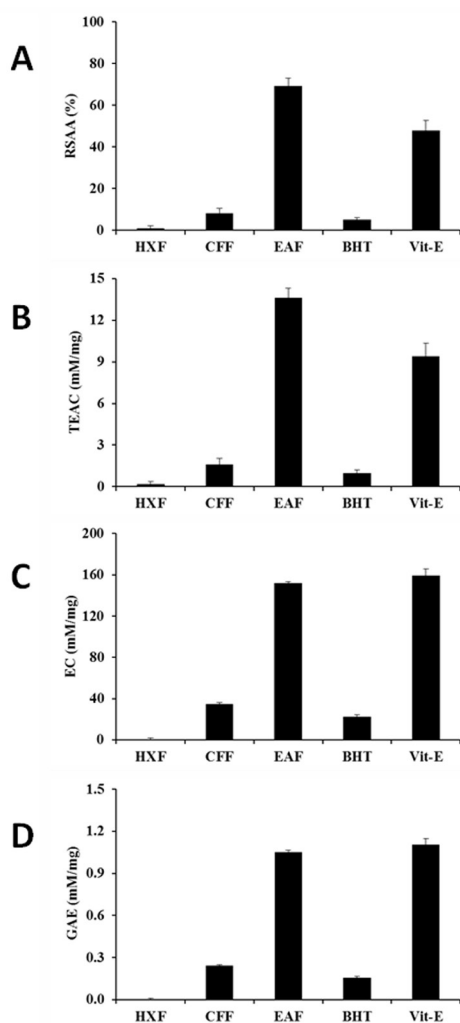


Figure 1. Antioxidant activities expressed as RSAA (A), TEAC (B), EC (C), and GAE (D) of HXF, CFF, and EAF in comparison with BHT and Vit-E.

radical scavenging property with the RSAA value of 69.3 ± 3.6 % and TEAC value of 13.6 ± 0.7 mM/mg. The TEAC values of BHT and Vit-E were found to be 0.9 ± 0.2 mM/mg and 9.4 ± 0.9 mM/mg, respectively. Therefore, the antioxidant activity of EAF was approximately 14 and 1.4 times higher than that of BHT and Vit-E, respectively. EAF also showed the highest reducing power with the EC and GAE values of 152 ± 2 mM/mg and 1.05 ± 0.01 mM/mg, respectively, which was about 6.7 times higher than that of BHT, but was 0.9 times less than that of Vit-E.

The antibacterial activity of the extracts investigated

Table 2. The percentage yield and antibacterial activities expressed as MIC and MBC values of EAF and different fractions of EAF against *S. aureus* by broth dilution method

Sample	Yield (% w/w)	MIC (mg/mL)	MBC (mg/mL)
EAF	100	0.50	0.50
Isolated fraction			
F1	0.05	> 0.02	> 0.02
F2	14.55	8.00	16.00
F3	2.30	1.00	2.00
F4	1.65	2.00	2.00
F5	0.10	> 0.04	> 0.04
F6	0.05	> 0.02	> 0.02

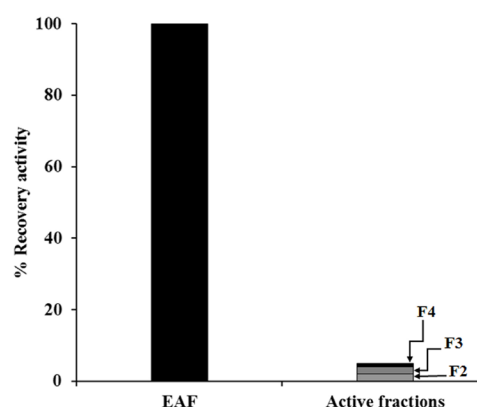


Figure 2. Recovery antibacterial activity of EAF and different active fractions; fraction 2 (F2), fraction 3 (F3), and fraction 4 (F4), from the preparative column chromatography.

by micro-dilution method demonstrated that EAF was the strongest inhibitory activity against *S. aureus* with the MIC and MBC values less than 1 mg/mL. The control antimicrobial agents shows equal values of their respective MIC and MBC. The MIC and MBC values of vancomycin was 0.5 μ g/mL whereas that of gentamicin was 1 μ g/mL.

3.2. Isolation of the highest antibacterial extract

As EAF presented the highest antioxidant and antibacterial activities, this extract was selected for isolation using silica gel 60 column chromatography. The percentage yield, MIC, and MBC values of each fraction from the isolation and EAF were compared in Table 2. Fraction 2 as eluted with chloroform:methanol at a ratio of 4:1 showed the highest yield of 14.6% (w/w) but less antibacterial activity whereas fraction 3 which obtained by elution with chloroform:methanol at a ratio of 3:2 gave the highest antibacterial activity with MIC and MBC values of 1.00 and 2.00 mg/mL, respectively. Considering the antibacterial activity in term of recovery activity as shown in Figure 2, the results indicated that the recovery activity of the sum of total different

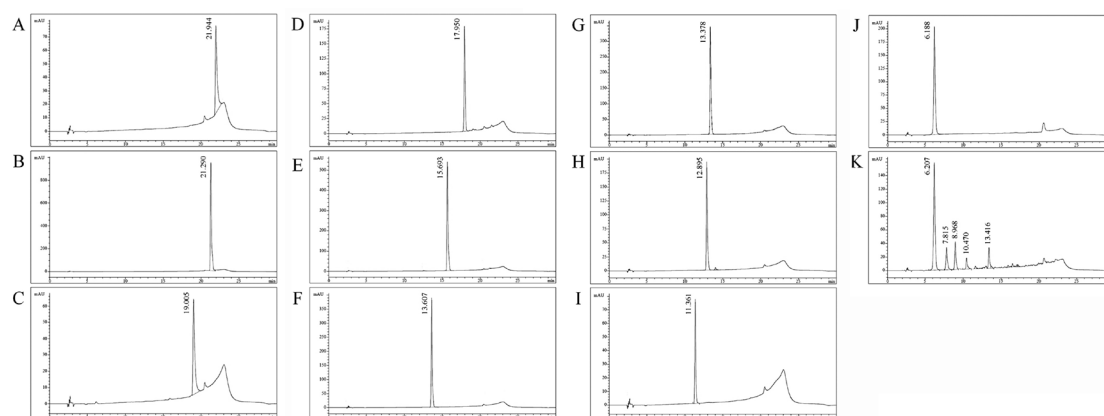


Figure 3. HPLC chromatograms of an individual standard quercetin (A), trans-cinnamic acid (B), ellagic acid (C), naringic acid (D), coumaric acid (E), syringin (F), caffeic acid (G), vanilic acid (H), catechin (I), gallic acid (J) and EAF (K) at 280 nm.

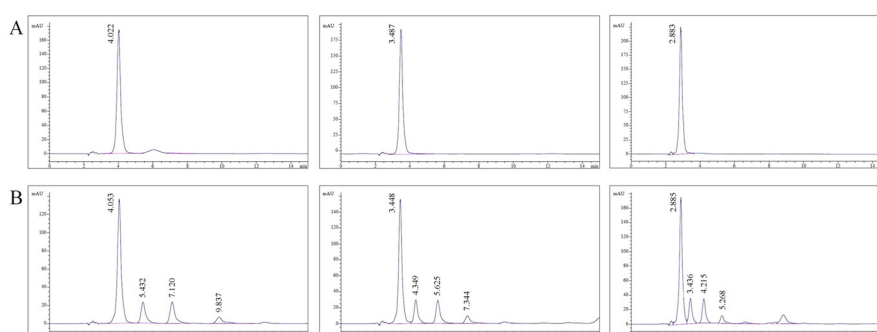


Figure 4. HPLC chromatograms of standard gallic acid (A) and EAF (B) using an eluting mixture containing 1% acetic acid in water and methanol at ratios of 90:10 (left), 85:15 (middle), and 80:20 (right) at 280 nm.

fractions was only 5% of EAF which was 20 times less than that of its original EAF (not isolated).

3.3. HPLC analysis

HPLC fingerprint of EAF was performed and compared with that of 10 standard phenolic compounds in order to identify the compounds existed in EAF. For this study, the concentrations of each standard compound and the extract were 100 $\mu\text{g/mL}$ and 1 mg/mL , respectively. It was found that the HPLC chromatograms of 10 standard compounds could be obtained using gradient eluents of 1% acetic acid in water and methanol for 30 min run time and detected at 280 nm when each of these compounds was observed individually. The chromatograms of all standard phenolic compounds in comparison with EAF were shown in Figure 3. The retention time of standard quercetin, trans-cinnamic acid, ellagic acid, naringic acid, coumaric acid, syringin, caffeic acid, vanilic acid, catechin, and gallic acid were 21.944, 21.290, 19.005, 17.950, 15.693, 13.607, 13.378, 12.895, 11.361, and 6.188 min, respectively. The HPLC fingerprint of EAF which obtained by elution with the same gradient condition of those standard compounds gave five distinct peaks at the retention times of 6.207, 7.815, 8.968, 10.470, and 13.416 min. It is noted that a

major peak of EAF exhibited at a retention time of 6.207 min. This peak resembled to the peak of standard gallic acid which eluted at a retention time of 6.188 min at the same detection wavelength.

To clarify the major compound existed in EAF whether it is gallic acid, the extract was subjected in various HPLC conditions and compared with HPLC chromatograms of the standard gallic acid. The HPLC chromatograms of EAF from various eluting ratios of 1% acetic acid in water and methanol detected at 280 nm exhibited a major peak which conformed to the peak of gallic acid in the same eluting conditions. As shown in Figure 4, the peak of gallic acid eluted by the ratios of 90:10, 85:15, and 80:20 presented at 4.022, 3.487, and 2.883 min, respectively, whereas the major peaks of EAF at the respective ratios were demonstrated at 4.053, 3.448, and 2.885 min, respectively.

4. Discussion

Bioactive agents from plants is currently interesting for alternative medicine (16). The research of effective natural compounds from medicinal plants which are potentiality, safety, and widely utilization has become considerable issue all over the world (28,29). The current study explores the antioxidant and antibacterial activities

of the most potential extract of *S. grandiflora*. The antibacterial activity of this plant is interesting because the plant has been used traditionally in the treatment of skin disorders and wound (30). In addition, the plant has been reported to have some other activities which related to antioxidant activity (1,3,31). Therefore, both antioxidant and antibacterial activities of *S. grandiflora* were investigated. In the antioxidant investigation, the extracts was evaluated by two methods. One is the determination of free radical scavenging activity using DPPH as free radicals and the other is determination of reducing power using FRAP methods. These two different assays are the most potential methods to determine antioxidant capacity of the plant extracts as both of them show high reproducibility and provide better understand the mechanism of action of a tested antioxidant (26). Vit-E is natural antioxidant and it is synthesized only by plant (32). Its mechanism of action has been reported to be free radical scavenging reaction (33,34). In the meanwhile, Vit-E *in vivo* has been reported to have high efficient in transferring a hydrogen atom to a lipid free radical like peroxy, alkoxy, and carbon-centered radicals (35,36). Therefore, Vit-E possesses both mechanisms of antioxidant action; free radical scavenging and reducing properties whereas the synthetic antioxidant BHT has been reported to predominate in reducing mechanism (37). Both Vit-E and BHT were used as positive controls in the current study. Among the three fractions of *S. grandiflora* bark extracts, EAF showed extremely high free radical scavenging action which significantly higher than Vit-E, therefore, the antioxidant activity of this extract was considered to be majorly due to the free radical scavenging mechanism. However, comparing to BHT which is the reducing antioxidant, EAF showed extremely higher EC value than BHT but slightly lower than Vit-E. Therefore, it was considered that reducing action is the minor mechanism of antioxidant action of the extract.

Many researchers report the use of phytochemicals from plant sources as an interesting choice to treat infectious diseases (38,39). EAF was therefore investigated for antibacterial activity. The antibacterial assay used in this study was a broth micro-dilution assay. This assay is appropriate for *in vitro* antibacterial activity investigation of plant extracts because it is higher repetition than agar diffusion assay (40). The results showed a great interest that among the tested extracts from *S. grandiflora* bark, EAF possessed the highest inhibitory activity against the tested pathogenic bacteria. Therefore, EAF was further isolated by preparative column chromatography. The results notified that the activity of each fraction was not strong inhibitory action. The recovery activity of the sum of total different fractions was only 5% of EAF while that of EAF as original extract (not isolated) was 100%. This low recovery might be due to an inactivation or simple loss of materials during the purification process. Moreover,

synergistic effect was also one of the possibilities. Many previous studies have shown that the combination of phytochemical compounds in natural products revealed synergistic effect (41,42). The synergistic effect indicate that associating of several compounds in the plant could give the stronger activity than the individual active compound for that activity (43-45). The antibacterial potency of EAF that significantly higher than the sum of total different fractions might be explained by the synergistic effect of many compounds existing in the extract.

The results of HPLC fingerprints informed that EAF consisted several elements. One of all constituents in the extract presented the major peak as a main compound which corresponded to a standard phenolic compound of gallic acid. Gallic acid was reported to have an inhibitory action against human pathogenic bacteria, such as *S. aureus* and *Corynebacterium accolans*, human pathogenic yeast such as *Candida albicans* (46), and also other pathogenic microorganisms (47,48). From these activities of gallic acid and in accordance with the HPLC consequences, it is considered that the major compound as a bioactive marker of EAF is gallic acid.

In conclusion, EAF of *S. grandiflora* bark possessed the highest biological actions of antioxidant and antibacterial activities. HPLC study confirmed that there are many compounds existed in EAF. Synergistic effect on antibacterial activity of EAF might be occurred from the combination of several compounds existed in EAF. The major bioactive compound in *S. grandiflora* bark possessing an antibacterial activity is gallic acid.

Acknowledgements

The authors are grateful the Royal Golden Jubilee PhD Program (RGJ) for financial support (Grant No. PHD/0043/2552). We also thank the Graduate School of Pharmaceutical Sciences, the University of Tokyo, Japan and Research Center of Pharmaceutical Nanotechnology, Chiang Mai University, Thailand for their support.

References

1. Sreelatha S, Padma PR, Umasankari E. Evaluation of anticancer activity of ethanol extract of *Sesbania grandiflora* (Agati Sesban) against Ehrlich ascites carcinoma in Swiss albino mice. *J Ethnopharmacol.* 2011; 134:984-987.
2. Gowri SS, Vansanta K. Free radical scavenging and antioxidant activity of leaves from agathi (*Sesbania grandiflora*) (L.) Pers. *Am Euras J Sci Res.* 2010; 5:114-119.
3. Kasture VS, Deshmukh VK, Chopde CT. Anxiolytic and anticonvulsive activity of *Sesbania grandiflora* leaves in experimental animals. *Phytother Res.* 2002; 16:455-460.
4. Krasaekoopt W, Kongkarchanatip A. Antimicrobial properties of Thai traditional flower vegetable extracts. *AU J Technol.* 2005; 9:71-74.

5. Ouattara MB, Konate K, Kiendrebeogo M, Ouattara N, Compaore M, Meda R, Millogo-Rasolodimby J, Nacoulma OG. Antibacterial potential and antioxidant activity of polyphenols of *Sesbania grandiflora*. *Curr Res J Biol Sci*. 2011; 3:351-356.
6. Patil RB, Nanjwade BK, Manv FV. Evaluation of anti inflammatory and anti arthritic effect of *Sesbania grandiflora* bark and fruit of *Terminalia chebula* in rats. *Int J Pharm Bio Sci*. 2011; 5:37-46.
7. Serti JA, Wieze G, Woisky RG, Carvalho JC. Antiulcer activity of the ethanol extract of *Sesbania grandiflora*. *Braz J Pharm Sci*. 2001; 37:107-111.
8. Karthikeyan P, Suresh V, Suresh A, Aldrin bright J, Senthilvelan S, Arunachalam G. Wound healing activity of *Sesbania grandiflora* (L) Poir. bark. *Int J Pharm Res Dev*. 2011; 3:87-93.
9. Coyle CH, Philips BJ, Morrisroe SN, Chancellor MB, Yoshimura N. Antioxidant effects of green tea and its polyphenols on bladder cells. *Life Sci*. 2008; 80:12-18.
10. Miguel MG. Antioxidant and anti-inflammatory activities of essential oils. *Molecules*. 2010; 15:9252-9287.
11. Umachigi SP, Kumar GS, Jayaveera K, Kishore KD, Ashok KC, Dhanapal R. Antimicrobial, wound healing and antioxidant activities of *Anthocephalus cadamba*. *Afr J Tradit Complement Altern Med*. 2007; 4:481-487.
12. Jitvaropas R, Saenthaweek S, Somparn N, Thuppia A, Sireeratawong S, Phoolcharoen W. Antioxidant, antimicrobial and wound healing activities of *Boesenbergia rotunda*. *Nat Prod Commun*. 2012; 7:909-912.
13. Barku VYA, Opoku-Boahen Y, Owusu-Ansah E, Dayie NTKD, Mensah FE. *In vitro* assessment of antioxidant and antimicrobial activities of methanol extracts of six wound healing medicinal plants. *J Nat Sci Res*. 2013; 3:74-80.
14. Narendhirakannan RT, Nirmala JG, Caroline A, Lincy S, Saj M, Durai D. Evaluation of antibacterial, antioxidant and wound healing properties of seven traditional medicinal plants from India in experimental animals. *Asian Pac J Trop Biomed*. 2012; 2:S1245-S1253.
15. Anantaworasakul P, Klayraung S, Okonogi S. Antibacterial activities of *Sesbania grandiflora* extracts. *Drug Discov Ther*. 2011; 5:12-17.
16. Chahad AM, Michalet S, Bechir AB, Tidjani A, Nkongmeneck BA, Dijoux-Franca M G. Medicinal plants from the Ouaddai province (Chad): An ethnobotanical survey of plants used in traditional medicine. *J Altern Complement Med*. 2015; 21:569-577.
17. Huang WY, Cai YZ, Zhang Y. Natural phenolic compounds from medicinal herbs and dietary plants: Potential use for cancer prevention. *Nutr Cancer*. 2009; 62:1-20.
18. Harborne JB. *Phytochemical Methods, A Guide to Modern Techniques of Plant Analysis*. Chapman & Hall, London, UK, 1973; pp. 33-41.
19. Boudet AM. Evolution and current status of research in phenolic compounds. *Phytochemistry*. 2007; 68:2722-2735.
20. Naik GH, Priyadarsini KI, Hari M. Free radical scavenging reactions and phytochemical analysis of Triphala, an ayurvedic formulation. *Curr Sci*. 2006; 90:1100-1105.
21. Sati SC, Sati N, Rawat U, Sati OP. Medicinal plants as a source of antioxidants. *Res J Phytochem*. 2010; 4:213-224.
22. Mradu G, Saumyakanti S, Sohini M, Arup M. HPLC profiles of standard phenolic compounds present in medicinal plants. *Int J Pharmacogn Phytochem Res*. 2012; 4:162-167.
23. Okonogi S, Tachakittirungrod S, Chowwanapoonpohn S, Anuchpreeda S, Duangrat C. Comparison of antioxidant capacity and cytotoxicity of certain fruit peels. *Food Chem*. 2007; 103:839-846.
24. Aliyu AB, Ibrahim MA, Ibrahim H, Musa AM, Lawal AY, Oshanimi JA, Usman M, Abdulkadir IE, Oyewale AO, Amupitan JO. Free radical scavenging and total antioxidant capacity of methanol extract of *Ethuliaconyzoides* growing in Nigeria. *Rom Biotechnol Lett*. 2012; 17:7458-7465.
25. Kenny O, Smyth TJ, Walsh D, Kelleher CT, Hewage CM, Brunton NP. Investigating the potential of under-utilised plants from the Asteraceae family as a source of natural antimicrobial and antioxidant extracts. *Food Chem*. 2014; 161:79-86.
26. Tachakittirungrod S, Okonogi S, Chowwanapoonpohn S. Study on antioxidant activity of certain plants in Thailand: Mechanism of antioxidant action of guava leaf extract. *Food Chem*. 2007; 103:381-388.
27. Siler B, Zivkovic S, Banjanac T, Cvetkovic J, Nestorovic ZJ, Ciric A, Sokovic M, Mistic D. Centauries as underestimated food additive: Antioxidant and antimicrobial potential. *Food Chem*. 2014; 147:367-376.
28. Dzoyem JP, Hamamoto H, Ngameni B, Ngadjui BT, Sekimizu K. Antimicrobial action mechanism of flavonoids from *Dorstenia* species. *Drug Discov Ther*. 2013; 7:66-72.
29. Rubens DM, Constantin OO, Moevi AA, Nathalie GK, Daouda T, David NJ, Mireille D, Joseph DA. Anti *Staphylococcus aureus* activity of the aqueous extract and hexanic fraction of *Thonningia sanguinea* (Cote ivoire). *Int J Pharmacogn Phytochem Res*. 2015; 7:301-306.
30. Venkateshwarlu G, Shantha TR, Shiddamallayya N, Kishore KR. Traditional and ayurvedic medicinal importance of agastya leaves (*Sesbania grandiflora* (L) Pers.) W.R.T. its pharmacognostic and physicochemical evaluation. *Int J Res Ayurveda Pharm*. 2012; 3:193-197.
31. Shyamalagowri S, Vasanth K. Free radical scavenging and antioxidant activity of leaves from agathi (*Sesbania grandiflora*) (L.) Pers. *Am Euras J Sci Res*. 2010; 5:114-119.
32. Fryer MJ. The antioxidant effects of thylakoid vitamin E (alpha-tocopherol). *Plant Cell Environ*. 1992; 15:381-392.
33. Van Acker SABE, Koymans LMH, Bast A. Molecular pharmacology of vitamin E: Structure aspects of antioxidant activity. *Free Radical Biol Med*. 1993; 15:311-328.
34. Yamauchi R. Vitamin E: Mechanism of its antioxidant activity. *Food Sci Technol Int Tokyo*. 1997; 3:301-309.
35. Liebler DC, Burr JA. Oxidation of vitamin E during iron-catalyzed lipid peroxidation: Evidence for electron-transfer reactions of the tocopheroxyl radical. *Biochemistry*. 1992; 31:8278-8284.
36. Ham AJL, Liebler DC. Vitamin E oxidation in rat liver mitochondria. *Biochemistry*. 1995; 34:5754-5761.
37. Nantitanon W, Yotsawimonwat S, Okonogi S. Factors influencing antioxidant activities and total phenolic content of guava leaf extract. *LWT-Food Sci Technol*. 2010; 43:1095-1103.
38. Clark AM. Natural products as a resource for new drug. *Pharm Res*. 1996; 13:1133-1144.
39. Cowan MM. Plant product as antimicrobial agents. *Clin Microbiol Rev*. 1999; 12:564-582.
40. Wilkinson JM. Methods for testing the antimicrobial

- activity of extracts. In: Modern phytomedicine: Turning medicinal plants into drugs (Ahmad I, Aquil F, Owais M., eds.). Wiley-VCH Verlag GmbH and Co. KGaA Weinheim, Germany, 2006; pp. 157-171.
41. China R, Mukherjee S, Sen S, Bose S, Datta S, Koley H, Ghosh S, Dhar P. Antimicrobial activity of *Sesbania grandiflora* flower polyphenol extracts on some pathogenic bacteria and growth stimulatory effect on the probiotic organism *Lactobacillus acidophilus*. Microbiol Res. 2012; 167:500-506.
 42. Kumar AS, Venkateshwaran K, Vanitha J, Saravanan VS, Ganesh M, Vasudevan M, Sivakumar T. Synergism between methanolic extract of *Sesbania grandiflora* (Fabaceae) flowers and oxytetracycline. Pharmacologyonline. 2008; 3:6-11.
 43. Vipin K, Arun GK, Rajesh G. Antimicrobial activity of *Sesbania grandiflora* (L.) Pers. Int Res J Pharm. 2011; 2:85-87.
 44. Zuo GY, Li Y, Wang T, Han J, Wang GC, Zhang YL, Pan WD. Synergistic antibacterial and antibiotic effects of bisbenzylisoquinoline alkaloids on clinical isolates of Methicillin-Resistant *Staphylococcus aureus* (MRSA). Molecules. 2011; 16:9819-9826.
 45. Naksuriya O, Okonogi S. Comparison and combination effects on antioxidant power of curcumin with gallic acid, ascorbic acid, and xanthone. Drug Discov Ther. 2015; 9:136-141.
 46. Fogliani B, Raharivelomanana P, Bianchini JP, Madjebi SB, Hnawia R. Bioactive ellagitannins from *Cunonia macrophylla*, an endemic Cunoniaceae from New Caledonia. Phytochemistry. 2005; 66:241-247.
 47. Moshe R. The antimicrobial activity of phenolic antioxidants in foods: A review. J Food Safety. 1984; 6:141-170.
 48. Clark AM, El-Ferally FS, Li WS. Antimicrobial activity of phenolic constituents of *Magnolia grandiflora* L. J Pharm Sci. 1981; 70:951-952.
- (Received February 23, 2017; Revised April 18, 2017; Accepted April 20, 2017)

Genomic analysis of vancomycin-resistant *Staphylococcus aureus* VRS3b and its comparison with other VRSA isolates

Suresh Panthee¹, Hiroshi Hamamoto¹, Atmika Paudel¹, Kazuhisa Sekimizu^{1,2,*}

¹Teikyo University Institute of Medical Mycology, Tokyo, Japan;

²Genome Pharmaceutical Institute Co., Ltd., Tokyo, Japan.

Summary

High-level vancomycin resistance among *Staphylococcus aureus* poses a grave threat to global health as the treatment options for this pathogen are very limited. A detailed evaluation of the genetic background of vancomycin-resistant *S. aureus* (VRSA) is expected to facilitate the understanding of its origin and pathogenicity. In this study, we performed the genetic analysis of the clinical VRSA isolates and identified the genetic basis of resistance to multiple antibiotics among these strains, based on the available draft genome sequences. In addition, we generated the draft genome of the strain VRS3b, which was considered to be same as VRS3a based on its isolation from the same patient. We found that strain VRS3b did not harbor the genes responsible for tetracycline and gentamicin, which was further confirmed by the sensitivity towards these antibiotics. Our results suggest that the strains VRS3a and VRS3b are different from the view of antibiotic resistance and highlight the possibility of generation of two distinct VRSA strains from the same patient.

Keywords: *Staphylococcus aureus*, resistance, vancomycin, methicillin, genomics

1. Introduction

Staphylococcus aureus, a gram-positive bacterium, can reside in the human body both as a commensal or as an opportunistic pathogen and accounts for the majority of the deaths and hospitalization globally. Staphylococcal infections caused by methicillin-sensitive *S. aureus* can easily be cured with penicillins or cephalosporins (1). Resistance to methicillin (defined as minimum inhibitory concentration (MIC) of oxacillin ≥ 4 $\mu\text{g}/\text{mL}$) (2), mediated mainly by the *mecA* gene, was observed shortly after the introduction of methicillin (3). Since then, methicillin-resistant *S. aureus* (MRSA) developed itself as a leading cause of death and major clinical threat with more than 60% *S. aureus* isolates becoming resistant to methicillin (4). Vancomycin, a glycopeptide antibiotic produced by *Amycolatopsis orientalis*, has been the mainstay of treatment against

infections caused by methicillin-resistant *S. aureus* (1). In 1996, *S. aureus* with reduced susceptibility to vancomycin (MIC 8 $\mu\text{g}/\text{mL}$), referred as vancomycin-intermediate *S. aureus* (VISA), was isolated in Japan (5). The first case of vancomycin-resistant *S. aureus* (VRSA) was first isolated in 2002 in the USA and following it, at least 14 cases of VRSA have been identified in the United States, and the first case in Europe was reported in 2013 (6). *vanA* type vancomycin resistance is the most prevalent vancomycin resistance and has been associated with the synthesis of an alternative, vancomycin-resistant pentatdepsipeptide peptidoglycan precursor (7). Genomic analysis of the strains resistant to vancomycin is critical to understand the genetic background and identify the difference between the strains, thus facilitating the development of novel anti-VRSA drugs.

S. aureus VRS3b was co-isolated with *S. aureus* VRS3a from nephrostomy tube exit site of a 64-year old female in New York, USA. As these two strains were isolated from the same patient, they were considered to be identical, and the characterization has been performed mainly for VRS3a. However, the vancomycin-resistant phenotype of VRS3b is more stable than VRS3a (8). Recently, the genome of

Released online in J-STAGE as advance publication April 30, 2017.

*Address correspondence to:

Dr. Kazuhisa Sekimizu, Teikyo University Institute of Medical Mycology, 359 Otsuka, Hachioji, Tokyo, 192-0395, Japan.

E-mail: sekimizu@main.teikyo-u.ac.jp

multiple VRSA strains has been sequenced (9) and the study excluded the strain VRS3b considering it to be same as the strain VRS3a. In this study, we sequenced and analyzed the draft genome of VRS3b strain to reveal the genetic basis of drug resistance and its difference with the strain VRS3a.

2. Materials and Methods

2.1. Draft genome sequences of VRSAs

Strain VRS3a and VRS3b were obtained from BEI Resources and grown at 37°C aerobically in tryptic soy broth containing 6 µg/mL vancomycin. Genomic DNA was isolated using Qiagen DNA-blood Mini Kit (Qiagen, Hilden, Germany) (10,11). One hundred ng of the DNA was subjected to fragmentation using Ion Xpress Plus Fragment Library Kit (Thermo Fisher Scientific, Waltham, MA, USA) to prepare 400 bp reads according to manufacturer's recommended protocol. The libraries were then enriched in an Ion Chef (Thermo Fisher Scientific) and subsequent sequencing was performed in Ion PGM System (Thermo Fisher Scientific). The reads were first assembled in the Ion Torrent Server (Thermo Fisher Scientific) and then analyzed in the CLC Genomics Workbench ver 9.5.3. (CLC bio, Aarhus, Denmark). The draft sequences were downloaded from NCBI using following GenBank accession numbers AHBK000000000 – VRS1; AHBL000000000 – VRS2; AHBM000000000 – VRS3a; NBPC000000000 – VRS3b; AHBN000000000 – VRS4; AHBO000000000 – VRS5; AHBP000000000 – VRS6; AHBQ000000000 – VRS7; AHBR000000000 – VRS8;

AHBS000000000 – VRS9; AHBT000000000 – VRS10; AHBU000000000 – VRS11a; AHBV000000000 – VRS11b; and JICL000000000 – BR-VRSA.

2.2. Genomic analysis of VRSAs

2.2.1. Sequencing typing

The draft genomes (9,11) were analyzed in the CLC Genomics Workbench. For multi locus sequence typing (MLST), the sequence of seven housekeeping genes: *arcC* (carbamate kinase); *aroE* (shikimate dehydrogenase); *glpF* (glycerol kinase); *gmk* (guanylate kinase); *pta* (phosphate acetyltransferase); *tpi* (triosephosphate isomerase); and *ycjI* (acetyl coenzyme A acetyltransferase) was collected and trimmed to extract the seven loci by using the standard sequence of a typical *S. aureus*. The trimmed sequences were then concatenated and submitted to clustalW for the generation of phylogenetic tree and to the MLST server (<http://saureus.beta.mlst.net/#>) for sequence typing. The trimmed sequence used for MLST can be found in the supplementary information (Supplementary Data, <http://www.ddtjournal.com/action/getSupplementalData.php?ID=10>).

2.2.2. Analysis of resistance genes

The recent database to find resistance was downloaded from the server (12). The database consisted of 2,156 genes known to be involved in the resistance against multiple antibiotics. The presence of resistance gene on the draft genome was scanned with a minimum identity

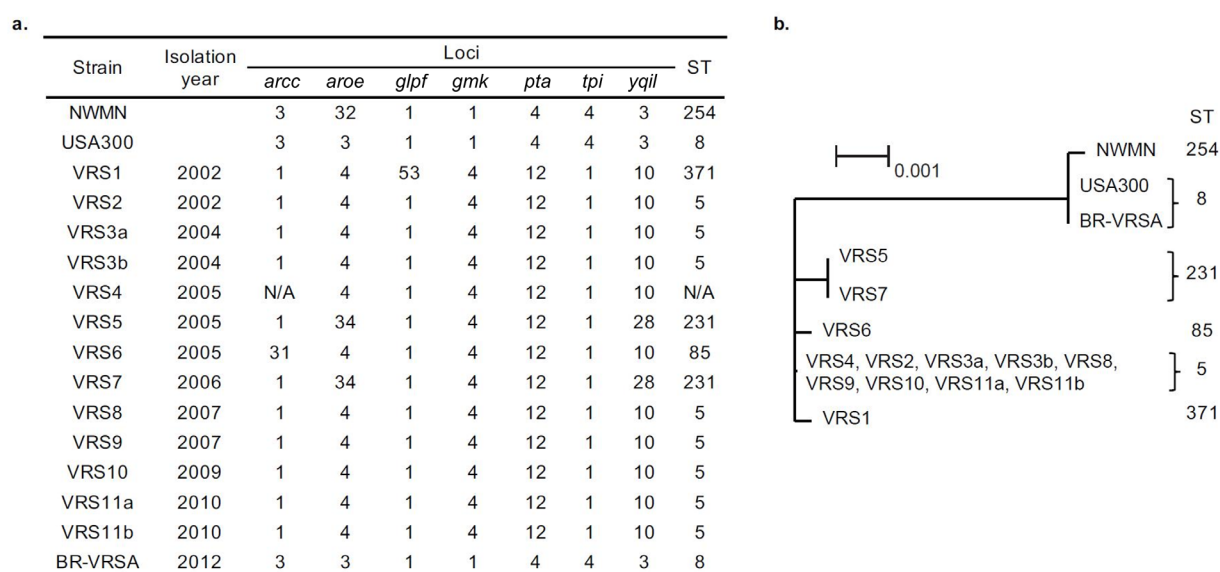


Figure 1. Multi locus sequence typing (a), and phylogenetic tree (b) of vancomycin-resistant *Staphylococci*. N/A: not analyzed. The *arcC* locus of strain VRS4 could not be analyzed as the size of the allele was different from standard allele size of 465. The distance scale of 0.001 in the phylogenetic tree indicates 0.1% differences between the groups. The nine strains from ST5 group had a highly similar concatenated sequence used for the tree construction.

Table 1. Genes involved in antibiotic resistance present in clinical isolates of VRSA

Staphylococcus aureus strain														
MRSA	VRSA													
	VRS1	VRS2	VRS3a	VRS3b	VRS4	VRS5	VRS6	VRS7	VRS8	VRS9	VRS10	VRS11a	VRS11b	BR-VRSA
<i>mecA</i>	<i>mecA</i>	<i>mecA</i>	<i>mecA</i>	<i>mecA</i>	<i>mecA</i>	<i>mecA</i>	<i>mecA</i>	<i>mecA</i>	<i>mecA</i>	<i>mecA</i>	<i>mecA</i>	<i>mecA</i>	<i>mecA</i>	<i>mecA</i>
<i>vanZ</i>	<i>vanZ</i>	<i>vanZ</i>	<i>vanZ</i>	<i>vanZ</i>	<i>vanZ</i>	<i>vanZ</i>	<i>vanZ</i>	<i>vanZ</i>	<i>vanZ</i>	<i>vanZ</i>	<i>vanZ</i>	<i>vanZ</i>	<i>vanZ</i>	<i>vanZ</i>
<i>vanX</i>	<i>vanX</i>	<i>vanX</i>	<i>vanX</i>	<i>vanX</i>	<i>vanX</i>	<i>vanX</i>	<i>vanX</i>	<i>vanX</i>	<i>vanX</i>	<i>vanX</i>	<i>vanX</i>	<i>vanX</i>	<i>vanX</i>	<i>vanX</i>
<i>vanR</i>	<i>vanR</i>	<i>vanR</i>	<i>vanR</i>	<i>vanR</i>	<i>vanR</i>	<i>vanR</i>	<i>vanR</i>	<i>vanR</i>	<i>vanR</i>	<i>vanR</i>	<i>vanR</i>	<i>vanR</i>	<i>vanR</i>	<i>vanR</i>
<i>vanY</i>	<i>vanY</i>	<i>vanY</i>	<i>vanY</i>	<i>vanY</i>	<i>vanY</i>	<i>vanY</i>	<i>vanY</i>	<i>vanY</i>	<i>vanY</i>	<i>vanY</i>	<i>vanY</i>	<i>vanY</i>	<i>vanY</i>	<i>vanY</i>
<i>vanH</i>	<i>vanH</i>	<i>vanH</i>	<i>vanH</i>	<i>vanH</i>	<i>vanH</i>	<i>vanH</i>	<i>vanH</i>	<i>vanH</i>	<i>vanH</i>	<i>vanH</i>	<i>vanH</i>	<i>vanH</i>	<i>vanH</i>	<i>vanH</i>
<i>vanA</i>	<i>vanA</i>	<i>vanA</i>	<i>vanA</i>	<i>vanA</i>	<i>vanA</i>	<i>vanA</i>	<i>vanA</i>	<i>vanA</i>	<i>vanA</i>	<i>vanA</i>	<i>vanA</i>	<i>vanA</i>	<i>vanA</i>	<i>vanA</i>
<i>vanS</i>	<i>vanS</i>	<i>vanS</i>	<i>vanS</i>	<i>vanS</i>	<i>vanS</i>	<i>vanS</i>	<i>vanS</i>	<i>vanS</i>	<i>vanS</i>	<i>vanS</i>	<i>vanS</i>	<i>vanS</i>	<i>vanS</i>	<i>vanS</i>
<i>vanR</i>	<i>vanR</i>	<i>vanR</i>	<i>vanR</i>	<i>vanR</i>	<i>vanR</i>	<i>vanR</i>	<i>vanR</i>	<i>vanR</i>	<i>vanR</i>	<i>vanR</i>	<i>vanR</i>	<i>vanR</i>	<i>vanR</i>	<i>vanR</i>
<i>aadD</i>	<i>aadD</i>	<i>aadD</i>	<i>aadD</i>	<i>aadD</i>	<i>aadD</i>	<i>aadD</i>	<i>aadD</i>	<i>aadD</i>	<i>aadD</i>	<i>aadD</i>	<i>aadD</i>	<i>aadD</i>	<i>aadD</i>	<i>aadD</i>
<i>spc</i>	<i>spc</i>	<i>spc</i>	<i>spc</i>	<i>spc</i>	<i>spc</i>	<i>spc</i>	<i>spc</i>	<i>spc</i>	<i>spc</i>	<i>spc</i>	<i>spc</i>	<i>spc</i>	<i>spc</i>	<i>spc</i>
<i>aac(6')-aph(2'')</i>	<i>aac(6')-aph(2'')</i>	<i>aac(6')-aph(2'')</i>	<i>aac(6')-aph(2'')</i>	<i>aac(6')-aph(2'')</i>	<i>aac(6')-aph(2'')</i>	<i>aac(6')-aph(2'')</i>	<i>aac(6')-aph(2'')</i>	<i>aac(6')-aph(2'')</i>	<i>aac(6')-aph(2'')</i>	<i>aac(6')-aph(2'')</i>	<i>aac(6')-aph(2'')</i>	<i>aac(6')-aph(2'')</i>	<i>aac(6')-aph(2'')</i>	<i>aac(6')-aph(2'')</i>
	<i>ant(6)-Ia</i>													
	<i>aph(3')-III</i>													
<i>blaZ</i>	<i>blaZ</i>	<i>blaZ</i>	<i>blaZ</i>	<i>blaZ</i>	<i>blaZ</i>	<i>blaZ</i>	<i>blaZ</i>	<i>blaZ</i>	<i>blaZ</i>	<i>blaZ</i>	<i>blaZ</i>	<i>blaZ</i>	<i>blaZ</i>	<i>blaZ</i>
<i>erm(A)</i>	<i>erm(A)</i>	<i>erm(A)</i>	<i>erm(A)</i>	<i>erm(A)</i>	<i>erm(A)</i>	<i>erm(A)</i>	<i>erm(A)</i>	<i>erm(A)</i>	<i>erm(A)</i>	<i>erm(A)</i>	<i>erm(A)</i>	<i>erm(A)</i>	<i>erm(A)</i>	<i>erm(A)</i>
	<i>erm(B)</i>													
	<i>erm(C)</i>													
	<i>mph(C)</i>													
	<i>mst(A)</i>													
	<i>tet(K)</i>													
	<i>tet(U)</i>													
	<i>tet(S)</i>													
	<i>dfcG</i>													

Genes conferring resistance: methicillin – *mecA*; vancomycin – *van* genes; aminoglycosides – *aadD*, *spc*, *aac(6')-aph(2'')*, *ant(6)-Ia*, *aph(3')-III*; beta lactams – *blaZ*; erythromycin – *erm* genes, *mst(A)*; streptogramin B – *mst(A)*; macrolide – *mph(C)*; tetracycline – *tet* genes; trimethoprim – *dfcG*. *: part of the gene was detected in VRSA3b.

Table 2. Minimum inhibitory concentrations of various antibiotics against VRS3a and VRS3b

Strain	MIC ($\mu\text{g/mL}$)			
	Vancomycin	Tetracycline	Kanamycin	Gentamicin
VRS3a	> 128	16	128	128
VRS3b	> 128	< 0.125	128	0.5
MSSA1	1	< 0.125	4	0.5

Table 3. List of the genes present in VRS3b that did not map in the VRS3a reads

Contig	ORF ID	Putative function
22	B6A35_13980	Arsenical efflux pump membrane protein ArsB
	B6A35_13985	ArsC
	B6A35_13990	Lactococcin 972 family bacteriocin
	B6A35_13995	Bacteriocin associated protein
23	B6A35_14125	Hypothetical protein
38	B6A35_14765	Arsenic transporter
	B6A35_14770	ArsC
	B6A35_14775	Lactococcin 972 family bacteriocin
	B6A35_14780	Bacteriocin associated protein
43	B6A35_14855	Hypothetical protein
	B6A35_14860	Hypothetical protein
	B6A35_14865	Hypothetical protein
44	B6A35_14870	Hypothetical protein

of 98% and minimum length of 60% in the CLC Genomics Workbench.

2.3. Determination of minimum inhibitory concentration

The MIC was determined by broth microdilution assay (13-15). Briefly, *Staphylococci* were grown with aeration in 50-mL falcon tube containing 5 mL Tryptic Soy Broth (TSB; Becton Dickinson and Company, Franklin Lakes NJ, USA) in a shaker maintained at 37°C. The medium was supplemented with 6 $\mu\text{g/mL}$ vancomycin as required. The overnight culture was diluted with cation-adjusted Muller-Hinton Broth (MHB; Becton Dickinson and Company) to have approximately 5×10^4 colony forming units (CFU) per 100 μL in each well in a round bottom 96-well plate. Serial dilutions of antibiotics were added to each well to obtain a final concentration of 128 $\mu\text{g/mL}$ to 0.0125 $\mu\text{g/mL}$. The plates were further incubated at 37°C for 20 h and MIC was determined as the lowest concentration that did not allow visible growth of cell.

3. Results

3.1. The phylogeny of VRSA

We found that the 14 VRSA were categorized among five sequence types (STs): ST5, ST8, ST85, ST231,

and ST371. ST5 was the most predominant group with eight VRSA falling within this group (Figure 1a). The strain VRS4 could not be typed as the *arcC* locus in this strain had a deletion of a nucleotide and the trimmed length was different from the standard length. Previous reports have characterized the strain VRS4 as ST5 (9). Further, we constructed a phylogenetic tree based on the sequences used for sequence typing and found that VRS4 clustered with other VRSA of ST5 group. The strain BR-VRSA was categorized to be ST8, same as the methicillin-resistant, vancomycin-sensitive strain USA300 strain and based on the phylogenetic tree, it also claded with the USA300 rather than other VRSA (Figure 1b).

3.2. Presence of antibiotic resistance genes in VRSA

When checked for the presence of antibiotic resistance genes, we found that all the strains of VRSA harbored *mecA* gene, involved in resistance to methicillin. Further, multiple genes involved in the resistance against clinically used antibiotics such as vancomycin, aminoglycosides, streptogramins and macrolides were identified in the draft genome (Table 1). This finding, in fact, indicated the complexity of VRSA treatment in the clinic. Interestingly, the drug resistance genes were not the same among these strains. This difference might reflect the clinical setting where most of the

patients from whom these VRSA were isolated had a history of several underlying conditions and were exposed to multiple antibiotics during isolation. Among the VRSA, VRS3a and VRS3b were considered to be same as these two strains were isolated from the same patient source. Our analysis indicated that antibiotic resistance genes were not the same among these two strains.

3.3. Comparative analysis of strains VRS3a and VRS3b

We found that VRS3b did not harbor the putative genes that conferred resistance to tetracycline and aminoglycosides such as kanamycin and gentamicin. To confirm this, we determined the MIC of these two strains and found that VRS3a was resistant to these antibiotics whereas VRS3b was sensitive to tetracycline and gentamicin but resistant to kanamycin (Table 2). Resistance to kanamycin but not to gentamicin in *S. aureus* might be ascribed to *aph(3')-III* gene (16). Given that the sequence we generated was a draft genome, we performed a blast search for this gene in all contigs generated from the VRS3b sequence. We found a part of *aph(3')-III* at the terminal position of a contig less than 1,000 bp suggesting that this might be responsible for resistance to kanamycin but not gentamicin in VRS3b. These results further suggested that these two strains were different. To confirm this notion, we mapped the reads obtained from *de novo* sequencing of VRS3a against the VRS3b contigs. We found that some of the genes present in VRS3b were missing from the VRS3a reads (Table 3).

3.4. Comparative analysis of *Tn1546*

Transposon *Tn1546*, obtained from vancomycin-resistant *Enterococcus* (17), has been shown to be one of the responsible elements of vancomycin resistance in VRSA (7). The analysis of the genome indicated that all the VRSA but VRS3a, VRS3b, and BR-VRSA harbored complete sets of genes from *Tn1546*. To further confirm this result, we independently mapped the reads from strains VRS3a and VRS3b and found that these strains did not harbor transposase and part of resolvase from *Tn1546* (Figure 2).

4. Discussion

The clinical isolates of MRSA with decreased susceptibility to vancomycin (VISA) and high-level vancomycin resistance (VRSA) pose a serious threat to public health. Comparative genomic analysis of the clinical isolates of VRSA will facilitate our understanding of how these strains acquired the antibiotic resistance gene. Successful growth of these isolates in mixed culture and their ability to overcome the continuous antibiotic selection pressure in the

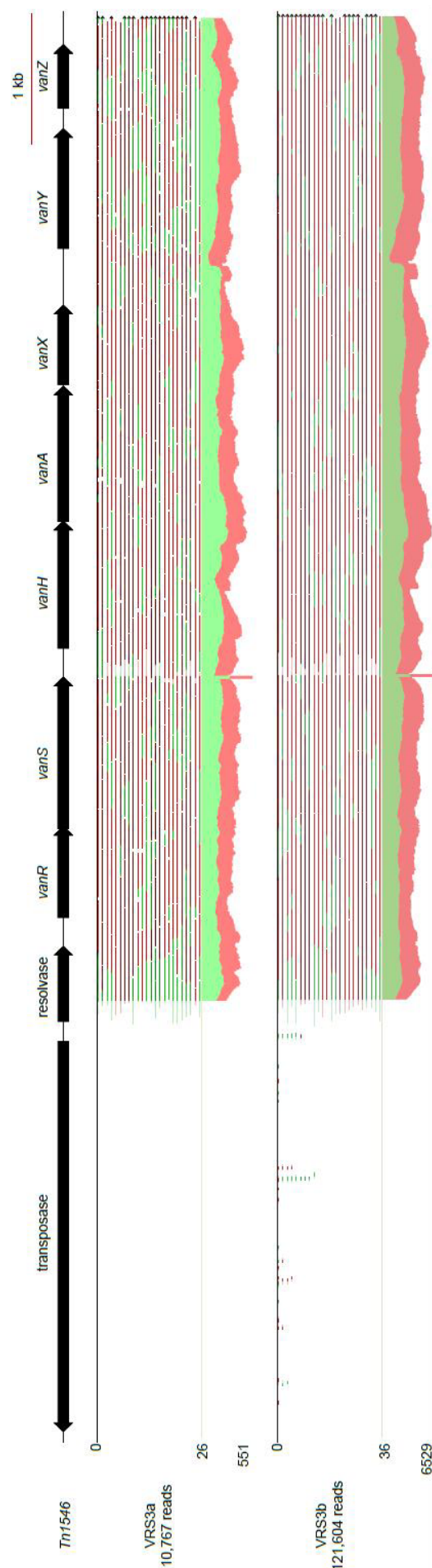


Figure 2. Mapping of VRS3a and VRS3b reads against transposon *Tn1546* reference sequence.

hospital further highlights the importance of this issue. Here, we showed that the genes conferring resistance to methicillin, vancomycin and erythromycin were common in all the VRSA and the genes conferring resistance to other antibiotics such as beta lactams, macrolide and tetracycline were distributed. Besides, we found that the strain VRS3b was typically different from VRS3a. Furthermore, we demonstrated that some of the genes present in VRS3b were missing in VRS3a. Although we could not precisely predict whether these two strains independently acquired vancomycin-resistance trait or diverged after the acquisition of the vancomycin resistance, our results suggested that these two strains acquired vancomycin-resistance in a similar manner. Our findings highlighted the possibility of generation of two different VRSA strains from the same source.

Acknowledgements

This work was supported by Grant-in-Aid for scientific research (S) (JP15H05783) and Drug Discovery Support Promotion Project from Japan Agency for Medical Research and Development, AMED to KS; and in part by Takeda Science Foundation to HH. *Staphylococcus aureus*, Strain VRS3a and VRS3b were provided by the Network on Antimicrobial Resistance in *Staphylococcus aureus* (NARSA) for distribution by BEI Resources, NIAID, NIH.

References

1. Rayner C, Munchhof WJ. Antibiotics currently used in the treatment of infections caused by *Staphylococcus aureus*. Intern Med J. 2005; 35:S3-S16.
2. Clinical and Laboratory Standards Institute. M100-S16 Performance standards for antimicrobial disk susceptibility testing; Sixteenth international supplement. Wayne, PA, 2006.
3. Jack Benner E, Kayser FH. Growing clinical significance of methicillin-resistant *Staphylococcus aureus*. The Lancet. 1968; 292:741-744.
4. National Nosocomial Infections Surveillance System. National Nosocomial Infections Surveillance (NNIS) System Report, data summary from January 1992 through June 2004, issued October 2004. Am J Infect Control. 2004; 32:470-485.
5. Hiramatsu K. Vancomycin-resistant *Staphylococcus aureus*: A new model of antibiotic resistance. Lancet Infect Dis. 2001; 1:147-155.
6. Melo-Cristino J, Resina C, Manuel V, Lito L, Ramirez M. First case of infection with vancomycin-resistant *Staphylococcus aureus* in Europe. The Lancet. 2013; 382:205.
7. Werner G, Strommenger B, Witte W. Acquired vancomycin resistance in clinically relevant pathogens. Future Microbiol. 2008; 3:547-562.
8. Weigel LM, Donlan RM, Shin DH, Jensen B, Clark NC, McDougal LK, Zhu W, Musser KA, Thompson J, Kohlerschmidt D, Dumas N, Limberger RJ, Patel JB. High-level vancomycin-resistant *Staphylococcus aureus* isolates associated with a polymicrobial biofilm. Antimicrob Agents Chemother. 2007; 51:231-238.
9. Kos VN, Desjardins CA, Griggs A, et al. Comparative genomics of vancomycin-resistant *Staphylococcus aureus* strains and their positions within the clade most commonly associated with methicillin-resistant *S. aureus* hospital-acquired infection in the United States. mBio. 2012; 3:e00112-12.
10. Panthee S, Hamamoto H, Suzuki Y, Sekimizu K. In silico identification of lysocin biosynthetic gene cluster from *Lysobacter* sp. RH2180-5. J Antibiot. 2017; 70:204-207.
11. Panthee S, Paudel A, Hamamoto H, Sekimizu K. Draft genome sequence of vancomycin-resistant clinical isolate *Staphylococcus aureus* VRS3b. Genome Announc. 2017; DOI: 10.1128/genomeA.00452-17
12. Jia B, Raphenya AR, Alcock B, et al. CARD 2017: Expansion and model-centric curation of the comprehensive antibiotic resistance database. Nucl Acids Res. 2017; 45:D566-D573.
13. Clinical and Laboratory Standards Institute. Methods for dilution antimicrobial susceptibility tests for bacteria that grow aerobically; approved standard – ninth edition (CLSI document M07–A9). Clinical and Laboratory Standards Institute, Wayne, PA, 2012.
14. Paudel A, Hamamoto H, Panthee S, Kaneko K, Matsunaga S, Kanai M, Suzuki Y, Sekimizu K. A novel spiro-heterocyclic compound identified by the silkworm infection model inhibits transcription in *Staphylococcus aureus*. Front Microbiol. 2017; 8:712.
15. Paudel A, Kaneko K, Watanabe A, Shigeki M, Motomu K, Hamamoto H, Sekimizu K. Structure-activity relationship study of novel iminothiadiazolo-pyrimidinone antimicrobial agents. J Antibiot. 2013; 66:663-667.
16. Freitas FIS, Guedes-Stehling E, Siqueira-Junior JP. Resistance to gentamicin and related aminoglycosides in *Staphylococcus aureus* isolated in Brazil. Lett Appl Microbiol. 1999; 29:197-201.
17. Arthur M, Molinas C, Depardieu F, Courvalin P. Characterization of Tn1546, a Tn3-related transposon conferring glycopeptide resistance by synthesis of depsipeptide peptidoglycan precursors in *Enterococcus faecium* BM4147. J Bacteriol. 1993; 175:117-127.

(Received April 14, 2017; Revised April 20, 2017; Accepted April 23, 2017)

Investigation of antiaromatase activity using hepatic microsomes of Nile tilapia (*Oreochromis niloticus*)

Tanongsak Sassa-deepaeng¹, Wasana Chaisri², Surachai Pikulkaew^{2,*}, Siriporn Okonogi^{3,*}

¹Nanoscience and Nanotechnology Program, the Graduate School, Chiang Mai University, Chiang Mai, Thailand;

²Department of Food Animal Clinic, Faculty of Veterinary Medicine, Chiang Mai University, Chiang Mai, Thailand;

³Department of Pharmaceutical Sciences, Faculty of Pharmacy, Chiang Mai University, Chiang Mai, Thailand.

Summary Microsomal aromatase enzymes of humans and rats have been used in antiaromatase assays, but enzyme activity is species-specific. The current study extracted hepatic microsomes of Nile tilapia (*Oreochromis niloticus*) to investigate and compare the antiaromatase activity of chrysin, quercetin, and quercitrin. This activity was evaluated using a dibenzylfluorescein (DBF) assay. Results revealed that the age and body weight of Nile tilapia affected the yield of extracted microsomes. Extraction of hepatic microsomes of Nile tilapia was most effective when using a reaction medium with a pH of 8.0. A DBF assay using Nile tilapia microsomes revealed significant differences in levels of antiaromatase activity for chrysin, quercetin, and quercitrin. Chrysin was the most potent aromatase inhibitor, with an IC₅₀ of 0.25 mg/mL. In addition, chrysin is an aromatase inhibitor that also inhibits the proliferation of cancer cells. Hepatic microsomes of Nile tilapia can be used to investigate and compare the antiaromatase activity of different compounds.

Keywords: Aromatase inhibitor, Nile tilapia, microsome, chrysin, pH effect

1. Introduction

Aromatase, a cytochrome P-450 enzyme consisting of a polypeptide chain of 503 amino acids, is key to estrogen biosynthesis (1,2). Aromatase is an essential component of the process of conversion of C-19 androgens to C-18 estrogens. Excessive aromatase activity can cause excessive synthesis of estrogen in breast tissue and lead to the development of breast cancer and increase the ability of immature breast tissue cells to strongly bind to carcinogens, decreasing their DNA repair capacity (3). Several recent studies have reported that a high concentration of estrogen promotes breast cancer (4-6). Therefore, inhibition of aromatase activity is a potential

approach to the treatment of breast cancer (7,8).

Aromatase is involved in sex differentiation and ovarian development in many species of animals (9,10) since the enzyme plays a key role in estrogen biosynthesis. Estrogen influences ovarian differentiation in non-mammalian vertebrates, including amphibians (11), reptiles (12), birds (13), and fish (14). In aquaculture, aromatase is involved in sex control. Sex control in fish is important because one sex may grow faster than the other (15). Efforts to control unwanted breeding have focused on male fish rather than female fish because of their faster growth rate and more distinctive coloration. Therefore, research on mechanisms of fish reproduction has sought to develop agents with potent anti-aromatase activity, i.e. aromatase inhibitors, in order to decrease estrogen synthesis and masculinize fish to complete the sex shift to males (16).

Many aromatase inhibitors used in the treatment of breast cancer (17) and in the process of producing only male fish in aquaculture (18) have different levels of potency. Antiaromatase activity can be evaluated in order to search for potent aromatase inhibitors using a dibenzylfluorescein assay; microsomal aromatase enzymes are usually extracted from human placenta (19,20), the rat liver (21), or the rat ovaries (22).

Released online in J-STAGE as advance publication March 19, 2017.

*Address correspondence to:

Dr. Siriporn Okonogi, Department of Pharmaceutical Sciences, Faculty of Pharmacy, Chiang Mai University, Chiang Mai, Thailand.

E-mail: okng2000@gmail.com

Dr. Surachai Pikulkaew, Department of Food Animal Clinic, Faculty of Veterinary Medicine, Chiang Mai University, Chiang Mai, Thailand.

E-mail: surapikulkaew@gmail.com

However, the applications of those enzymes are limited by animal species because the microsomes of each species are specific to certain animals. Nile tilapia (*Oreochromis niloticus*) is an economic teleost fish cultured in Thailand, and Nile tilapia has garnered attention worldwide as a food source. Male fish of this species have received greater attention than female fish because of their faster growth rate and larger size at the same age. Aromatase from Nile tilapia microsomes is therefore an essential component of a search for potent aromatase inhibitors. To the extent known, no study has used Nile tilapia microsomes for this purpose. The current study extracted microsomal aromatase from the liver of Nile tilapia and it tested compounds for their anti-aromatase activity. The effects of body weight and age of Nile tilapia on microsome yield and the effect of pH on the aromatase activity of the microsomes obtained were investigated. Three active compounds, chrysin, quercetin, and quercitrin, were previously reported to have antiaromatase activity (23,24). However, the antiaromatase activity of these compounds has yet to be compared. The current study is the first to examine the antiaromatase potency these compounds and to investigate their inhibition of the proliferation of breast cancer cells.

2. Materials and Methods

2.1. Materials

Chrysin, quercetin, quercitrin, dibenzylfluorescein, and thiazolyl blue tetrazolium blue (MTT) were purchased from Sigma-Aldrich (St. Louis, MO, USA). Potassium chloride (KCl) and methanol were obtained from Merck (Darmstadt, Germany). Acetic acid was obtained from RCI Labscan (Bangkok, Thailand). 4-(2-Hydroxyethyl)-1-piperazineethanesulfonic acid (HEPES) was purchased from AMRESCO (Solon, OH, USA). Nicotinamide adenine dinucleotide phosphate (NADPH) was obtained from Tocris (Ellisville, MO, USA). Antibiotic-antimycotic Dulbecco's modified Eagle's medium (DMEM) and fetal bovine serum (FBS) were obtained from Gibco BRL Life Technologies (Grand Island, NY, USA). Dimethyl sulfoxide (DMSO) was obtained from Amresco (Salon, OH, USA). All solvents were of analytical grade. Ninety-six-well plates were obtained from Costar (Cambridge, MA, USA). Ultra-clear centrifuge tubes were purchased from Beckman Coulter Inc. (Brea, CA, USA).

2.2. Microsome preparation

This study was approved by the Animal Experimentation Committee, Faculty of Veterinary Medicine, Chiang Mai University, Thailand. Hepatic microsomes from Nile tilapia were prepared as previously described (25) with some modifications. Briefly, female fish were

anesthetized by hypothermic shock in an ice bucket and then killed by decapitation. The liver was quickly removed and placed in 1.15% KCl solution. The liver was then chopped into small pieces and flash frozen in liquid nitrogen. The three volumes (w/v) of chilled 1.15% KCl solution was added to a homogenizer for 30 min. Homogenized liver samples were pooled and centrifuged at 10,000× g, 4°C for 30 min. The lipid layer was removed and the supernatant was subjected to ultracentrifugation at 105,000× g, 4°C for 1 h. The liquid solution containing microsomes was lyophilized for further experiments.

2.3. Scanning electron microscopy (SEM)

SEM was performed to observe the morphology of fish microsomes after lyophilization. Samples were placed in a standard sample holder and examined under a scanning electron microscope (Phenom Pure Desktop SEM, Phenom-World BV, Eindhoven, Netherlands).

2.4. Protein determination

Total protein content of the obtained microsomes was determined using NanoDrop™ 2000 (Thermo Scientific, USA). The instrument was first calibrated using distilled water and then 2 µL of a 2-fold serial dilution of the sample was placed on the pedestal. The proteins contain aromatic side chains that influence light absorption at 280 nm. The protein concentration was automatically calculated with the NanoDrop™ 2000 software.

2.5. Effect of pH on the aromatase activity of fish microsomes

The aromatase activity of hepatic Nile tilapia microsomes was quantified by measuring the fluorescent intensity of fluorescein, a dibenzylfluorescein product, in black 96-well microplates as described previously (26) with some modifications. Briefly, Nile tilapia microsomes were resuspended in water and adjusted with HEPES at a pH of 7.2, 7.4, 7.6, 7.8, or 8.0 to obtain a microsomal protein concentration of 350 µg/mL. Precisely 100 µL of the mixture was added to a 96-well plate (Corning™ 96-Well Black, Costar, Cambridge, MA, USA), and the plate was incubated at room temperature for 60 min. Afterwards, 10 µL of dibenzylfluorescein was added, and the plate was further incubated for 30 min at room temperature. Precisely 10 µL of 0.3 mM NADPH was added to the mixture and dibenzylfluorescein was allowed to generate a fluorescent product. The signal was measured at 485 nm (excitation) and 530 nm (emission). The experiment was performed in triplicate.

2.6. Antiaromatase activity assay

An antiaromatase activity assay was performed in the

similar manner as described in Section 2.5. Briefly, Nile tilapia microsomes were resuspended in water and adjusted to the desired microsomal protein concentration with HEPES at a pH of 8.0. Precisely 10 μ L of the test compound (chrysin, quercetin, or quercitrin) at the desired concentration was added to 96-well plates pre-incubated with 100 μ L of 350 μ g/mL microsomal protein for 60 min at room temperature. Afterwards, 10 μ L of dibenzylfluorescein was added and plates were further incubated for 30 min at room temperature. Precisely 10 μ L of 0.3 mM NADPH was added to the mixture and dibenzylfluorescein was allowed to generate a fluorescent product. The signal was measured at 485 nm (excitation) and 530 nm (emission). The experiment was performed in triplicate. Concentrations of the aromatase inhibitors used were varied to generate dose response curves and IC₅₀ values were calculated.

2.7. Anti-proliferative activity assay

Two cancer cell lines, HepG2 human hepatoma and MCF-7 human breast cancer cells from the American type Culture Collection (Rockville, MD, USA), were cultured in a 75-cm² sterile flat-bottomed bottle containing DMEM supplemented with 10% FBS and 10% of antibiotic-antimycotic in a humidified atmosphere of 5% CO₂ at 37°C until confluent. An anti-proliferative activity assay was performed using the method previously described (27) with some modifications. Cells (5×10^5 cells/well) were seeded in 96-well plates (Thermo Scientific™ Nunc™ MicroWell™ Plates with Nunclon™ Delta Surface, Nunc™, Nalge Nunc, Denmark). Various concentrations of the tested sample were added and the plates were incubated at 37°C for 20 h. DMSO was used as a vehicle control. Afterwards, the medium was drained and 100 μ L of (5 mg/mL) MTT was added to each well. Plates were further incubated at the same temperature for 4 h. Finally, the cells were dissolved by adding DMSO before measuring the absorbance of the resulting purple solution at 570 nm with a microplate reader (Tecan Sunrise, Software Magellan V.5.00, Switzerland). Absorbance at 630 nm served as a reference. All treatments were done in quadruplicate.

2.8. Statistical analysis

The experiment was performed in triplicate. Data are presented as the mean \pm S.D. Statistical analysis was performed using ANOVA and p values less than 0.05 were considered significant.

3. Results

3.1. Microsome preparation and SEM images

The outer appearance of the liver of Nile tilapia and

the homogenized liver is shown in Figure 1(a) and 1(b), respectively. After the first centrifugation at 10000 \times g, the fractions of unbreakable cells, nuclei, and mitochondria were precipitated while the soluble enzymes and fragmented endoplasmic reticulum containing microsomes remained in the supernatant. After ultracentrifugation at 105,000 \times g, the microsomes appeared as a gel-like mass at the bottom of the tube that was reddish color, as shown in Figure 1(c). Under SEM, fish microsomes had an irregular shape as shown in Figure 1(d). The yields of microsomes are shown in Table 1. Results suggested that a higher yield of fish microsomes can be extracted from adult fish with a heavier weight.

3.2. Effect of pH on the aromatase activity of Nile tilapia microsomes

The aromatase activity of Nile tilapia microsomes at different pHs was examined. As shown in Figure 2, results indicated that fish microsomes dissolved in a

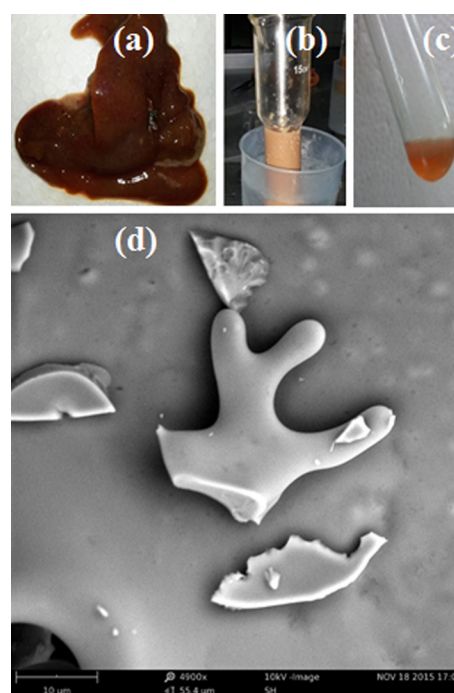


Figure 1. The outer appearance of (a) the liver of Nile tilapia, (b) homogenized liver of Nile tilapia, (c) extract from the liver of Nile tilapia microsomes, and (d) SEM image of Nile tilapia microsomes.

Table 1. Effects of age and body weight of Nile tilapia on the yield of microsomes ($n = 3$)

Body weight (g)	Age (month)	Extracted microsomes (mg)
150-160	3-4	0 \pm 0
170-180	3-4	0 \pm 0
190-200	3-4	0 \pm 0
220-230	5-6	27 \pm 6
240-250	5-6	41 \pm 16
300-320	5-6	198 \pm 33

medium with a pH of 7.2-7.8 had significantly less aromatase activity than microsomes dissolved in a medium with a pH of 8.0. At microsome concentrations of 21.9-175 µg/mL, the activity of the enzyme was independent of its dose. Dose-dependent activity was noted only when the enzyme was in medium with a pH of 8.0.

3.3. Antiaromatase activity

Three active compounds, chrysin, quercetin, and quercitrin, were used in the current study because they have similar structures, as shown in Figure 3. Results indicated that all 3 assayed compounds inhibited the aromatase activity of Nile tilapia microsomes in a dose-dependent manner. However, that level of inhibition differed, as shown in Figure 4. Chrysin had the most potent antiaromatase activity, with an IC_{50} of 0.25 mg/mL. This activity was approximately 2 times that of quercetin (0.44 mg/mL). Quercitrin had the lowest activity, with an IC_{50} that could not be detected.

3.4. Anti-proliferative activity

Chrysin was chosen to determine whether it inhibited the proliferation of HepG2 human hepatoma and MCF-7 human breast cancer cells. Results indicated that chrysin significantly inhibited the proliferation of both types of cells in a dose-dependent manner. As shown in Figure 5,

treatment with chrysin for 20 h dramatically decreased the viability of cancer cells as the concentration of chrysin increased. The anti-proliferative activity of chrysin against both types of cancer cells differed slightly. The IC_{50} of chrysin with respect to HepG2 cells was 8.76 ± 0.79 µg/mL while its IC_{50} with respect to MCF-7 cells was 9.77 ± 1.21 µg/mL.

4. Discussion

During sex differentiation, overexpression of estrogens or androgens in genetically male or female individuals, respectively, is known to transform the sexual phenotype to the opposite gender (9,10). In fish, aromatase enzymes can irreversibly convert androgens into estrogens

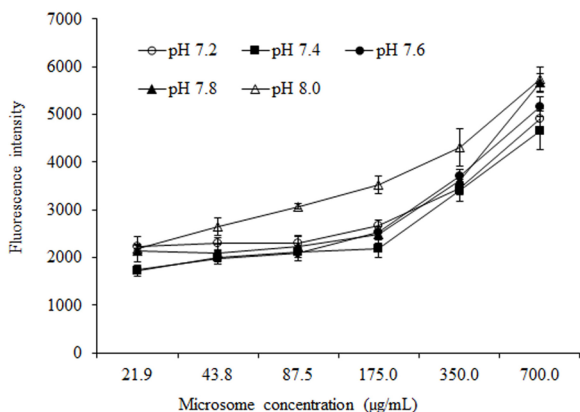


Figure 2. Effect of pH on aromatase activity of Nile tilapia microsomes measured with fluorescence intensity.

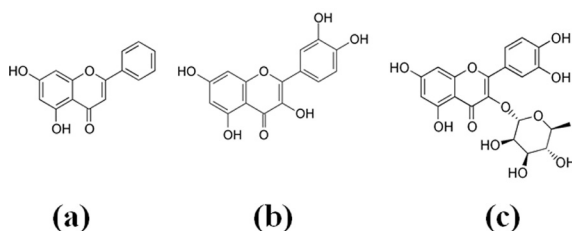


Figure 3. Chemical structure of (a) chrysin, (b) quercetin, and (c) quercitrin.

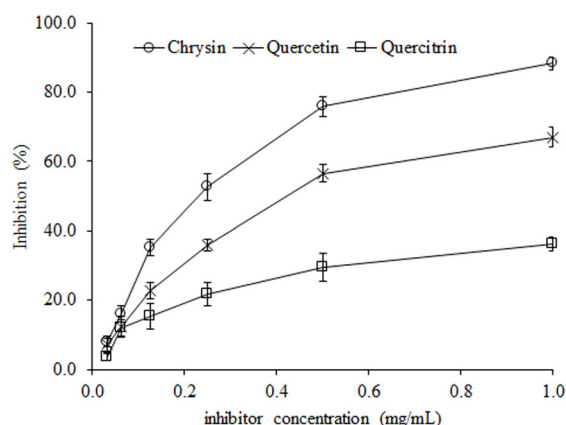


Figure 4. Inhibition of aromatase by the tested compounds.

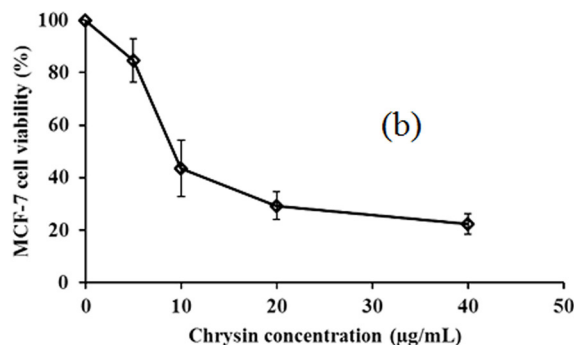
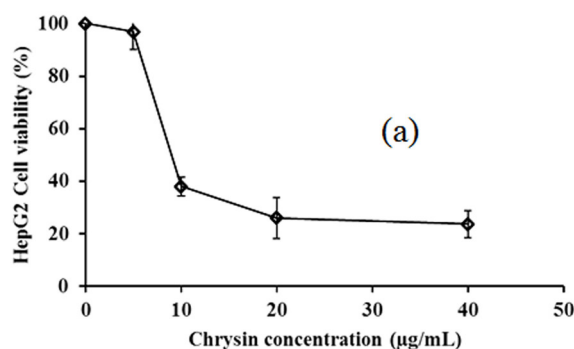


Figure 5. Anti-proliferative activity of chrysin against (a) HepG2 and (b) MCF-7 cancer cells.

(14). Hence, aromatase is essential to establishing the final sex phenotype of fish. A high level of expression of aromatase enzymes is associated with ovarian differentiation while a low level is associated with testicular differentiation. Male Nile tilapia grow at a rate 20% faster than female fish (15). Therefore, male fish need to be produced when aquaculturing Nile tilapia. For years, aromatase inhibitors have been used as sex inversion agents to produce all-male populations of fish since they can significantly reduce the biosynthesis of estrogen (16,18). The antiaromatase activity of different compounds should be compared in order to search for the most potent aromatase inhibitor. Microsomes of some fish species such as rainbow trout (*Oncorhynchus mykiss*), carp (*Cyprinus carpio*), and seabream (*Sparus aurata*) have previously been used to assay antiaromatase activity (28,29). However, Nile tilapia microsomes have not been used for this purpose. The current study therefore sought to investigate whether the hepatic microsomes of Nile tilapia could be a source of aromatase enzymes and whether they would be suitable for testing or comparing the antiaromatase activity of different compounds.

Microsomes are vesicle-like fractions of the endoplasmic reticulum (ER) found in healthy living cells. Microsomes can feasibly be isolated when eukaryotic cells are dissolved and centrifuged (30). Many organs of fish have been used to extract microsomes. However, the parts that are normally rich in microsomes are the liver (28), brain (31), and ovaries (32). The liver was selected for the source of microsomes in the current study because of its larger size and ease of isolation. To the extent known, the current study is the first to extract hepatic microsomes of Nile tilapia for use in an assay of antiaromatase activity.

As expected, results indicated that the hepatic microsomes of Nile tilapia obtained were reddish in color due to the presence of heme (33). Fish of two age groups, 3-4 months and 5-6 months, were compared. Results clearly indicated that the older fish yielded more microsomes. Moreover, fish in the same age group but with different weights yielded different amounts of microsomes. Fish with a heavier weight yielded a larger amount of microsomes. Based on the fish body weight, the percent yield from fish with the lightest average weight (225 g) was only 0.12% whereas that from the heaviest average weight (310 g) was 0.63%. Thus, the percent yield was almost three times greater. The yield of hepatic microsomes from Nile tilapia was influenced by the age and body weight of fish.

The pH of fish blood is reported to fluctuate due to species variation, environment, electrolytes, temperature, and stress (34). Moreover, the pH of a reaction medium occasionally plays a key role in many reactions (35,36). The current study found that pH played an important role in the aromatase activity of Nile tilapia microsomes. The pH of the medium was adjusted to 8.0, which was the

most effective pH, since aromatase enzymes behaved in a dose-dependent manner. Therefore, this pH was chosen for further study of the antiaromatase activity of different compounds.

Three compounds, chrysin, quercetin, and quercitrin, were tested for their antiaromatase activity. These compounds have the same core structure of 5,7 dihydroxy flavone as is found in chrysin. Addition of two hydroxyl groups to chrysin at C3' and C4' yields quercetin, which is the aglycone part of many important flavonoid glycosides. Substitution of deoxy sugar rhamnose at C3 of quercetin yields quercitrin, a glycoside. Comparison of the antiaromatase activity of these three compounds in hepatic microsomes from Nile tilapia revealed different levels of antiaromatase activity. Results also indicated the effects that the structure-activity relationship of the compounds had. Substitution of OH group to chrysin, such as in quercetin molecule, caused significant decrease in antiaromatase activity. In addition, consideration between a flavonoid quercetin and its glycoside formed from deoxyrhamnose substitution, quercitrin, resulted that the aglycone quercetin possessed higher activity than its corresponding glycoside, quercitrin. Since the active site of aromatase is highly hydrophobic (37), the compounds with alkyl or higher hydrophobic aromatic groups could have higher affinity to this enzyme leading to a higher efficiently block enzyme activity. Substituting OH groups or sugar moieties in chrysin can decrease its hydrophobicity. Chrysin had the highest hydrophobicity and most potent antiaromatase activity, so chrysin was investigated for its inhibition of the proliferation of cancer cells.

A study has reported that estrogen-dependent breast carcinogenesis can be treated by blocking estrogen activity using aromatase inhibitors (38). Recent studies have indicated that some aromatase inhibitors inhibit the proliferation of cancer cells as well (39,40). Chrysin had the most potent antiaromatase activity among the compounds tested in the current study, so chrysin was selected to investigate its ability to inhibit the proliferation of MCF-7 human breast cancer cells. To confirm a compound's ability to inhibit the proliferation of cancer cells, HepG2 human hepatoma cells were also used. Results indicated that chrysin efficiently inhibited the growth of both cancer cell lines but at different levels. Chrysin has been reported to have anti-inflammatory action (41). The current study used hepatic microsomes from Nile tilapia as a novel source of test enzymes. Results indicated that chrysin inhibited the proliferation of MCF-7 and HepG2 cancer cells and that it had potent antiaromatase activity.

In conclusion, the current study indicated that hepatic microsomes from Nile tilapia are a high specific means of investigating the activity of aromatase inhibitors *in vitro*. The age and body weight of Nile tilapia significantly affected the yield of the extracted microsomes. The aromatase activity of Nile tilapia

microsomes was influenced by the pH of the reaction medium. A pH of 8.0 is the most effective pH at which to assay the antiaromatase activity of different compounds. The antiaromatase activity of chrysin, quercetin, and quercitrin differed. Chrysin was the most potent aromatase inhibitor. Results confirmed that chrysin is an aromatase inhibitor and indicated that chrysin inhibits the proliferation of cancer cells as well.

Acknowledgements

The authors wish to thank Rajamangala University of Technology Lanna, Thailand for its financial grant to TS. The authors also wish to thank Dr. Kassara Pattamapun, Dr. Sakornrat Khongkhunthian, and Dr. Phenphichar Wanachantararak of the Faculty of Dentistry, Chiang Mai University, as well as Dr. Rawiwan Wongpoomchai and Dr. Ariyapong Wongnoppavich of the Faculty of Medicine, Chiang Mai University for their advice and assistance.

References

- Chumsri S, Howes T, Bao T, Sabnis G, Brodie A. Aromatase, aromatase inhibitors, and breast cancer. *J Steroid Biochem Mol Biol*. 2011; 125:13-22.
- Smith IE, Dowsett M. Aromatase inhibitors in breast cancer. *N Engl J Med*. 2003; 348:2431-2442.
- Gray J, Evans N, Taylor B, Rizzo L, Walker M. State of the evidence: The connection between breast cancer and the environment. *Int J Occup Environ Health*. 2009; 15:43-78.
- Brueggemeier RW, Richards JA, Joomprabutra S, Bhat AS, Whetstone JL. Molecular pharmacology of aromatase and its regulation by endogenous and exogenous agents. *J Steroid Biochem Mol Biol*. 2001; 79:75-84.
- Yadav MR, Barmade MA, Tamboli RS, Murumkar PR. Developing steroidal aromatase inhibitors – An effective armament to win the battle against breast cancer. *Eur J Med Chem*. 2015; 105:1-38.
- Chan HJ, Petrossian K, Chen S. Structural and functional characterization of aromatase, estrogen receptor, and their genes in endocrine-responsive and -resistant breast cancer cells. *J Steroid Biochem Mol Biol*. 2016; 161:73-83.
- Miller WR. Biological rationale for endocrine therapy in breast cancer. *Best Pract Res Clin Endocrinol Metab*. 2004; 8:1-32.
- Recanatini M, Cavalli A, Valenti P. Nonsteroidal aromatase inhibitors: Recent advances. *Med Res Rev*. 2002; 22:282-304.
- Young G, Kagawa H, Nagahama Y. Evidence for a decrease in aromatase activity in the ovarian granulosa cells of amago salmon (*Oncorhynchus rhodurus*). *Zoolog Sci*. 2003; 20:1399-1404.
- Desvages G, Pierau C. Aromatase activity in gonads of turtle embryos as a function of the incubation temperature of eggs. *J Steroid Biochem Mol Biol*. 1992; 41:851-853.
- Miyata S, Kubo T. *In vitro* effects of estradiol and aromatase inhibitor treatment on sex differentiation in *Xenopus laevis* gonads. *Gen Comp Endocrinol*. 2000; 119:105-110.
- Pieau C, Dorizzi M. Oestrogens and temperature-dependent sex determination in reptiles: All is in the gonads. *J Endocrinol*. 2004; 181:367-377.
- Smith CA, Sinclair AH. Sex determination: Insights from the chicken. *Bioessays*. 2004; 26:120-132.
- Nakamura M, Alam MA, Kobayashi Y, Bhandari RK. Role of sex hormones in sex change of grouper. *J Mar Sci Technol*. 2007; 15:23-27.
- Devlin R, Nagahama Y. Sex determination and sex differentiation in fish: An overview of genetic, physiological, and environmental influences. *Aquaculture*. 2002; 208:191-364.
- Gormaz JG, Fry JP, Erazo M, Love DC. Public health perspectives on aquaculture. *Curr Environ Health Rep*. 2014; 1:227-238.
- Mouridsen HT, Robert NJ. The role of aromatase inhibitors as adjuvant therapy for early breast cancer in postmenopausal women. *Eur J Cancer*. 2005; 41:1678-1689.
- Fatima S, Adams M, Wilkinson R. Sex reversal of brook trout (*Salvelinus fontinalis*) by 17 α -methyltestosterone exposure: A serial experimental approach to determine optimal timing and delivery regimes. *Anim Reprod Sci*. 2016; 175:39-47.
- Shimizu Y, Yarborough CP, Elger W, Chwalisz K, Osawa Y. Inhibition of aromatase activity in human placental microsomes by 13-retro-antiprogestins. *Steroids*. 1995; 60:234-238.
- Wójtowicz AK, Milewicz T, Gregoraszczyk EL. DDT and its metabolite DDE alter steroid hormone secretion in human term placental explants by regulation of aromatase activity. *Toxicol Lett*. 2007; 173:24-30.
- Tao X, Piao H, Canney DJ, Borenstein MR, Nnanea IP. Biotransformation of letrozole in rat liver microsomes: Effects of gender and tamoxifen. *J Pharm Biomed Anal*. 2007; 43:1078-1085.
- Satoh K, Nonaka R, Ishikawa F, Ogata A, Nagai F. *In vitro* screening assay for detecting aromatase activity using rat ovarian microsomes and estrone ELISA. *Biol Pharm Bull*. 2008; 31:357-362.
- Seralini GE, Moslemi S. Aromatase inhibitors: Past, present and future. *Mol Cell Endocrinol*. 2001; 178:117-131.
- Otake Y, Nolan AL, Walle UK, Walle T. Quercetin and resveratrol potently reduce estrogen sulfotransferase activity in normal human mammary epithelial cells. *J Steroid Biochem Mol Biol*. 2000; 73:265-270.
- Iwata N, Mukai T, Hara S, Endo T, Tomoda A. Rapid and large scale isolation of microsomal fraction of mouse liver by lyophilization and low speed centrifugation. *Tohoku J Exp Med*. 1996; 180:65-71.
- Stresser DM, Turner SD, McNamara J, Stocker P, Miller VP, Crespi CL, Patten CJ. A high-throughput screen to identify inhibitors of aromatase (CYP19). *Anal Biochem*. 2000; 284:427-430.
- Finco FDDBA, Kloss L, Graeve L. Bacaba (*Oenocarpus bacaba*) phenolic extract induces apoptosis in the MCF-7 breast cancer cell line via the mitochondria-dependent pathway. *NFS J*. 2016; 5:5-15.
- Zlabek V, Burkina V, Borrisser-Pairo F, Sakalli S, Zamaratskaia G. Phase I metabolism of 3-methylindole, an environmental pollutant, by hepatic microsomes from carp (*Cyprinus carpio*) and rainbow trout (*Oncorhynchus mykiss*). *Chemosphere*. 2016; 150:304-310.
- Aydemir DH, Sen A. Characterization of brain and liver aromatase of gilthead seabream (*Sparus aurata* L., 1758)

- using dibenzylfluorescein. *J Nat Appl Sci.* 2013; 17:5-14.
30. Abas L, Luschnig C. Maximum yields of microsomal-type membranes from small amounts of plant material without requiring ultracentrifugation. *Anal Biochem.* 2010; 401:217-227.
 31. Strobl-Mazzulla PH, Lethimonier C, Gueguen MM, Karube M, Fernandino JI, Yoshizaki G, Patiño R, Strüßmann CA, Kah O, Somoza GM. Brain aromatase (Cyp19A2) and estrogen receptors, in larvae and adult pejerrey fish *Odontesthes bonariensis*: Neuroanatomical and functional relations. *Gen Comp Endocrinol.* 2008; 158:191-201.
 32. Shilling AD, Carlson DB, Williams DE. Rainbow trout, *Oncorhynchus mykiss*, as a model for aromatase inhibition. *J Steroid Biochem Mol Biol.* 1999; 70:89-95.
 33. Richards IS, Bourgeois M. Phase I reaction and cytochrom P450. *Principles and Practice of Toxicology in Public Health.* 2nd, Jones & Bartlett learning, Burlington, MA, 2014; p. 165.
 34. Burton RF. The dependence of normal arterial blood-pH on sodium concentration in teleost fish. *Comp Biochem Physiol A Mol Integr Physiol.* 1996; 114:111-116.
 35. Rios F, Lechuga M, Fernandez-Serrano M, Fernandez-Arteaga A. Aerobic biodegradation of amphoteric amine-oxide-based surfactants: Effect of molecular structure, initial surfactant concentration and pH. *Chemosphere.* 2017; 171:324-331.
 36. Abboud MM, Khleifat KM, Batarseh M, Tarawneh KA, Al-Mustafa A, AlMadadhah M. Different optimization conditions required for enhancing the biodegradation of linear alkylbenzenesulfonate and sodium dodecyl sulfate surfactants by novel consortium of *Acinetobacter calcoaceticus* and *Pantoea agglomerans*. *Enzyme Microb Tech.* 2007; 41:432-439.
 37. Bonfield K, Amato E, Bankemper T, Agard H, Steller J, Keeler JM, Roy D, McCallum A, Paula S, Ma L. Development of a new class of aromatase inhibitors: Design, synthesis and inhibitory activity of 3-phenylchroman-4-one (isoflavanone) derivatives. *Bioorgan Med Chem.* 2012; 20:2603-2613.
 38. Benson JD, Chen YNP, Cornell-Kennon SA, Dorsch M, Kim S, Leszczyniecka M, Sellers WR, Lengauer C. Validating cancer drug targets. *Nature.* 2006; 441:451-456.
 39. Kim J, Jayaprakasha GK, Patil BS. Obacunone exhibits anti-proliferative and anti-aromatase activity *in vitro* by inhibiting the p38 MAPK signaling pathway in MCF-7 human breast adenocarcinoma cells. *Biochimie.* 2014; 105:36-44.
 40. Murthy KNC, Guddadarangavvanahally K, Jayaprakasha GK, Patil BS. Cytotoxicity of obacunone and obacunone glucoside in human prostate cancer cells involves Akt-mediated programmed cell death. *Toxicology.* 2015; 329:88-97.
 41. Byun EB, Jang BS, Byun EH, Sung NY. Effect of gamma irradiation on the change of solubility and anti-inflammation activity of chrysin in macrophage cells and LPS-injected endotoxemic mice. *Radiat Phys Chem.* 2016; 127:276-285.

(Received January 18, 2017; Revised February 12, 2017; Accepted February 14, 2017)

Ultrastructural and physico-chemical characterization of saliva during menstrual cycle in perspective of ovulation in human

Ganesan Saibaba¹, Mahalingam Srinivasan¹, Archunan Priya Aarth², Velliyangiri Silambarasan¹, Govindaraju Archunan^{1,*}

¹ Centre for Pheromone Technology, Department of Animal Science, School of Life Sciences, Bharathidasan University, Tiruchirappalli, Tamilnadu, India;

² Tagore Medical College and Hospital, Rathinamangalam, Chennai, India.

Summary

Human saliva is a potential diagnostic fluid and any alteration in body might be reflected in saliva so that saliva is considered as "mirror of the body". Variations in salivary hormone level, ultra structure, pH, flow rate, buffering capacity and electrolytes level are found during menstrual cycle in regard to ovulation. Thirty healthy volunteers were used for the assessment of physico-chemical changes in saliva. Reproductive cycle was categorized as pre-ovulation phase (5 to 12 days), ovulation phase (13 or 14 days) and post-ovulation phase (15 to 25 days) according to salivary arborization test and hormonal analysis. Estradiol and luteinizing hormone was gradually increased and attained peak at the level of 2.28 ± 0.20 pg/mL and 1.35 ± 0.41 mIU/mL respectively during the ovulation phase. The electrolytes result clearly indicates that the influx of common electrolytes is important for crystallization and help to induce clear ferning pattern in ovulation phase. Sodium (Na) and chloride (Cl) were found to be high during ovulation phase only. Average salivary pH was 7.5, 7.1, and 7.3 during ovulation, pre- and post-ovulation phases respectively. Buffering capacity of saliva was normal during pre- and post- ovulation phases. In contrast, in ovulation phase the buffer capacity was slightly higher. At the first time, the scanning electron microscopy (SEM) studies revealed the ultra structure difference of saliva during menstrual cycle. During ovulation phase a compact network-shaped mesh was appeared; such structure was not appeared in pre- and post ovulation phases. Additionally, we observed the saliva is arrayed as a fine mosaic-like structure during ovulation. Based on physico-chemical properties and hormonal levels may lead to develop a detection kit/sensor for detecting the ovulation phase in human.

Keywords: Buffer capacity, SEM, luteinizing hormone, estradiol, electrolytes

1. Introduction

Saliva is secreted from three paired extrinsic salivary glands in humans such as parotid, submandibular, and sublingual glands under the control of both the parasympathetic (PNS) and sympathetic nervous

systems (SNS) (1). Parotid glands and submandibular glands are contributing around 25% and 70%, whereas the sublingual glands account for only 5% of total salivary output (2,3). In recent years, more blood borne substances have been detected in saliva, which leads to saliva as an essential, noninvasive diagnostic medium. On the other hand, saliva is composed of 95% water and 5% of various minerals, electrolytes, hormones, enzymes, immunoglobulins, cytokines, etc. (4).

Ovulation is a complex mechanism in which mature ova is likely to respond to surge of luteinizing hormone (LH) and rupture to release fertilizable oocytes. The LH-induced transition of ovarian tissue is prerequisite for the process of ovulation which is caused by

Released online in J-STAGE as advance publication April 14, 2017.

*Address correspondence to:

Dr. Govindaraju Archunan, Centre for Pheromone Technology, Department of Animal Science, Bharathidasan University, Tiruchirappalli 620024, Tamilnadu, India.
E-mail: garchu56@yahoo.co.in

multi-gene and multi-step process. Particularly, LH surge initiates a cascade of proteolytic events that control ovulation. Mainly, the LH gene activates the progesterone receptor (5). During ovulation numerous cell types get altered namely granulosa, theca cells, fibroblasts and endothelial cells, as well as the ovarian surface epithelium (6). Additionally, various protease enzymes mediate the ovulation during LH surge; for instance, proteins are thought to be mediators of ovulation such as: plasminogen activators (PAs), matrix metalloproteinases (MMPs), kallikreins and tissue-specific inhibitors of MMPs (TIMPs) (7).

Recently, attention has been paid to the development of noninvasive methods for ovulation detection (8,9). Saliva is a good investigative tool for various diagnostic purposes. It is reported that the sympathetic nervous system, parasympathetic nervous system, hypothalamic-pituitary-adrenal axis and immune system are response to change their biomolecules in saliva due to stress (10). Ovulation has been linked to an inflammatory-like response (11) and well considered as stress to women. Perhaps, one or more salivary proteins would serve as a potential non-invasive biomarker that would be characterized to predict ovulation (12). Report revealed that, uridine diphosphoacetylglucosamine pyrophosphorylase (UDP)-N-acetylglucosamine pyrophosphorylase was found to be a specific protein differentially expressed in human saliva during the ovulation phase (13). Most recently, the salivary protein expression differs particularly the high 14.5 kDa protein expression were high in ovulation phase (14). In general, LH assay in serum and ultrasonography methods are used to predict the ovulation time, even though, these methods are invasive, high cost and needs technically skilled persons. In the present scenario, the time of ovulation in women is highly essential to avoid unwanted pregnancy and *in vitro* fertilization to effective implementation of assisted reproductive technology (ART). However, presently there is no reliable, cost effective indicator for detection of ovulation in women accurately. As of now, there is an increasing demand to promote cost effective method or tool to predict fertile period in women. The present study was undergone to analyze LH and estradiol levels, pH, buffer capacity, flow rate, and electrolytes during the phases of menstrual cycle. Furthermore, for the first time the ultra-structure of saliva in different phases of menstrual cycle was spotted using scanning electron microscopy.

2. Materials and Methods

2.1. Ethics statement

Sample collection from local women volunteers and all experimental protocols were approved by Institutional Ethical Committee (IEC) (Approval

No: DM/2014/101/38), Bharathidasan University, Tiruchirappalli, India. All the methods were carried out in accordance with the Indian Council for Medical Research (ICMR, New Delhi) approved guidelines and regulations. Volunteers were duly informed and subsequently given a written consent.

2.2. Volunteer's inclusion criteria

Thirty healthy female volunteers (ranges from 18-30 years) without any chronic diseases of oral system, infectious diseases, systemic illness, cardiac, renal, respiratory or hepatic failure, ovarian dysfunction or any medications known to alter sex hormone levels were selected. Volunteers were excluded from the study if they did not meet the above criteria.

2.3. Saliva sampling and process

The saliva samples were collected without any stimulus in the morning (8.00 to 9.00 a.m.) from female volunteers. The volunteers were instructed to brush the teeth 30 min before the collection of saliva. Further, all subjects abstained from eating or drinking for a minimum of 1 h before saliva collection. The saliva samples were collected by expectorating into polypropylene tubes within 5 min according to the protocol followed by Navazesh (15). The samples were centrifuged at 16,000 g for 15 min to remove insoluble materials and cells, if any. The samples were stored at -80°C until further use.

2.4. Confirmation of ovulation

The saliva samples were assigned among the three phases, preovulatory (day 6 to 12), ovulatory (days 13 or 14) and postovulatory (day 15 to 26) phases according to the salivary hormone concentrations and fern pattern analysis (13). In addition, the ovarian follicle status was assessed with ultrasonography to validate the day of ovulation. The concentration of hormones such as estradiol, LH (luteinizing hormone), and FSH (follicle-stimulating hormone) were determined by enzyme immunoassay (EIA) using commercial kits (Pathozyne Oestradiol OD477 EIA kits, Omega House, Scotland, UK).

2.5. pH, buffer capacity and flow rate

Saliva pH was measured using a pHTestr[®] 30 (Thermo Scientific Eutech products, Ayer Rajah Crescent, Singapore). To measure buffering capacity of saliva, after measuring pH, 1 mL of 0.1 N HCl was added to 1 mL of saliva and pH was recorded (16). Buffer capacity was calculated according to changes in pH. For flow rate, the sample tubes were first weighed and reweighed with tubes containing saliva samples.

2.6. Electrolytes measurement

Electrolytes (Na, Cl, K and Ca) were analyzed in Atomic Absorption Spectrophotometer (AAS) (AAS iCE 3000 series, Thermo Fischer, Waltham, Massachusetts, USA) after calibrating for each element using standard solution of known concentration

2.7. Scanning electron microscopy analysis

Saliva samples were fixed in 3% glutaraldehyde solution in 0.25 M cacodylate buffer at 4°C for 48 h. After the fixation period, the specimens were washed twice in a 0.25 M cacodylate buffer for 30 min each time, to remove the remaining fixer. Then they were dehydrated in an ascending gradient in acetone concentration. For this, the specimens went through 30%, 50%, 70%, 90% and 100% (v/v) concentration acetone solutions, remained in each solution for 120 min as described in Barros *et al.* (17). Followed by auto gold coating, the samples were examined at 10.00K x magnification at 10 kV. SEM Observations were made with a ZEISS FE-SEM (Carl Zeiss NTS Ltd, Oberkochen, Germany) scanning electron microscope.

2.8. Energy-dispersive X-ray spectroscopy

Energy-dispersive X-ray spectroscopy (EDX) analysis

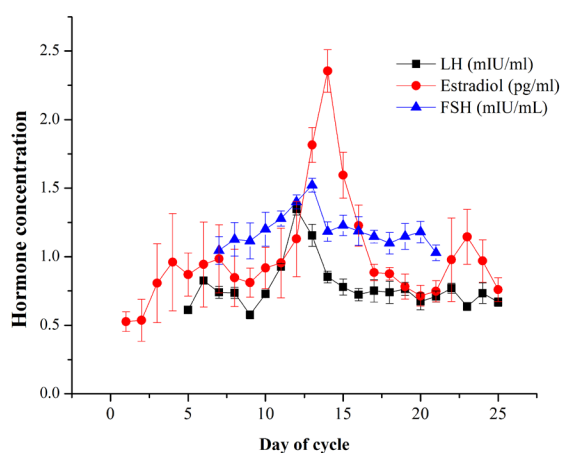


Figure 1. Salivary LH and estradiol level during menstrual cycle. The daily pattern of LH and estradiol level was recorded in subject's saliva sample ($n = 30$). The timing of LH and estradiol peak were appears around 12th and 14th day of menstrual cycle respectively. Data are presented as mean \pm SD ($p < 0.05$).

was applied to the area nearest to the smear surfaces of the samples. EDX analysis was performed using ZEISS FE-SEM instrument equipped with EDX.

2.9. Statistical analysis

All data represented as mean \pm SE and analyzed using one-way analysis of variance (ANOVA) with LSD post-hoc comparisons. A p value ≤ 0.05 was considered statistically significant. All statistical analysis was performed using the software package Statistical Package for Social Sciences (SPSS) for Windows, version 16.0 (SPSS Inc., Cary, NC, USA).

3. Results

3.1. Hormones level in saliva

The levels of salivary estradiol and LH during various phases of menstrual cycle were shown in Figure 1. A peak LH was observed during menstrual cycle at 12th day, whereas, the mean concentration of estradiol began to increase after LH shut down and reached its peak level during 14th day of cycle (Figure 1). The FSH concentration also differed in a significant level ($p < 0.05$) during the menstrual cycle which was highest during the ovulatory phase. The concentrations of hormones varied in preovulatory, ovulatory and postovulatory phases according to their physiological condition. The mean level of salivary estradiol, LH are during ovulation phase 2.35 ± 0.15 pg/mL and 1.34 ± 0.04 mIU/mL respectively.

3.2. pH, buffer capacity and flow rate

The results show that the pH was significantly (7.53 ± 0.073 , $p = 0.01$) increased during ovulation phase as compared to pre- and postovulation phases (Figure 2A, Table 1). Normal buffer capacity was observed in phases of menstrual cycle but a slight change was found in ovulation phase (2.21 ± 0.23) as compared to other phases, but the difference was not significant ($p = 0.145$) (Figure 2B, Table 1). The mean value of flow rate was decreased significantly in ovulation phase (2.09 ± 0.18 mL/5 min, $p = 0.01$) as compared to pre- and postovulation phases are $2.23 \pm .09$ mL/5 min and 2.47 ± 0.01 mL/5 min respectively (Figure 2C, Table 1). A significant positive correlation was found between

Table 1. Physico-chemical properties during ovulation phase

Physico-chemical properties	Pre-ovulation	Ovulation	Post-ovulation	p value
pH	7.18 ± 0.08	$7.53 \pm 0.07^*$	7.35 ± 0.07	0.01
Buffer capacity	2.13 ± 0.20	2.21 ± 0.23	1.65 ± 0.20	-
Flow rate (ml/5 min)	2.23 ± 0.09	$2.09 \pm 0.18^*$	2.47 ± 0.06	0.00

*Differences ($p < 0.05$) with pre- and post-ovulation phases. Data are presented as mean \pm SE.

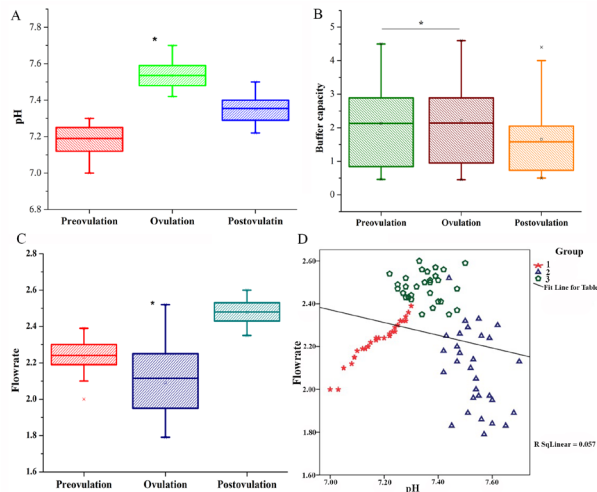


Figure 2. Physico-chemical properties of saliva. A) pH level of saliva during different phases of menstrual cycle, B) Buffer capacity of saliva, C) Flow rate of saliva, D) Correlation slope for saliva between pH and flow rate.

salivary pH and flow rate ($r = 0.751$ and $r^2 = 0.565$, $p < 0.05$) (Figure 2D).

3.3. Major electrolytes level

The salivary electrolytes were observed around the menstrual cycle (Figure 3). The concentrations of sodium in saliva significantly increased during ovulation phase (0.27 ± 0.08 mmol/mL, $p = 0.002$), whereas the chloride concentration was significantly less during preovulation phase and rapidly increased during ovulation phase (0.045 ± 0.010 mmol/mL, $p = 0.05$) and reached maximum in postovulation phase (0.062 ± 0.009 mmol/mL, $p = 0.008$). The mean potassium and calcium level in saliva did not alter during the phases of menstrual cycle. The potassium and calcium levels during ovulation phase were observed as 0.05 ± 0.005 mmol/mL, $p = 0.292$ and 0.003 ± 0.001 mmol/mL, $p = 0.195$.

3.4. Scanning electron microscopy analysis

The ultra-structure of saliva revealed by SEM analysis and a significant structural change were observed in different phases of menstrual cycle. Three different saliva structures were found in saliva such as, micro globules, compact network-shaped mesh and network-shaped mesh with pores at 10 K X magnification. The micro globules were exclusively found in pre-ovulation phase saliva with 2 μ m scale (Figure 4A). Likewise, the ovulation phase saliva shows a unique compact network-shaped mesh structure, which is recorded as the highest relative abundance (Figure 4B). In post-ovulation, the network-shaped meshes denatures and pores were developed (Figure 4C), which indicates that mesh structure started to lose their structural arrangement due to decrease the ion content.

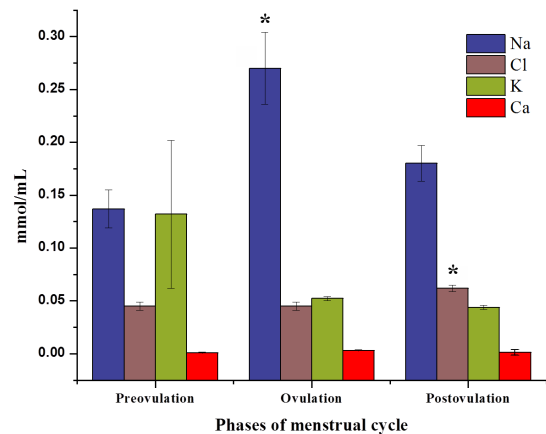


Figure 3. Major salivary electrolytes level. Bar diagram shows that level of Na, Cl, K, Ca electrolytes in saliva during menstrual cycle. The Na and Cl level were significantly high during ovulation and post-ovulation phase respectively compared to other phases using Fisher's least significant difference post-hoc comparisons ($p < 0.05$). Data are presented as mean \pm SE.

3.5. SEM-EDX analysis

In saliva, the presence of elements was recorded using EDX analysis. The following elements were detected namely: calcium, sodium, chloride, potassium and magnesium. Interestingly, the Cl element was appeared exclusively during ovulation phase and it may have vital role in crystals formation during ovulation phase (Figures 4D-4I).

4. Discussion

This is the first approach to investigate the salivary physico-chemical properties and ultrastructure in relation to the ovulation phase during menstrual cycle. Ovarian hormones cause the cyclic changes in the endometrium of uterus; particularly, estradiol produced by a mature ovarian follicle which triggers a surge release of GnRH (gonadotropin-releasing hormone) from the hypothalamus through positive feedback mechanism. Saliva samples have been demonstrated to enable differentiation between the follicular and luteal phase by assessing progesterone (18) and estradiol (19). Chatterton *et al.*, (20) found that the mean estradiol 2 level in the follicular phase across three consecutive cycles was 22.1 ± 2.7 pmol/L while mean luteal phase progesterone was 436 ± 34 pmol/L. Similarly, the present study confirms the variation in hormonal level around the menstrual cycle with peak concentration for estradiol (2.28 ± 0.20 pg/mL) and LH (1.35 ± 0.41 mIU/mL) during ovulation phase. Comparing our results with previous findings estradiol and LH are found to be equal concentrations in saliva during ovulation phase (8,21). It is well reported that the ferning pattern in women saliva was formed due to NaCl (sodium chloride), which is cyclically increased

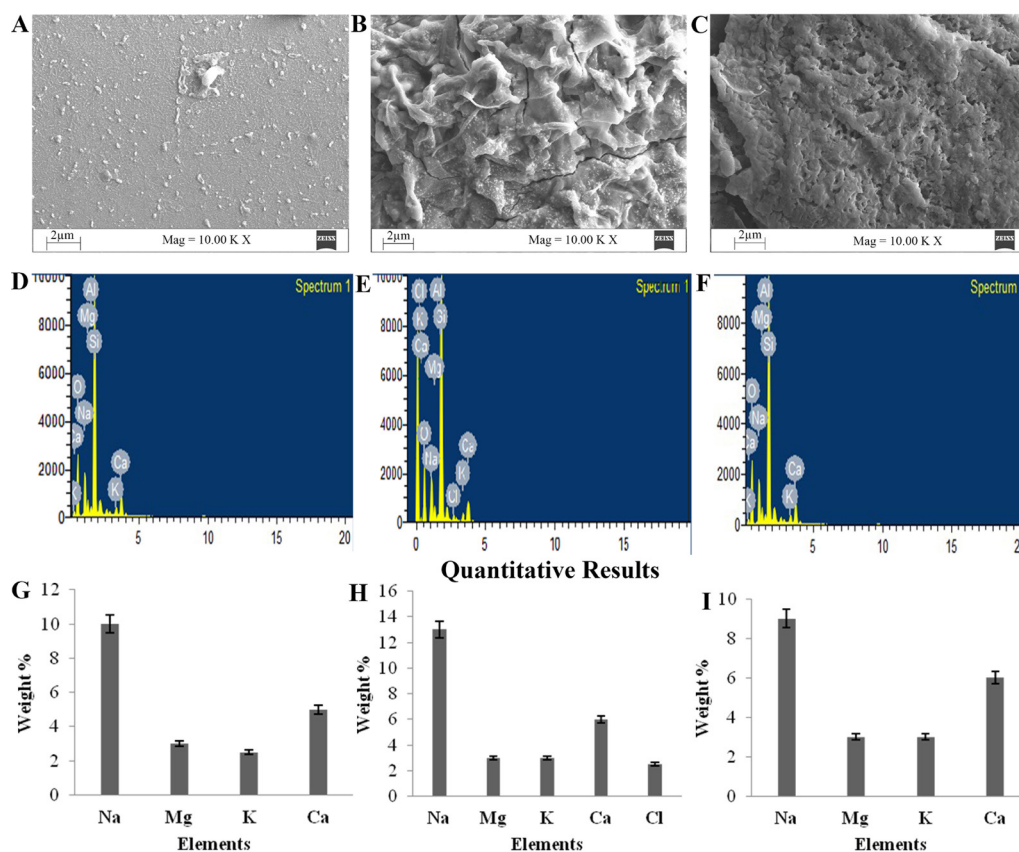


Figure 4. Scanning electron microscopic and SEM-EDX analysis of saliva during menstrual cycle. SEM analysis of **A)** pre-ovulation phase shows microglobules, **B)** Compact network-shaped mesh of ovulation phase, **C)** Network-shaped mesh with formation of pores of post-ovulation phase, at 10.00 K X in magnification and Bar = 2 μm . **D, G)** EDX electrolytes analysis of the pre-ovulation phase. **E, H)** EDX electrolytes analysis of ovulation phase. **F, I)** EDX electrolytes analysis of the post-ovulation phase saliva.

under the influence of estrogen (22-24). Barbato *et al.* (25) reported that the strong relationship is found among salivary ferning pattern and physiological condition during menstrual cycle.

A previous study revealed that the sodium and chlorine concentration level increased in sweat and saliva of cystic fibrosis (CF) patients (26,27). Likewise, a decreased potassium concentration level was found in rheumatoid arthritis patients (28). Recently, the level of sodium, potassium, chloride, calcium and phosphorus were identified as higher in Down syndrome patients saliva compared to healthy individuals (29). The concentration of sodium (Na), potassium (K) and chloride (Cl) ions in saliva was higher in diabetic patients when compared to that of non-diabetic patients those are having dental caries (30). In the present study, higher levels of sodium and chloride were found in saliva during ovulation phase compared to that of other phases. Our previous report showed that the salivary electrolytes are responsible for fern pattern formation during the ovulation phase (23), the present study further affirms the elevated level of salivary electrolytes during the ovulation phase.

The results obtained in this study indicated that significant difference was recorded in salivary pH and

buffer capacity during ovulation phase compared to other phases of menstrual cycle. Preethi *et al.*, (31) showed that the buffering capacity of the saliva was lower in children having caries as compared to healthy children. According to our data, salivary flow is lesser in ovulation phase of women, which may lead to oral dryness seen in females (32). It is found that women have a low saliva flow rate than men for stimulated and un-stimulated parotid saliva (33). Possibly female sexual hormones, specifically estrogen, have a significant role in the suppression of saliva flow (31,34). Recently, it is reported that individuals with increased inorganic salivary calcium, phosphate, pH and increased flow rate may chance for periodontitis formation (35). Additionally, findings from the present study suggest that the sexual hormones may influence the changes in salivary flow rate and pH during ovulation phase. Electrolyte level, pH, buffer capacity, flow rate and ultra structure have been studied in saliva in reference to several diseases and physiological conditions (26-30,33,36-42). The present study revealed the difference in the electrolytes, pH, buffer capacity and flow rate of saliva during the ovulation phase. Likewise, the salivary protein expressions are varies in regard to ovulation phase (14).

Commonly, the typical endocrine pattern of the menstrual cycle controls the functions of the cervix and, thereby controls the biophysical properties of the cervical mucus (38). At earlier period the mesh type morphology was demonstrated in cervical mucus during ovulatory phase (43). Even though, in the human salivary ultra structure is not yet studied during menstrual cycle in regard to ovulation phase. Now, the SEM-EDX study reveals the difference in elements concentration during ovulation phase as compared to other phases.

On the basis of our findings, we suggest that human saliva has distinctive variation in physico-chemical properties during ovulation phase, which would help to set a reference for the identification of fertile period in women. Further, studies are required to understand the composition of saliva during the fertile period in women. In conclusion, micro and macro molecules which involved in the ultra structural variation and electrolytes would lead to the development of biosensor for ovulation detection.

Acknowledgements

G.S. thanks the Indian Council of Medical Research (ICMR-New Delhi, India; File No. 45/5/2014-BIO/BMS) for the award of Senior Research Fellowship. The facility availed from Bharathidasan University, ICAR-National Fund, DST-FIST-Phase-I (Stage-II) and UGC-SAP-DRS-II is greatly acknowledged. Authors thank Dr. A.S. Rao, Honorary Professor, Department of Biotechnology, Bharathidasan University, Tiruchirappalli-620024 for critical reading of manuscript.

References

1. Marieb EN, Hoehn K. Human anatomy & physiology (8th ed.). Benjamin Cummings, San Francisco, USA, 2010.
2. Martini FH, Nath JL. Fundamentals of Anatomy and Physiology (8th ed.). Pearson/Benjamin Cummings, San Francisco, USA, 2009.
3. Farnaud SJ, Kostic O, Getting SJ, Renshaw D. Saliva: physiology and diagnostic potential in health and disease. *ScientificWorldJournal*. 2010; 10:434-456.
4. Edgar WM. Saliva: its secretion, composition and functions. *Br Dent J*. 1992; 172:305-312.
5. Robker RL, Russell DL, Yoshioka S, Sharma SC, Lydon JP, O'Malley BW, Espey LL, Richards JS. Ovulation: a multi-gene, multi-step process. *Steroids*. 2000; 65:559-570.
6. Espey LL, Lipner H. Ovulation. In: *The Physiology of Reproduction* (Knobil E, Neill JD, eds.). Raven Press, New York, 1994; pp. 725-780.
7. Nothnick WB, Keeble SC, Curry TE Jr. Collagenase, gelatinase, and proteoglycanase messenger ribonucleic acid expression and activity during luteal development, maintenance, and regression in the pseudopregnant rat ovary. *Biol Reprod*. 1996; 54:616-624.
8. Alagendran S, Archunan G, Prabhu SV, Orozco BE, Guzman RG. Biochemical evaluation in human saliva with special reference to ovulation detection. *Indian J Dent Res*. 2010; 21:165-168.
9. Martinez AR. Prediction and detection of the fertile phase of the menstrual cycle: an overview. *Adv Contracept*. 1997; 13:131-138.
10. Khaustova S, Shkurnikov M, Tonevitsky E, Artyushenko V, Tonevitsky A. Noninvasive biochemical monitoring of physiological stress by Fourier transform infrared saliva spectroscopy. *Analyst*. 2010; 135:3183-3192.
11. Espey LL. Ovulation as an inflammatory reaction—a hypothesis. *Biol Reprod*. 1980; 22:73-106.
12. Saibaba G, Archunan G. Does salivary protein(s) act an ovulation indicator for women? A hypothesis. *Med Hypotheses*. 2015; 84:104-106.
13. Alagendran S, Saibaba G, Muthukumar S, Rajkumar R, Guzman RG, Archunan G. Characterization of salivary protein during ovulatory phase of menstrual cycle through MALDI-TOF/MS. *Indian J Dent Res*. 2013; 24:157-163.
14. Saibaba G, Rajesh D, Muthukumar S, Sathiyarayanan G, Padmanabhan P, Akbarsha MA, Gulyás B, Archunan G. Proteomic analysis of human saliva: An approach to find the marker protein for ovulation. *Reprod Biol*. 2016; 16:287-294.
15. Navazesh M. Methods for collecting saliva. *Ann N Y Acad Sci*. 1993; 694:72-77.
16. Tulunoglu O, Demirtas S, Tulunoglu I. Total antioxidant levels of saliva in children related to caries, age, and gender. *Int J Paediatr Dent*. 2006; 16:186-191.
17. Barros C, Arguello B, Jedlicki A, Vigil P, Herrera E. Scanning electron microscope study of human cervical mucus. *Gamete Res*. 1985; 12:85-89.
18. Choe JK, Khan-Dawood FS, Dawood MY. Progesterone and estradiol in the saliva and plasma during the menstrual cycle. *Am J Obstet Gynecol*. 1983; 147:557-562.
19. Gröschl M, Rauh M, Schmid P, Dörr HG. Relationship between salivary progesterone, 17-hydroxyprogesterone, and cortisol levels throughout the normal menstrual cycle of healthy postmenarcheal girls. *Fertil Steril*. 2001; 76:615-617.
20. Chatterton RT Jr, Mateo ET, Hou N, Rademaker AW, Acharya S, Jordan VC, Morrow M. Characteristics of salivary profiles of oestradiol and progesterone in premenopausal women. *J Endocrinol*. 2005; 186:77-84.
21. Gandara BK, Leresche L, Mancl L. Patterns of salivary estradiol and progesterone across the menstrual cycle. *Ann N Y Acad Sci*. 2007; 1098:446-450.
22. Alagendran S, Archunan G, Achiraman S. Prediction of ovulation in women through the occurrence of salivary fern prototype. *ICFAI J Life Sci*. 2007; 1:7-15.
23. Alagendran S, Archunan G, Bonnila Armando EO, Guzman RG. Evaluation of salivary electrolytes during normal menstrual cycle with special reference to ovulation. *Am J Appl Sci*. 2010; 7:1066-1072.
24. Fernando RS, Regas J, Betz G. Ovulation prediction and detection with the CUE Ovulation Predictor. *Hum Reprod*. 1988; 3:419-424.
25. Barbato M, Pandolfi A, Guida M. A new diagnostic aid for natural family planning. *Adv Contracept*. 1993; 9:335-340.
26. Di Sant'agnese PA, Darling RC, Perera GA, Shea E. Abnormal electrolyte composition of sweat in cystic fibrosis of the pancreas; clinical significance and

- relationship to the disease. *Pediatrics*. 1953; 12:549-563.
27. Jiménez-Reyes M, Sánchez-Aguirre FJ. Sodium and chlorine concentrations in mixed saliva of healthy and cystic fibrosis children. *Appl Radiat Isot*. 1996; 47:273-277.
 28. Syrjänen S, Lappalainen R, Markkanen H. Salivary and serum levels of electrolytes and immunomarkers in edentulous healthy subjects and in those with rheumatoid arthritis. *Clin Rheumatol*. 1986; 5:49-55.
 29. Singh V, Arora R, Bhayya D, Singh D, Sarvaiya B, Mehta D. Comparison of relationship between salivary electrolyte levels and dental caries in children with Down syndrome. *J Nat Sci Biol Med*. 2015; 6:144-148.
 30. Hegde MN, Tahiliani D, Shetty SS, Devadiga D. Salivary electrolyte as a biomarker in caries active type II diabetes-A comparative study. *Nitte Uni J Health Sci*. 2014; 4:85-89.
 31. Preethi BP, Reshma D, Anand P. Evaluation of flow rate, pH, buffering capacity, calcium, total proteins and total antioxidant capacity levels of saliva in caries free and caries active children: An *in vivo* study. *Indian J Clin Biochem*. 2010; 25:425-428.
 32. Sreebny LM. Saliva in health and disease: an appraisal and update. *Int Dent J*. 2000; 50:140-161.
 33. Lukacs JR, Largaespada LL. Explaining sex differences in dental caries prevalence: saliva, hormones, and "life-history" etiologies. *Am J Hum Biol*. 2006; 18:540-555.
 34. Temple DH. Variability in dental caries prevalence between male and female foragers from the Late/Final Jomon period: Implications for dietary behavior and reproductive ecology. *Am J Hum Biol*. 2011; 23:107-117.
 35. Rajesh KS, Zareena, Hegde S, Arun Kumar MS. Assessment of salivary calcium, phosphate, magnesium, pH, and flow rate in healthy subjects, periodontitis, and dental caries. *Contemp Clin Dent*. 2015; 6:461-465.
 36. Brunelli R, Papi M, Arcovito G, Bompiani A, Castagnola M, Parasassi T, Sampaolese B, Vincenzoni F, De Spirito M. Globular structure of human ovulatory cervical mucus. *FASEB J*. 2007; 21:3872-3876.
 37. Ceric F, Silva D, Vigil P. Ultrastructure of the human periovulatory cervical mucus. *J Electron Microsc (Tokyo)*. 2005; 54:479-484.
 38. Elstein M. Cervical mucus: its physiological role and clinical significance. *Adv Exp Med Biol*. 1982; 144:301-318.
 39. Gipson IK, Moccia R, Spurr-Michaud S, Argüeso P, Gargiulo AR, Hill JA 3rd, Offner GD, Keutmann HT. The Amount of MUC5B mucin in cervical mucus peaks at midcycle. *J Clin Endocrinol Metab*. 2001; 86:594-600.
 40. Muthukumar S, Rajkumar R, Karthikeyan K, Liao CC, Singh D, Akbarsha MA, Archunan G. Buffalo cervico-vaginal fluid proteomics with special reference to estrus cycle: heat shock protein (HSP)-70 appears to be an estrus indicator. *Biol Reprod*. 2014; 90:97.
 41. Vigil P, Cortés ME, Zúñiga A, Riquelme J, Ceric F. Scanning electron and light microscopy study of the cervical mucus in women with polycystic ovary syndrome. *J Electron Microsc (Tokyo)*. 2009; 58:21-27.
 42. Wentz AC, McCranie WM. Circulating hormone levels in a case of granulosa cell tumor. *Fertil Steril*. 1976; 27:167-170.
 43. Menárguez M, Pastor LM, Odeblad E. Morphological characterization of different human cervical mucus types using light and scanning electron microscopy. *Hum Reprod*. 2003; 18:1782-1789.
- (Received January 29, 2017; Revised March 25, 2017; Accepted April 3, 2017)

Comparison of three acute stress models for simulating the pathophysiology of stress-related mucosal disease

Bhagawati Saxena¹, Sanjay Singh^{2,*}

¹Department of Pharmacology, L. J. Institute of Pharmacy, Ahmedabad, Gujarat, India;

²Division of Pharmacology and Toxicology, Department of Pharmaceutics, Indian Institute of Technology (Banaras Hindu University), Varanasi, U.P., India.

Summary

Stress-related mucosal disease (SRMD) is highly prevalent in intensive care patients leading to increasing treatment cost and mortality. SRMD is a disease elusive of ideal treatment. Evaluation of drugs is very pertinent for the efficient and safe treatment of SRMD. It relies mainly on in vivo screening models. There are various stress models, and till date, none of them is validated for simulating the SRMD pathophysiology. The present study aims to choose the best model, which reproduce pathophysiology of SRMD, among previously established stress models. This study evaluates ulcer index, hexosamine content, microvascular permeability, and gastric content in three acute stress models (cold-restraint, restraint, and water immersion restraint). Macroscopic pictures of the ulcerogenic stomach explain that in contrast to other models, cold-restraint stress (CRS) exposure produced marked ulcers on the fundic area of the stomach. Results of the present study depicted that each stress model significantly increased ulcer index, microvascular permeability and decreased hexosamine level, however, the maximum in the case of CRS-exposed rats. Total acidity and pH of the gastric content remains unchanged in all the stress models. On the contrary, the gastric volume significantly decreased only in case of CRS, while unchanged in other stress models. The overall results revealed that the CRS resembles the pathophysiology of SRMD closely. It is the best and feasible model among all the models to evaluate drugs for the treatment of SRMD.

Keywords: Mucosal barrier, microvascular permeability, gastric mucosal blood flow, restraint stress, cold-restraint stress, water immersion restraint stress

1. Introduction

Stress-related mucosal disease (SRMD) commonly known as stress ulcer is described as continuum conditions ranging from superficial mucosal damage to deep focal mucosal damage (1). SRMD is observed in critically ill patients during a serious illness such as surgery, trauma, sepsis, severe burns, etc., within

twenty-four hours of their admittance to intensive care unit (ICU) (2,3). SRMD is a considerable reason of morbidity in addition to mortality in critically ill patients in ICU (4). Upper gastrointestinal (GI) bleeding observed in SRMD patients places critically ill patients at a high risk of death (5,6). SRMD in the ICU patients also adds to the cost of treatment by increasing the stay of patients at the hospital (2,7). Therefore, due to the above reasons, SRMD prophylaxis has become a regular practice in ICU (8). The primary goal of clinical therapy of SRMD is to prevent bleeding. Current preventive treatment strategies use histamine-2 receptor antagonists (H₂RAs), proton pump inhibitors (PPIs) and sucralfate. H₂RAs and PPIs suppress acid secretion. Sucralfate provides a protective barrier against the acid in the GI tract. These drugs have their limitations (9). H₂RAs,

Released online in J-STAGE as advance publication March 19, 2017.

*Address correspondence to:

Dr. Sanjay Singh, Division of Pharmacology and Toxicology, Department of Pharmaceutics, Indian Institute of Technology (Banaras Hindu University), Varanasi, U.P. 221005, India.
E-mail: sssingh.phe@iitbhu.ac.in

PPIs, and sucralfate are also commonly prescribed for the treatment of the peptic ulcer.

Peptic ulcer and SRMD are dissimilar in several aspects. Ordinary peptic ulcers are found mainly in the gastric antrum and the duodenal bulb, while SRMD is found majorly in acid producing area of the stomach like fundic mucosa and corpus (1). Primary pathological factor for peptic ulcer is mostly considered to be the increased acid output, and thus gastric mucosa is exposed to a very low intraluminal pH. Hyperacidity is not a primary pathological factor of SRMD, as normal or slightly decreased gastric acid volume is seen in affected patients. Rather, ischemia is considered as a major pathological factor of SRMD (1,10,11). It is reported that even without intragastric hydrochloric acid, ischemia followed by reperfusion caused histologic mucosal injury in the stomach (12). These findings suggest that the pathology of SRMD is probably related to a reduction in gastric mucosal blood flow, which leads to ischemia. The breakdown of the mucosal defensive barrier by ischemia and reperfusion allows offensive factors (low acid secretion) to produce gastric ulceration.

Treatment of SRMD remains a major challenge to health professionals and represents a disease elusive of ideal treatment. Therefore, evaluation of drugs leading to the efficient and safe treatment of SRMD is very pertinent. The improvement of new therapeutics for the treatment of SRMD relies mainly on *in vivo* screening models. From the experimental point of view, the selection of a model for producing SRMD in the stomach is highly required. Pyloric ligation, ethanol, aspirin, indomethacin-induced ulcer models are among several models frequently used for screening antiulcer action of drugs. However, these models are based on the aggravation of offensive factor, while the weakening of defensive barrier is a primary pathological factor of SRMD. Additionally, these are local models, whereas, the model that needs to reproduce the SRMD pathology should be central. SRMD have been developing in critically ill patients secondary to physiological stress (8). Currently, various stress models are available like restraint stress (RS), cold-restraint stress (CRS), water immersion restraint stress (WRS), food deprivation stress, activity wheel stress, chronic unpredictable stress, chronic foot shock stress, *etc.* SRMD is an acute stress condition. WRS, RS, and CRS models are acute stress models while food deprivation stress (13), activity wheel stress (14), chronic unpredictable stress (15), and chronic footshock stress (16) models are chronic stress models for ulcer formation. Till now, none of the existing acute stress models are studied for simulating the SRMD pathophysiology. Therefore, this study aims to select a model that imitates the pathological condition of SRMD, among previously established three acute stress models (CRS, RS, and WRS).

2. Materials and Methods

2.1. Materials

Evans blue and D-glucosamine hydrochloride were acquired from Sigma-Aldrich (St. Louis, MD, USA). All the other solvents and chemicals were purchased from Loba Chemie (Mumbai, Maharashtra, India).

2.2. Animals

Experimentations were conducted on male Wistar albino rats (180-220 g). Animals were issued from the Central Animal House, Institute of Medical Sciences, Banaras Hindu University. The animals were kept in polypropylene cages. The temperature of $25 \pm 10^\circ\text{C}$, relative humidity of 45-55%, and a 12:12 h light/dark cycle was maintained. The rats were fed commercial food pellets (Doodh dhara pashu ahar, India) as well as water *ad libitum*. Institutional Ethical Committee approved all the experimental methodology. All experimental procedures were conducted as per committee for the purpose of control and supervision of experiments on animals (CPCSEA).

2.3. Stress models

2.3.1. Cold-restraint stress

In a cold-restraint stress (CRS) model, the rats ($n = 6$) fasted overnight and immobilized by tying the fore and hind limbs separately on a wooden block with an adhesive tape. Finally, all the rats were kept at $4-7^\circ\text{C}$ for two hours (17).

2.3.2. Restraint stress

In a restraint stress (RS) model, the rats ($n = 6$) were immobilized for four hours in restraint cages ($5 \times 5 \times 20 \text{ cm}^3$) after overnight of fasting at room temperature during the early phase of the light cycle (18).

2.3.3. Water immersion restraint stress

In a water immersion restraint stress (WRS) model, rats fasted overnight and immobilized similar to RS then immersed vertically up to the xiphoid in the water bath ($20-25^\circ\text{C}$). The body was wiped dry after four hours of stress, and the rats were then returned to their home cages (19).

2.4. Estimation of ulcer index and hexosamine content

Rats ($n = 6$) were randomly assigned to control and three stress groups (CRS, RS, and WRS). Except for control group, other groups were exposed to CRS, RS, and WRS, respectively. Lastly, all the animals were

killed by cervical dislocation, and their stomachs were taken out for estimation of ulcer index and hexosamine. Hexosamine is an index of mucosal content.

2.4.1. Ulcer index

Ulcer scoring was done as per Sanyal (20). The scoring as per the severity of the ulcer has been explained in Table 1. The score of the ulcers as per severity was determined by a person unaware of the experimental protocol. Ulcer index is the summation of the number of ulcers multiplied by their score per stomach. Ulcer index = 1 X (No. of ulcer of score 1) + 2 X (No. of ulcer of score 2) + 3 X (No. of ulcer of score 3) + 4 X (No. of ulcer of score 4).

2.4.2. Hexosamine estimation

The content of hexosamine was estimated as per Dische (21) with slight modification. Briefly, 0.5 mL of the scrapped mucosa of the stomach was taken, and mixed with 0.5 mL of acetylacetone reagent. Then 0.1 mL of sodium carbonate (0.5 N) was added to 1 mL of the mixture. The mixture was kept on boiling water bath for 20 min and then cooled to room temperature. 1.5 mL of glacial acetic acid (90%) was added to above mixture. The absorbance was measured after 30 min by the spectrophotometer at 530 nm (λ_{\max}). Distilled water was used as blank. A standard curve was prepared by using D-glucosamine hydrochloride and concentration of hexosamine was expressed in mg/g of tissue.

2.5. Estimation of microvascular permeability

The microvascular permeability was measured by injecting Evans blue (10 mg/kg) intravenously through the tail vein under light halothane anesthesia. Animals of all groups except control were exposed to CRS, WRS, RS, respectively. Finally, all the rats were killed by cervical dislocation. Dye from the gastric tissue was extracted, and measured as per method adopted by Katayama (22).

Briefly, the gastric content was soaked overnight in 2 mL of 3.5 N KOH. Then, 18 mL of a mixed solution of 4 N H_3PO_4 and acetone (1.75:16.25) was added to make the volume up to 25 mL. The tube was shaken vigorously and centrifuged at 3,000 rpm for 15 min. The color intensity of the supernatant was measured at 620 nm (λ_{\max}) by the spectrophotometer. The amount of dye recovered from the gastric contents was expressed as $\mu\text{g/g}$ of gastric tissue.

2.6. Estimation of gastric volume, acidity and pH of gastric content of pyloric ligated rats

Rats were randomly divided into four groups (control, CRS, RS, and WRS) of six animals each. In all the

Table 1. Score and severity of ulcer

Score	Features
0	No ulcer
1	Pin point ulcer and changes limited to superficial layers of mucosa
2	Ulcer less than 1 mm in size
3	Ulcer more than 1 mm but less than 2 mm in sizes.
4	Ulcer more than 2 mm or perforation of ulcer.

animals, pyloric ligation was done as per Debnath (23). Briefly, animals were anesthetized by intraperitoneal injection of pentobarbitone (35 mg/kg). The abdomen of the anesthetized rat was opened, and a knot of the thread was tied around the pyloric sphincter. The stomach was put back carefully, and the abdomen wall was closed with interrupted sutures. The skin was cleaned from any blood spots and bleeding, and the collodion was applied over the wound. The rats were kept in a separate cage and allowed for recovery. All the pyloric ligated (PL) rats of all groups except control were exposed to CRS, WRS, RS, respectively.

Lastly, all the animals were killed by cervical dislocation and evaluation of acidity, volume, and pH of gastric content was done. The gastric content was collected in a centrifuge tube and centrifuged for ten mins at 1,000 rpm. The volume was noted as gastric volume. The pH of this solution was recorded with the help of a pH meter. 1 mL of supernatant was pipetted out and diluted up to 10 mL with distilled water. The solution was titrated with NaOH (0.01 N) using Topfer's agent and phenolphthalein as an indicator. Titration was done until the solution turns to pink color. It is used for detection and estimation of hydrochloric acid and total acidity in gastric fluids. The volume of NaOH was noted. Acidity ($\mu\text{Eq/mL}$) can be expressed as: Acidity = (Vol. of NaOH in mL \times Normality \times 1,000).

2.7. Statistical analysis

The values were expressed as mean \pm SEM. GraphPad Prism 5 (San Diego, CA, USA) was used to analyze the data. Statistical significance of all the experimental data were analyzed by one-way ANOVA followed by Tukey test. A *p*-value less than 0.05 was considered to be statistically significant in all the analysis.

3. Results

3.1. Effect of CRS, RS, and WRS on ulcer index and hexosamine content

The macroscopic analysis and ulcer index in control, CRS, RS, and WRS models, respectively are represented in Figures 1 and 2. Macroscopic pictures of the ulcerogenic stomach illustrate that in contrast to other models, CRS exposure produced marked ulcers on the fundic area of the stomach. One-way ANOVA

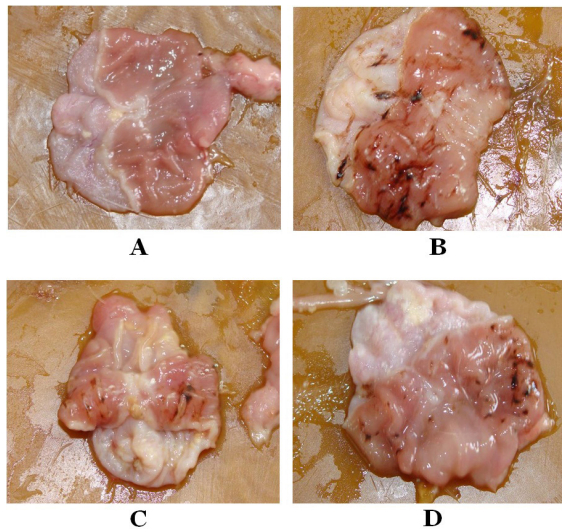


Figure 1. Macroscopic analyses showing ulcerogenesis in the stomach of rats in different stress models. Macroscopic pictures of stomach of (A) rat without stress and rats exposed to (B) CRS, (C) RS, and (D) WRS.

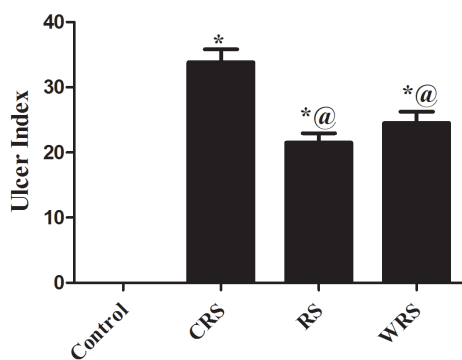


Figure 2. Ulcer index in control, CRS, RS and WRS exposed rats. Results are expressed in each column as the mean ± SEM ($n = 6$). * $p < 0.05$ and [@] $p < 0.05$ compared to control and CRS group, respectively (one way ANOVA followed by Tukey's test).

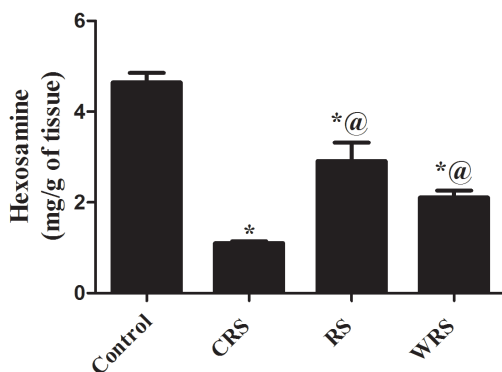


Figure 3. Hexosamine content in control, CRS, RS, and WRS exposed rats. Results are expressed in each column as the mean ± SEM ($n = 6$). * $p < 0.05$ and [@] $p < 0.05$ compared to control and CRS group, respectively (one way ANOVA followed by Tukey's test).

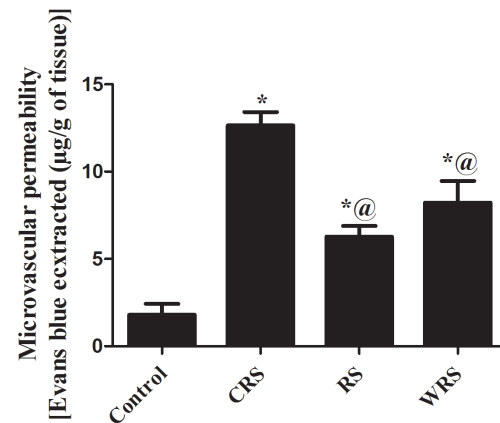


Figure 4. Microvascular permeability in control, CRS, RS, and WRS exposed rats. Results are expressed in each column as the mean ± SEM ($n = 6$). * $p < 0.05$ and [@] $p < 0.05$ compared to control and CRS group, respectively (one way ANOVA followed by Tukey's test).

revealed significant differences in ulcer index among the groups [$F(3, 23) = 536.7, p < 0.0001$]. All the stress models (CRS, RS, and WRS) increased ulcer index significantly in comparison to control. However, the ulcer index is maximum in the CRS-exposed rats.

The content of hexosamine in three stress models, as well as in control is demonstrated in Figure 3. One-way ANOVA revealed significant differences in the hexosamine content among the groups [$F(3, 23) = 39.02, p < 0.0001$]. All the stress models (CRS, RS, and WRS) significantly decreased hexosamine level in comparison to control. Hexosamine content decreased maximum in CRS model.

3.2. Effect of CRS, RS, and WRS on microvascular permeability

Figure 4 elucidates the microvascular permeability measured in all the groups. One-way ANOVA aptly demonstrated significant differences in microvascular permeability in terms of the Evans blue concentrations among the groups [$F(3, 23) = 28.29, p < 0.0001$]. All the stress models (CRS, RS, and WRS) increased microvascular permeability significantly in comparison to control. Microvascular permeability increased maximum in CRS model.

3.3. Effect of CRS, RS, and WRS on gastric content of pyloric ligated rats

The effect of CRS, RS, and WRS on acidity, pH, and volume of gastric content in PL rats is shown in Figure 5. No significant difference in acidity and pH of gastric content among the groups were found. However, gastric volume decreased significantly only in PL rats exposed to CRS ($p < 0.05$).

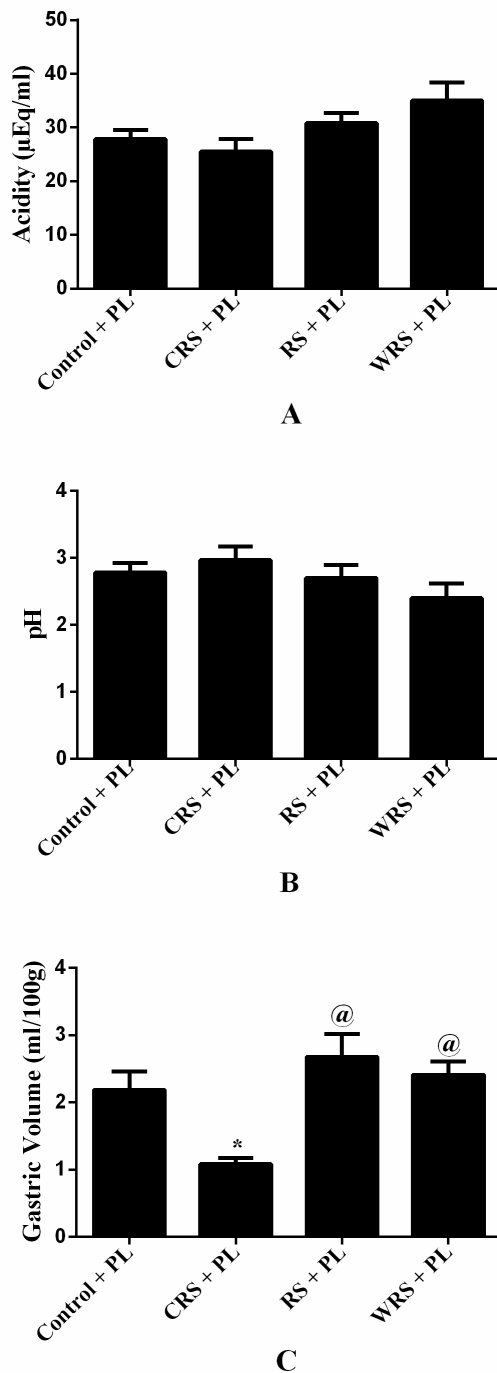


Figure 5. Effect of different stress models on gastric content of pyloric ligated rats. Bar diagram representing (A) acidity, (B) pH and (C) gastric volume of gastric content of pyloric ligated (PL) rats in different stress models (CRS, RS, and WRS). Results in each column are expressed as the mean \pm SEM ($n = 6$). * $p < 0.05$ and @ $p < 0.05$ compared to control + PL and CRS + PL group, respectively (one way ANOVA followed by Tukey's test).

4. Discussion

Results of the present study demonstrated that the CRS exposure produced marked ulcers on the fundic area of the stomach, contrary to other stress models. Each of the stress models significantly increased ulcer index and microvascular permeability while decreased hexosamine

level. However, these stress-induced changes in ulcer index, microvascular permeability and hexosamine occurred to a greater extent in the case of CRS model. Total acidity and pH of the gastric content remains unchanged in all the stress models. The gastric volume significantly decreased in case of CRS while unchanged in other stress models.

Macroscopic pictures elucidate that significant ulcers were clearly visible in the fundic area of the stomach of CRS-exposed rats. The well known characteristic feature of SRMD is that the ulcers are found in the fundic area of the stomach (1). Hexosamine level declined in all the stress models. Hexosamine level decreased is the maximum in the CRS model. Hexosamine is the marker of the mucosal barrier. Thus, the mucosal barrier is considerably damaged in the CRS. Decreased mucosal blood flow results in the decreased mucosal secretion (10), which is the ultimate cause of decreased mucosal content.

Results depict that all the stress models lead to an increase in microvascular permeability. Earlier it was reported that stress decreased gastric mucosal blood flow (24). Decreased blood flow results in ischemia followed by reperfusion. Ischaemia followed by reperfusion increased gastric microvascular permeability (25). Microvascular permeability increased maximum in the case of CRS model. The gastric blood flow was markedly influenced by the exposed temperature (26). Therefore, cold exposure to immobilized rats might decrease the mucosal blood flow greater than other immobilization stress. Thus, a remarkable increase in microvascular permeability in the CRS ulcer may be the result of ischemia followed by reperfusion. As ischemia followed by reperfusion is an important pathological factor of SRMD, CRS model emulates the pathophysiology of SRMD.

In the present study, the pylorus ligated rats were exposed to CRS, RS, and WRS. Stress-exposed to PL rats results in hemorrhagic ulcers in the stomach. The gastric volume significantly decreased in case of CRS-exposed PL rats, while unchanged in other rats. However, the total acidity, as well as pH of the gastric content in all the stress models remained unchanged. The above observations represent that gastric secretion is lowered in the CRS-exposed rats without affecting the acidity and pH of released acid. The acid secretion is not a primary characteristic feature of SRMD pathology. Contrary to the patients with severe burn and head injury, in most of the critically ill patients acid secretion in the GI tract is normal or low (9). Thus, as decreased gastric volume was observed in CRS-exposed rats, it can be predicted that CRS model simulates the SRMD pathophysiology in this aspect also.

The overall results of the present study illustrated that the CRS resembles the pathophysiology of SRMD closely. It is the best and feasible model among all the models to evaluate drugs for the treatment of SRMD.

Acknowledgements

This work was supported by a grant from the Council of Scientific and Industrial Research (CSIR), New Delhi, India in the form of Senior Research Fellowship.

References

1. Spirt MJ. Stress-related mucosal disease: Risk factors and prophylactic therapy. *Clin Ther.* 2004; 26:197-213.
2. Brett S. Science review: The use of proton pump inhibitors for gastric acid suppression in critical illness. *Crit Care.* 2005; 9:45-50.
3. Brown TH, Davidson PF, Larson GM. Acute gastritis occurring within 24 hours of severe head injury. *Gastrointest Endosc.* 1989; 35:37-40.
4. Tabeefer H, Beigmohammadi MT, Javadi MR, Abdollahi M, Mahmoodpoor A, Ahmadi A, Honarmand H, Najafi A, Mojtahedzadeh M. Effects of pantoprazole on systemic and gastric pro- and anti-inflammatory cytokines in critically ill patients. *Iran J Pharm Res.* 2012; 11:1051-1058.
5. Cook DJ, Fuller HD, Guyatt GH, Marshall JC, Leasa D, Hall R, Winton TL, Rutledge F, Todd TJ, Roy P, Lacroix J, Griffith L, Willan A. Risk factors for gastrointestinal bleeding in critically ill patients. Canadian critical care trials group. *N Engl J Med.* 1994; 330:377-381.
6. Zuckerman GR, Shuman R. Therapeutic goals and treatment options for prevention of stress ulcer syndrome. *Am J Med.* 1987; 83:29-35.
7. Cook DJ, Griffith LE, Walter SD, Guyatt GH, Meade MO, Heyland DK, Kirby A, Tryba M. The attributable mortality and length of intensive care unit stay of clinically important gastrointestinal bleeding in critically ill patients. *Crit Care.* 2001; 5:368-375.
8. Sesler JM. Stress-related mucosal disease in the intensive care unit: An update on prophylaxis. *AACN Adv Crit Care.* 2007; 18:119-128.
9. Metz DC. Preventing the gastrointestinal consequences of stress-related mucosal disease. *Curr Med Res Opin.* 2005; 21:11-18.
10. Beejay U, Wolfe MM. Acute gastrointestinal bleeding in the intensive care unit. The gastroenterologist's perspective. *Gastroenterol Clin North Am.* 2000; 29:309-336.
11. Navab F, Steingrub J. Stress ulcer: Is routine prophylaxis necessary? *Am J Gastroenterol.* 1995; 90:708-712.
12. Yasue N, Guth PH. Role of exogenous acid and retransfusion in hemorrhagic shock-induced gastric lesions in the rat. *Gastroenterology.* 1988; 94:1135-1143.
13. Yi I, Stephan FK. The effects of food deprivation, nutritive and non-nutritive feeding and wheel running on gastric stress ulcers in rats. *Physiol Behav.* 1998; 63:219-225.
14. Houser VP, Cash RJ, van Hart DA. The effects of metiamide on the "activity-stress" ulcer in rats. *Psychopharmacologia.* 1975; 44:37-41.
15. Rasheed N, Ahmad A, Singh N, Singh P, Mishra V, Banu N, Lohani M, Sharma S, Palit G. Differential response of a 68930 and sulphiride in stress-induced gastric ulcers in rats. *Eur J Pharmacol.* 2010; 643:121-128.
16. Pramanik SS, Sur TK, Debnath PK, Bhattacharyya D. Effect of Pueraria tuberosa tuber extract on chronic foot shock stress in Wistar rats. *Nepal Med Coll J.* 2010; 12:234-238.
17. Kulkarni MP, Juvekar AR. Attenuation of acute and chronic restraint stress-induced perturbations in experimental animals by nelumbo nucifera gaertn. *Indian J Pharm Sci.* 2008; 70:327-332.
18. Shah ZA, Gilani RA, Sharma P, Vohora SB. Attenuation of stress-elicited brain catecholamines, serotonin and plasma corticosterone levels by calcined gold preparations used in indian system of medicine. *Basic Clin Pharmacol Toxicol.* 2005; 96:469-474.
19. Ueyama T, Saika M, Koreeda C, Senba E. Water immersion-restraint stress induces expression of immediate-early genes in gastrointestinal tract of rats. *Am J Physiol.* 1998; 275:G287-295.
20. Sanyal AK, Pandey BL, Goel RK. The effect of a traditional preparation of copper, tamrabhasma, on experimental ulcers and gastric secretion. *J Ethnopharmacol.* 1982; 5:79-89.
21. Dische Z, Shettles LB. A specific color reaction of methylpentoses and a spectrophotometric micromethod for their determination. *J Biol Chem.* 1948; 175:595-603.
22. Katayama S, Shionoya H, Ohtake S. A new method for extraction of extravasated dye in the skin and the influence of fasting stress on passive cutaneous anaphylaxis in guinea pigs and rats. *Microbiol Immunol.* 1978; 22:89-101.
23. Debnath PK, Gode KD, Das DG, Sanyal AK. Effects of propranolol on gastric secretion in albino rats. *Br J Pharmacol.* 1974; 51:213-216.
24. Bregonzio C, Armando I, Ando H, Jezova M, Baiardi G, Saavedra JM. Anti-inflammatory effects of angiotensin II AT1 receptor antagonism prevent stress-induced gastric injury. *Am J Physiol Gastrointest Liver Physiol.* 2003; 285:G414-423.
25. Mojzis J, Pomfy M, Kohut A, Benes L, Nicak A, Mirossay L. Effect of stobadine on gastric mucosal injury after ischaemia/reperfusion. *Physiol Res.* 1996; 45:399-403.
26. Arai I, Muramatsu M, Aihara H. Body temperature dependency of gastric regional blood flow, acid secretion and ulcer formation in restraint and water-immersion stressed rats. *Jpn J Pharmacol.* 1986; 40:501-504.

(Received December 12, 2016; Revised February 12, 2017; Accepted February 26, 2017)

1,2,3-Triazolyl esterization of PAK1-blocking propolis ingredients, artemillin C (ARC) and caffeic acid (CA), for boosting their anti-cancer/anti-PAK1 activities along with cell-permeability

Hideaki Takahashi^{1,*}, Binh Cao Quan Nguyen^{2,*}, Yoshihiro Uto¹, Md Shahinozzaman^{2,3}, Shinkichi Tawata², Hiroshi Maruta^{4,**}

¹Tokushima University, Tokushima, Japan;

²PAK Research Center (Lab), Okinawa, Japan;

³Kagoshima University, Kagoshima, Japan;

⁴PAK Research Center (Office), Melbourne, Australia.

Summary

Artemillin C (ARC) and caffeic acid (CA) are among the major anti-cancer ingredients of propolis, and block the oncogenic/melanogenic/ageing kinase PAK1. However, mainly due to their COOH moiety, cell-permeability of these herbal compounds is rather limited. Thus, in this study, in an attempt to increase their cell-permeability without any significant loss of their water-solubility, we have esterized both ARC and CA with the water-soluble 1,2,3-triazolyl alcohol through Click Chemistry. We found that this esterization boosts the anti-cancer activity of ARC and CA by 100 and over 400 folds, respectively, against the PAK-dependent growth of A549 lung cells, but show no effect on the PAK1-independent growth of B16F10 melanoma cells. Confirming this "selective" toxicity, these esters are still capable of blocking the kinase PAK1 strongly in cell culture (with IC₅₀ around 5 μM), and the anti-PAK1 activity of 15A (ARC ester) and 15C (CA ester) appears to be 30-fold and 140-fold higher than ARC and CA, respectively. The 15A and 15C are 8-fold and 70-fold more cell-permeable (through the multi-drug resistant cell line EMT6) than ARC and CA, respectively. These data altogether suggest that both 15A and 15C would be far more useful than propolis for the treatment of a wide variety of PAK1-dependent diseases/disorders such as cancers, Alzheimer's diseases (AD), hypertension, diabetes (type 2), and hyper-pigmentation.

Keywords: PAK1, artemillin C, caffeic acid, click chemistry, triazolyl esters

1. Introduction

The bee product called "propolis", an ethanol extract of bee cumb, has been well known to be among potent antibiotics effective against both bacteria and viruses since the ancient Egyptian era. Around the late 1980s, it was discovered as a potent anti-cancer herb (1). The anti-cancer ingredients of propolis depend on the areas where each propolis is harvested. For instance, the

major anti-cancer ingredient in Brazilian green propolis is artemillin C (ARC), whereas those in European, US, Far-East, and Oceanian propolis are caffeic acid (CA) and its ester called caffeic acid phenethyl ester (CAPE) (1,2). Interestingly, both ARC and CA as well as CAPE block the oncogenic/melanogenic/ageing kinase PAK1 (3,4). Most interestingly, Okinawa propolis, based on nymphaeols A, B and C that inhibit the kinase PAK1 directly, extends the healthy lifespan of *C. elegans* (5).

However, IC₅₀ of ARC, CA and CAPE against the growth of A549 lung cancer cells are 25, 100 and 10 μM, respectively. The major reason for the relatively high IC₅₀ of ARC and CA is their COOH moiety, their negative charge which prevents their permeability through negatively charged phospholipid-based plasma membranes. In support of this notion, CAPE, a natural ester of CA, is 10 times more potent to inhibit the

Released online in J-STAGE as advance publication April 24, 2017.

*These authors contributed equally to this works.

**Address correspondence to:

Dr. Hiroshi Maruta, PAK Research Center, Melbourne, Australia.

E-mail: maruta20420@yahoo.co.jp

cancer growth than CA. More recently, 1,2,3-triazolyl esterization of PAK1-blocking compounds ursolic acid (UA) and ketorolac boosts their anti-cancer activity by 200-fold and 500-fold, respectively (6,7). Accordingly, in this study, through the same Click Chemistry, we have esterized both ARC and CA with 1,2,3-triazolyl alcohol, in an attempt to boost their cell-permeability without loss of their water-solubility.

2. Materials and Methods

2.1. Cell lines and reagents

Human lung cancer (A549) and murine melanoma (B16F10) cell lines were obtained from American Type Culture Collection (Rockville, MD, USA), and mouse breast cancer cell line (EMT6) supplied by Dr. Shin-ichiro Masunaga, Kyoto University, Kyoto, Japan. Artepillin C (ARC) was synthesized by us as previously described (8). Caffeic Acid (CA) was purchased from Tokyo Chemicals (Tokyo, Japan), while propargyl alcohol and 2-azidoanisole were obtained from Sigma-Aldrich (St. Louis, MO, USA).

2.2. Synthesis of 15A from artepillin C (ARC) and 15C from caffeic acid by Click Chemistry

2.2.1. Preparation of 1,2,3-triazolyl derivative of artepillin C (ARC) (15A or PRC-15A)

Step a: To solution of compound **1** (ARC, 161 mg, 536 μmol) in propargyl alcohol (6 mL) at 0°C, EDC (100 μL , 567 μmol) and DMAP (17 mg, 139 μmol) were added. The reaction mixture was stirred at room temperature and monitored by TLC till its completion in around a day. The crude mixture was then evaporated. The residue was purified through flash silica gel column chromatography (n-hexane:EtOAc = 3:1) to give pure **2** (100 mg, 295 μmol , 55% yield) as a pale yellow solid. $^1\text{H-NMR}$ (400 MHz, CDCl_3) δ = 7.66 (d, J = 15.9 Hz, 1H), 7.17 (s, 2H), 6.29 (d, J = 15.9 Hz, 1H), 5.30 (t, J = 7.30 Hz, 2H), 4.79 (d, J = 2.27 Hz, 2H), 3.33 (d, J = 7.14 Hz, 4H), 2.49 (t, J = 2.44 Hz, 1H), 1.77 (d, J = 8.76 Hz, 12H).

Step b: To solution of compound **2** (52 mg, 154 μmol) in t-BuOH:H₂O (2:1, 4 mL), sodium ascorbate (6 mg, 30.3 μmol) and CuSO₄ (4 mg, 25.1 μmol) were added at room temperature. To this mixture, 2-azidoanisole (0.5 M solution, 310 μL , 155 μmol) was added and the reaction mixture was sonicated at 42°C till its completion around 7 h, monitored by TLC. The crude mixture was extracted with ethyl acetate (3 \times 20 mL) and organic layer was washed with water and brine, then dried over sodium sulfate and purified through flash silica gel column chromatography (n-hexane:EtOAc = 3:1) to give pure **3** (52 mg, 107 μmol , 69% yield) as a pale yellow solid. $^1\text{H-NMR}$ (400 MHz, CDCl_3) δ = 8.20 (s, 1H), 7.77 (d, J

= 7.79 Hz, 1H), 7.63 (d, J = 16.1, 1H), 7.42 (t, J = 7.78 Hz, 1H), 7.15 (s, 2H), 7.12-7.07 (m, 2H), 6.30 (d, J = 15.6 Hz, 1H), 5.42 (s, 2H), 5.28 (t, J = 6.49 Hz, 2H), 3.89 (s, 3H), 3.32 (d, J = 7.27 Hz, 4H), 1.76 (d, J = 7.27, 12H). HRMS calcd for C₂₉H₃₄N₃O₄ (M+H)⁺ m/z 488.2549, found m/z 488.2586.

2.2.2. Preparation of 1,2,3-Triazolyl derivative of caffeic acid (CA) (15C or PRC-15C)

Step c: To solution of compound **4** (CA, 382 mg, 2.12 mmol) in DMF (3 mL) at 0°C, EDC.HCl (423 mg, 2.21 mmol) and DMAP (72 mg, 589 μmol) were added. To this solution, propargyl alcohol (400 μL , 6.87 mmol) was added and the reaction mixture was stirred at room temperature for 17 h. After quenching the reaction with cooled HCl aq. (0.5 M, 20 mL), crude product was extracted with ethyl acetate:n-hexane (1:1) three times. Organic layer was washed with aqueous solution of saturated sodium hydrogen carbonate and brine, and then dried over sodium sulfate. This crude product was purified through flash silica gel column chromatography (n-hexane:EtOAc = 1:1) to give pure **5** (143 mg, 655 μmol , 31% yield) as a milky white solid. $^1\text{H-NMR}$ (400 MHz, CDCl_3) δ = 7.62 (d, J = 16.1 Hz, 1H), 7.07 (d, J = 2.08 Hz, 1H), 7.00 (d, J = 8.00 Hz, 1H), 6.87 (d, J = 8.30 Hz, 1H), 6.27 (d, J = 16.1 Hz, 1H), 4.80 (d, J = 2.60 Hz, 2H), 2.50 (t, J = 2.60 Hz, 1H).

Step d: To solution of compound **5** (130 mg, 595 μmol) in THF:H₂O (1:1, 4 mL), sodium ascorbate (61 mg, 308 μmol) and CuSO₄ (17 mg, 107 μmol) were added at room temperature. To this mixture, 2-azidoanisole (0.5 M solution, 1.20 mL, 600 μmol) was added and the reaction mixture was stirred at room temperature till its completion around 5 h. The crude mixture was extracted with ethyl acetate (3 \times 20 mL). Organic layer was washed with water and brine, and then dried over magnesium sulfate. Without column chromatography, the pure **6** (185 mg, 504 μmol) was obtained in 85% yield as a milky white powder. $^1\text{H-NMR}$ (400 MHz, CD₃OD) δ = 8.37 (s, 1H), 7.64 (d, J = 8.04 Hz, 1H), 7.58 (d, J = 15.6 Hz, 1H), 7.50 (t, J = 7.92 Hz, 1H), 7.23 (d, J = 8.30 Hz, 1H), 7.12 (t, J = 7.79 Hz, 1H), 7.02 (d, J = 2.08 Hz, 1H), 6.93 (d, J = 8.04 Hz, 1H), 6.75 (d, J = 8.30 Hz, 1H), 6.28 (d, J = 15.6 Hz, 1H), 5.35 (s, 2H), 3.89 (s, 3H). HRMS calcd for C₁₉H₁₈N₃O₅ (M+H)⁺ m/z 368.1246, found m/z 368.1250.

2.3. Assay for anti-cancer activity in cell culture

2.3.1. MTT and trypan blue assays for anti-cancer activity against A549 lung cancer and B16F10 melanoma cells

The number of viable cells after treatment with ARC or CA was measured by MTT assay as described previously

(7,9). The number of viable cells after treatment with "15A" or "15C" was measured by Trypan blue assay in a hemocytometer as described previously (7,9), because both "15A" and "15C" themselves interferes with MTT-based colorimetry, as they are converted to colored "azo" dyes as is MTT by mitochondrial reductase. Briefly, A549 or B16F10 cells (2×10^5 cells/well) were seeded for 24 h, and then treated with either ARC, CA or their esters ("15A" or "15C") at the indicated concentrations for 96 h, to measure the number of viable cells by the corresponding protocol. The number of viable cells from non-treated samples was used as the negative control for calculating the anti-cancer activity of each test compound.

2.3.2. Crystal violet assays for anti-cancer activity against multi-drug resistant cancer cell line (EMT6)

EMT6 cells (2×10^3 cells/well) were treated with test acids or esters such as "15A" and "15C" at various concentrations for 24 h, and their viability/growth was measured by crystal violet assay as previously described (10) at the wavelength 570 nm.

2.4. Anti-PAK1 (kinase) assay in cell culture

The kinase activity of PAK1 in A549 cancer cells treated with either "15A" or "15C", in comparison with those of ARC or CA was assayed according to the procedure ("Macaroni-Western" ATP-Glo kinase assay) previously described (9). Briefly, A549 cells (2×10^5 cells/well) were seeded for 24 h, and then treated with "15A" or "15C" at two concentrations (1 and 5 μ M), in comparison with ARC (100 and 300 μ M) or CA (400 and 1200 μ M), for 24 h. After the drug treatment, cells were lysed, and PAK1 was immune-precipitated (IP) with anti-PAK1 antibody conjugated with protein A-beads, and after each IP was washed with saline thoroughly, the IP (PAK1) was incubated with ATP and MBP (myelin basic protein), substrates for the kinase, for 60 min with continuous shaking, and the resultant reaction mixture was further incubated with ATP_Glo kinase assay kit for 30 min, to measure the amount of remaining ATP by fluorometry. PAK1 activity from the non-treated cells was used as the negative control for calculating the anti-PAK1 activity of four test compounds.

2.5. Uptake of herbal acids (ARC or CA) and their esters into cells

To compare the uptake between acids and their esters into cells, we have chosen the multi-drug resistant (MDR) cancer cell line (EMT6) which could survive 30-100 μ M of these PAK1-blockers at least for 12 h. The IC_{50} of ARC and "15A" against the growth of this cell line for 24 h were 169 μ M and 22 μ M, respectively, indicating that this esterization boosts the toxicity

Table 1. Increase in anti-cancer activity of several herbal acids by their esterization

Items	IC_{50} (μ M)		
	A549	B16F10	EMT6
ARC	25	ND	170
15A (ester of ARC)	0.25	> 1	22
CA	100	ND	1,000
15C (ester of CA)	0.225	> 1	8
Ketorolac ^a	13	30	4,000
15K (ester of Ketorolac) ^a	0.024	0.006	450
UA ^b	20	ND	ND
13U (ester of UA) ^b	0.10	ND	ND

^areference 7, ^breference 6, ND: not determined.

towards EMT6 cells by 8-fold (see Table 1). The IC_{50} of CA and "15C" against the growth of this cell line for 24 h were 1 mM and 8 μ M, respectively, indicating that this esterization boosts the toxicity towards EMT6 cells by 125-fold (see Table 1). To compare the uptake between ARC and 15A or between CA and 15C, this cancer cell line was treated with either ARC or 15A at 100 μ M for 24 h. However, to compare the uptake between CA and 15C, this cancer cell line was treated with either CA (100 μ M) or 15C (30 μ M) for 24 h, simply because 100 μ M of 15C is too toxic for even 12 h treatment of EMT6 cells. Their uptake into 1×10^5 cells mainly during the indicated hours was quantitated by separation of the original herbal acids and their esters taken by cells through HPLC column chromatography as described previously (7), and the amount of each compound was estimated by photometry at the wavelength 322 nm (for detail, see the legend of Figure S1). After 12 h, the cell content of these esters was significantly reduced (see Figure 6), mainly due to both their cytotoxicity and conversion to pigments (detected at wavelength 500-600 nm) by mitochondrial reductase which also converts the tetrazolium MTT to a formazan product(s).

2.6. Statistical analysis

Data are expressed as mean values with their standard errors. Statistical comparisons were performed by oneway ANOVA followed by Duncan's multiple-range test. Statistical analysis was conducted using SAS (release 9.2; SAS Institute, Cary, NC, USA) and $p < 0.05$ was considered significant.

3. Results and Discussion

3.1. Preparation of 1,2,3-triazolyl esters from artemillin C (ARC) and caffeic acid (CA) through Click Chemistry

Both Artemillin C (ARC) and caffeic acid (CA), the

two major anti-cancer and PAK1-blocking ingredients in propolis, have the carboxyl moiety that hampers their cell-permeability. CAPE (caffeic acid phenethyl ester), a natural ester of CA in propolis, is 10 folds more potent than CA for inhibiting cancer cell growth. However, CAPE is less water-soluble than CA or ARC. Thus, in this study, we try to develop a far more cell-permeable and yet water-soluble ester of both ARC and CA. 1,2,3-Triazolyl alcohol is a positively charged water-soluble alcohol, and its esters with two acidic PAK1-blockers called ursolic acid (UA, a triterpene from rosemary leaves) and ketorolac (a synthetic pain-killer) turned out to be both highly cell-permeable and water-soluble, and strongly block PAK1 in cell culture (6,7).

Similarly, as summarized in Figures 1 and 2, we have synthesized the 1,2,3-triazolyl esters called 15A and 15C from ARC and CA, respectively, through the "two-step" Click Chemistry, with the relatively high "over-all" yield (around 40% and 25%, respectively), in an attempt to boost the cell-permeability of these two herbal acids abundant in propolis.

3.2. Increase in the anti-cancer activity of artepillin C (ARC) and caffeic acid (CA) by esterization with 1,2,3-triazolyl alcohol

As summarized in Figure 3, ARC inhibits the growth of A549 lung cancer cells with the IC_{50} around 25 μ M, while its 1,2,3-triazolyl ester called 15A inhibits the growth of the same cancer cells with the IC_{50} around 250 nM. Thus, this esterization boosts the anti-cancer activity of ARC by 100 folds.

CA inhibits the growth of the same cancer cells with the IC_{50} around 100 μ M as previously published (11). As shown in Figure 4, its 1,2,3-triazolyl ester called 15C inhibits their growth with the IC_{50} around 225 nM, indicating that 15C is over 400 folds more potent

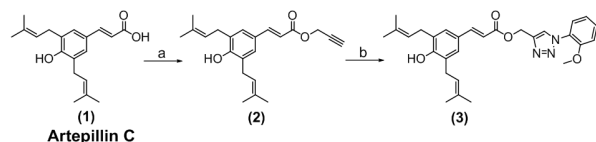


Figure 1. Click chemistry turning artepillin C (ARC) into 15A (or PRC-15A). (A) Propargyl alcohol, EDC·HCl, DMAP, rt, 55% yield; (B) 2-Azidoanisole, sodium ascorbate, $CuSO_4$, THF:H₂O (1:1), rt, 69% yield.

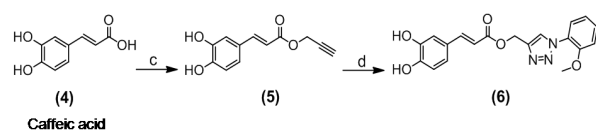


Figure 2. Click chemistry turning caffeic acid (CA) into 15C (or PRC-15C). (C) Propargyl alcohol, EDC·HCl, DMAP, rt, 31% yield; (D) 2-Azidoanisole, sodium ascorbate, $CuSO_4$, THF:H₂O (1:1), rt, 85% yield.

than CA as the anti-cancer drug. Among the CA esters, CAPE is the best known herbal compound abundant in propolis, and inhibits the growth of cancer cells with the IC_{50} around 10 μ M (11). Recently a more potent CA ester called 10C was developed, and 10C directly inhibits the enzyme called AKR (aldo-keto reductase) 1B10 with the IC_{50} around 6 nM, while CAPE inhibits AKR1B10 with the IC_{50} around 80 nM (11). However, 10C inhibits the growth of AKR-over-expressing brain cancer cell line with the IC_{50} around 1 μ M (11), suggesting that its cell-permeability is still rather poor. Thus, 15C is so far the most potent cancer-killing CA ester.

As summarized in Table 1, however, either 15A or 15C showed no significant effect on the PAK1-independent growth of B16F10 melanoma cells up to 1 μ M. Since this melanoma cell line is clearly 4-fold more sensitive to 15K, the 1,2,3-triazolyl ester of

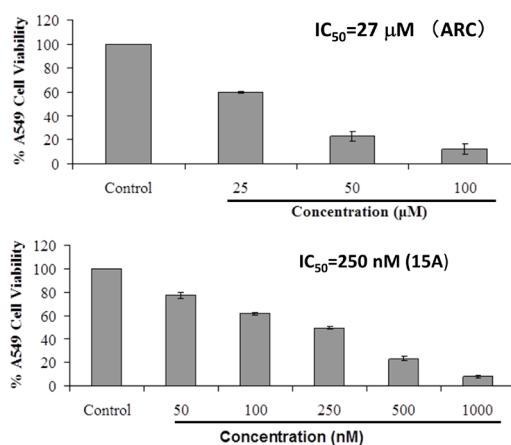


Figure 3. Increase in anti-cancer activity of artepillin C (ARC) against A549 cancer cells by its esterization. A549 lung cancer cells were treated with either ARC or 15A at indicated concentrations for 96 h, stained with trypan blue, and the viable (non-stained) cells were counted. The IC_{50} of 15A is around 250 nM, indicating that the esterization of ARC boosted its anti-cancer activity by over 100 folds. The results are mean \pm SE. Data have the statistical significance at $p \leq 0.01$.

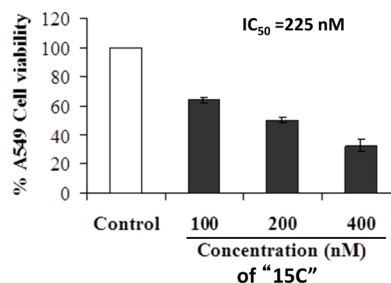


Figure 4. Increase in anti-cancer activity of caffeic acid (CA) against A549 cancer cells by its esterization. A549 lung cancer cells were treated with either CA or 15C at indicated concentrations for 96 h, stained with trypan blue, and the viable (non-stained) cells were counted. The IC_{50} of 15C is around 225 nM, indicating that the esterization of CA boosted its anti-cancer activity by over 400 folds. The results are mean \pm SE. Data have the statistical significance at $p \leq 0.01$.

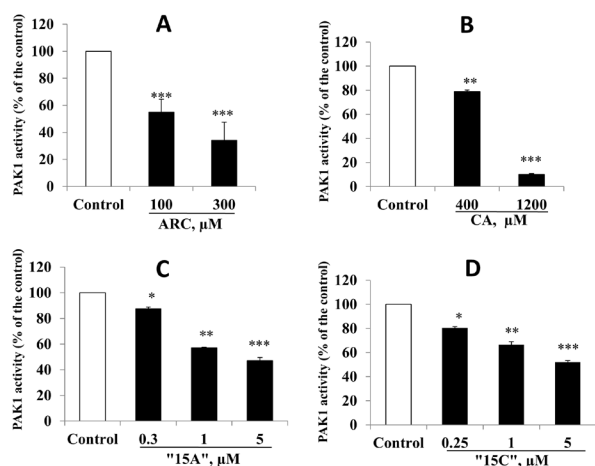


Figure 5. Boosting the anti-PAK1 activity of ARC (A) and CA (B) in cell culture by their esterization. After A549 cancer cells were treated with (A) ARC, (B) CA, (C) "15A" or (D) "15C" at the indicated concentrations for 24 h, PAK1 in cell lysates was IPed and its kinase activity was measured by "Macaroni-Western ATP_Glo" kinase assay. IC_{50} of "15A" and "15C" against PAK1 in cell culture is around 4.5 and 5.4 μ M, respectively, compared with that of ARC and CA (around 140 and 740 μ M, respectively).

ketorolac, than A549 lung cancer cell line (7), these observations altogether suggest that the anti-cancer action of both 15A and 15C is highly specific for the PAK1-dependent cell growth.

3.3. Anti-PAK1 activity of ARC ester (15A) and CA ester (15C)

Both ARC and CA are known to inhibit the PAK1-dependent growth of A549 lung cancer cells which carry the oncogenic mutant of Ki-RAS by blocking the oncogenic kinase PAK1 (12). Thus, we have examined if their esters also are able to block PAK1 in cell culture. As shown in Figure 5, both 15A and 15C block the PAK1 activity in cell culture in a concentration-dependent manner with IC_{50} around 5 μ M, confirming that both 15A and 15C are still potent PAK1-blockers. Furthermore, the anti-PAK1 activity of 15A and 15C appears to be 30 and 140 fold higher than those of ARC and CA (see Figure 5).

3.4. Uptake of 15A and 15C into cells compared with artepillin C (ARC) and caffeic acid (CA)

Since esterization of these acids generally abolishes their negative charge, their esters should be far more cell-permeable than the original herbal acids. Thus, here we have compared the cell-permeability between ARC and its ester (15A) as well as between CA and its ester (15C) using a drug-resistant breast cancer cell line (EMT6). At the tested concentrations (100 μ M of ARC, CA and 15A or 30 μ M of 15C), none of these compounds causes any serious effect on the growth or viability of this drug-resistant cell line for at least 12

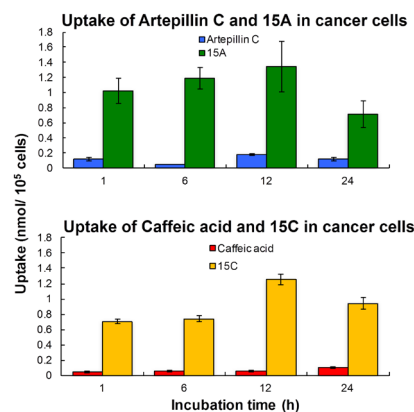


Figure 6. Increase in cell-permeability of ARC and CA by their esterization. The changes in the amount of (A, top) ARC and "15A" or (B, bottom) CA and "15C" taken into EMT6 cells during the first 12 h was monitored by HPLC analysis. "15A" is 8 fold more cell-permeable than ARC for the first hr, while "15C" is 20 fold more permeable than CA for 12 h. Data are mean \pm SEM.

h. However, 15C at 100 μ M is significantly toxic for this cancer cell line for 24 h (IC_{50} = 8 μ M, see Table 1). Uptake of each compound into cells was monitored by the HPLC-based analysis described previously (7) using the photometry at the wave-length 322 nm. As shown in Figure 6A, uptake of 15A is 8 folds faster than ARC during the first hour. However, the uptake of CA is rather slow, and that of 15C is over 20 fold (20-70 folds) more than CA during 12 h (see Figure 6B). Since both 15A and 15C are converted to a colored azo dye(s) by mito-chondrial reductase, as is the tetrazolium MTT, uptake of both 15A and 15C rapidly reduced shortly after 12 h treatment of cells with these esters.

Nevertheless, it is now clear that esterization of both ARC and CA boosts significantly their cell-permeability, and it is most likely that the dramatic increase in their anti-cancer activity is at least partly due to the increase of their cell-permeability.

References

- Grunberger D, Banerjee R, Eisinger K, Oltz EM, Efron L, Caldwell M, Estevez V, Nakanishi K. Preferential cytotoxicity on tumor cells by caffeic acid phenethyl ester isolated from propolis. *Experientia*. 1988; 44:230-232.
- Kimoto T, Arai S, Kohguchi M, Aga M, Nomura Y, Micallef MJ, Kurimoto M, Mito K. Apoptosis and suppression of tumor growth by artepillin C extracted from Brazilian propolis. *Cancer Detect Prev*. 1998; 22:506-515.
- Xu JW, Ikeda K, Kobayakawa A, Ikami T, Kayano Y, Mitani T, Yamori Y. Downregulation of Rac1 activation by caffeic acid in aortic smooth muscle cells. *Life Sci*. 2005; 76:2861-2872.
- Messerli SM, Ahn MR, Kunimasa K, Yanagihara M, Tatefuji T, Hashimoto K, Mautner V, Uto Y, Hori H, Kumazawa S, Kaji K, Ohta T, Maruta H. Artepillin C (ARC) in Brazilian green propolis selectively blocks

- oncogenic PAK1 signaling and suppresses the growth of NF tumors in mice. *Phytother Res.* 2009; 23:423-427.
- Taira N, Nguyen BCQ, Be Tu PT, Tawata S. Effect of Okinawa propolis on PAK1 activity, *Caenorhabditis elegans* longevity, melanogenesis, and growth of cancer cells. *J Agric Food Chem.* 2016; 64:5484-5489.
 - Rashid S, Dar BA, Majeed R, Hamid A, Bhat BA. Synthesis and biological evaluation of ursolic acid-triazolyl derivatives as potential anti-cancer agents. *Eur J Med Chem.* 2013; 66:238-245.
 - Nguyen BCQ, Takahashi H, Uto Y, Shahinozzaman Md, Tawata S, Maruta H. 1,2,3-Triazolyl ester of Ketorolac: A "Click Chemistry"-based highly potent PAK1-blocking cancer-killer. *Eur J Med Chem.* 2017; 126:270-276.
 - Uto Y, Hirata A, Fujita T, Takubo S, Nagasawa H, Hori H. First total synthesis of artepillin C established by o,o'-diprenylation of p-halophenols in water. *J Org Chem.* 2002; 67:2355-2357.
 - Nguyen BCQ, Be Tu PT, Tawata S, Maruta H. Combination of immunoprecipitation (IP)-ATP_Glo kinase assay and melanogenesis for the assessment of potent and safe PAK1-blockers in cell culture. *Drug Discov Ther.* 2015; 9:289-295.
 - Feoktistova I M, Geserick P, Leverkus M. Crystal violet assay for determining viability of cultured cells. *Cold Spring Harb Protoc.* 2016; 343-346.
 - Soda M, Hu D, Endo S, Takemura M, Li J, Wada R, Ifuku S, Zhao HT, El-Kabbani O, Ohta S, Yamamura K, Toyooka N, Hara A, Matsunaga T. Design, synthesis and evaluation of caffeic acid phenethyl ester-based inhibitors targeting a selectivity pocket in the active site of human aldo-keto reductase 1B10. *Eur J Med Chem.* 2012; 48:321-329.
 - Maruta H. Herbal therapeutics that block the oncogenic kinase PAK1: A practical approach towards PAK1-dependent diseases and longevity. *Phytother Res.* 2014; 28:656-672.
- (Received February 8, 2017; Revised March 29, 2017; Accepted April 14, 2017)

Supplementary Materials

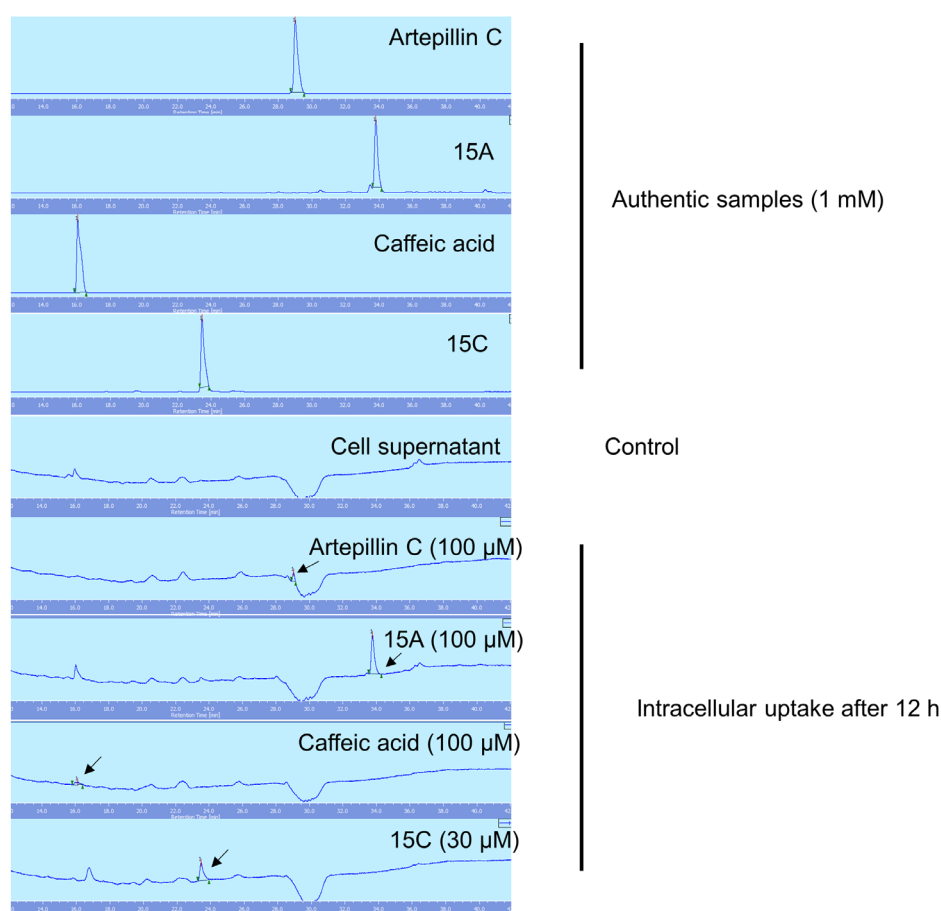


Figure S1. HPLC analysis of "15A" and "15C" compared with ARC and CA uptake into cells. After treating EMT6 (1×10^6 cells) with either "15A" (100 μ M), "15C" (30 μ M), ARC (100 μ M) or CA (100 μ M) for 1, 6, or 12 hrs, cells were washed twice with PBS and then lysed with 400 μ L of 2% Triton. 10 μ L of each lysate was injected into an analytical HPLC column (GL-Science Inertsustain C18, 4.6 mm \times 150 mm) equilibrated with 0.1% TFA in mQ water (A). The column was eluted with 1% acetonitrile (B) for 5 min, then with a linear gradient from 1% to 100% B over 30 min, and finally 100% B for 10 min, at a flow rate 1.0 mL/min. The eluate was monitored at wavelength 322 nm.

Fronodoside A from sea cucumber and nymphaeols from Okinawa propolis: Natural anti-cancer agents that selectively inhibit PAK1 *in vitro*

Binh Cao Quan Nguyen¹, Kazuki Yoshimura², Shigenori Kumazawa², Shinkichi Tawata¹, Hiroshi Maruta^{3,*}

¹PAK Research Center, University of the Ryukyus, Okinawa, Japan;

²Department of Food and Nutritional Sciences, University of Shizuoka, Shizuoka, Japan;

³PAK Research Center, Melbourne, Australia.

Summary

A sulfated saponin called "Fronodoside A" (FRA) from sea cucumber and ingredients from Okinawa propolis (OP) have been previously shown to suppress the PAK1-dependent growth of A549 lung cancer as well as pancreatic cancer cells. However, the precise molecular mechanism underlying their anti-cancer action still remains to be clarified. In this study, for the first time, we found that both FRA and OP directly inhibit PAK1 *in vitro* in a selective manner (far more effectively than two other oncogenic kinases, LIMK and AKT). Furthermore, at least two major anti-cancer ingredients of OP, nymphaeols A and C, also directly inhibit PAK1 *in vitro* in a selective manner. To the best of our knowledge, FRA is the first marine compound that selectively inhibits PAK1. Likewise, these nymphaeols are the first propolis ingredients that selectively inhibit PAK1.

Keywords: Propolis, sea cucumber, frondoside A, nymphaeols, PAK1, cancers

1. Introduction

Since conventional chemotherapeutics such as DNA/microtubule poisons cause serious side effects such as hair-loss and suppression of immune response, recently cancer patients, in particular those who suffer from formidable pancreatic or lung cancers, started seeking an alternative approach for cancer therapy by using natural remedies that do not cause any serious side effect. A bee product called "propolis" has been used as one of these herbal cancer therapeutics for last three decades. Two major propolis products available in the market are ARC (artepillin C)-based Brazilian green propolis (GP) and CAPE (caffeic acid phenethyl ester)-based propolis called Bio 30 or Bio 100 from New Zealand (1-3). However, recently, propolis from subtropical regions

such as Okinawa, Taiwan, and Hawaii has been studied extensively, mainly because of its unique ingredients such as geranylated flavonoids (nymphaeols) (4-6). Very recently, we found that Okinawa propolis (OP) is highly anti-angiogenic *in ovo* (fertilized eggs), clearly several times more potent than GP as a herbal anti-cancer remedy, and blocks the oncogenic/ageing kinase PAK1 at least in cell culture (4,7). Furthermore, we confirmed that OP is a potent elixir extending the healthy lifespan of *C. elegans* (7).

In addition to these three distinct propolis products, the potent anti-cancer activity of a sulfated saponin called "frondoside A" (FRA) from an edible sea cucumber (*Cucumaria frondosa*) has recently drawn much attention of pancreatic and lung cancer patients. According to previous studies by Thomas Adrian and others, FRA inhibits the growth of A549 lung cancer and pancreatic cancer cells with IC₅₀ ranging 1-3 μM in cell culture, and up-regulates the tumor-suppressor p21, an inhibitor of CDKs (cyclin-dependent kinases) (8,9). *In vivo* (xenograft in nude mice) FRA (1 mg/kg/day, *i.p.*) significantly suppresses the growth of human pancreatic cancer (9). We have shown previously that the expression of p21 gene is suppressed by PAK1 (10). Furthermore,

Released online in J-STAGE as advance publication April 24, 2017.

*Address correspondence to:

Dr. Hiroshi Maruta, PAK Research Center, Melbourne, Australia 3055, Australia.

E-mail: maruta20420@yahoo.co.jp

since both A549 lung cancer and pancreatic cancer cells carry the oncogenic Ki-RAS mutant, and their growth depends on PAK1, it would not be unreasonable for us to suspect that FRA might block the oncogenic/ageing kinase PAK1 somehow. Here, we have confirmed that both OP and FRA as well as nymphaeols directly inhibit PAK1 *in vitro* in a selective manner.

2. Materials and Methods

2.1. Chemicals and reagents

Human lung cancer cell line A549 was purchased from Japanese Collection of Research Bioresources Cell Bank (Osaka, Japan). Alcohol extract of Okinawa propolis (OP) was prepared as previously described (7). Nymphaeols were isolated from OP through HPLC as previously described (4). Frondoside A (FRA) was purchased from Sigma-Aldrich (St. Louis, MO, USA). Both recombinant PAK1 and LIMK were obtained from SignalChem Pharmaceuticals Inc. (Richmond, British Columbia, Canada).

2.2. Assay for anti-cancer activity in cell culture

The number of viable cells after treatment with either frondoside A or nymphaeols (see Figure 1 for their chemical structures) was measured by Trypan blue

assay in a hemocytometer as described previously (11). Briefly, A549 lung cancer cells (2×10^5 cells/well) were seeded for 24 h, and then treated with various test compounds at the indicated concentrations for 72 h, and the number of viable (unstained) cells were counted after Trypan blue staining.

2.3. *In vitro* anti-kinase (PAK1/LIMK/AKT) assay

The kinase activity of PAK1, LIMK, and AKT was measured *in vitro* by ADP-Glo kinase assay kit (Promega, Madison, WI, USA), according to the manufacturer's instruction, as previously described (12). Briefly, the recombinant human PAK1 (10 ng) or LIMK (10 ng) per reaction was treated with either OP, FRA or nymphaeols at the indicated concentrations in the presence of ATP, with either myelin basic protein (MBP) for PAK1 assay or cofilin for LIMK assay as their protein substrates, during the 40 min *in vitro* kinase reaction. Then the reaction was terminated with the ADP-Glo reagent. In the case of AKT assay, instead of using the recombinant AKT, A549 lung cancer cells were cultured for 48 h, and cell lysates were immuno-precipitated (IP) with anti-AKT IgG in the presence of protein A-agarose beads (11), and the resultant AKT in IP was treated with various test compounds at the indicated concentrations in the presence of ATP and MBP during 40 min *in vitro* kinase assay, which was then terminated with the ADP-

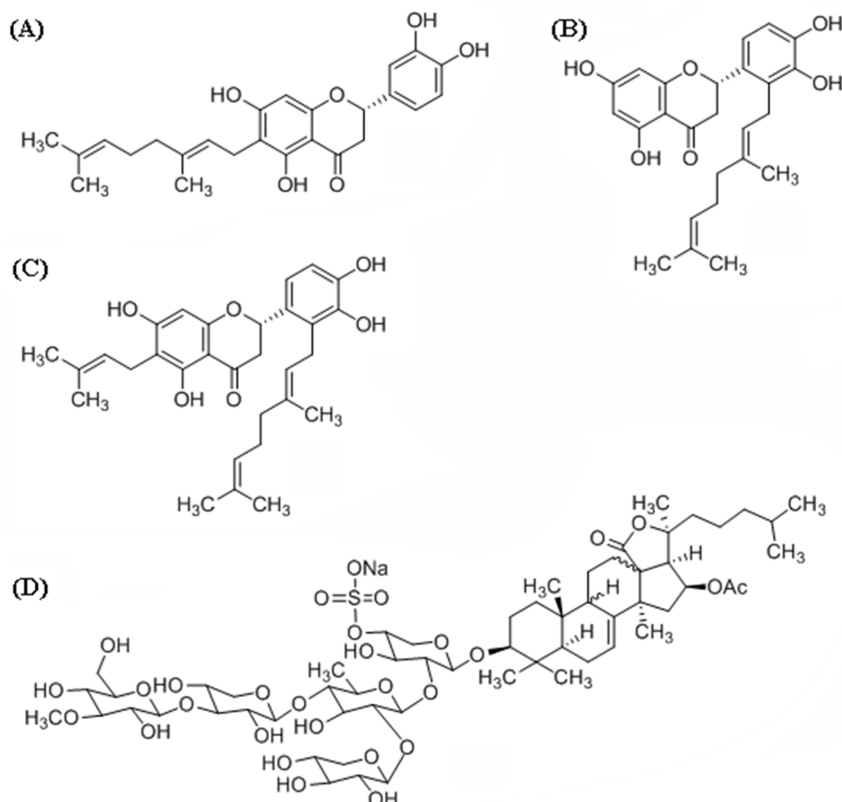


Figure 1. Chemical structures of nymphaeols A-C and frondoside A. (A) nymphaeol A; (B) nymphaeol B; (C) nymphaeol C; (D) frondoside A.

Glo reagent. To these reaction mixtures was added the kinase detection reagent that converts ADP to ATP which eventually generates a luciferin-luciferase based fluorescence.

2.4. Statistical analysis

Data are expressed as mean values with their standard errors. Statistical comparisons were performed by one-way ANOVA. Statistical analysis was conducted using SPSS (release 16.0, Chicago, Illinois) and $p < 0.05$ was considered significant.

3. Results and Discussion

3.1. Okinawa propolis (OP) and its major ingredients directly inhibit PAK1 *in vitro*

3.1.1. Okinawa propolis (OP) directly inhibits PAK1 *in vitro*

We have previously found that Okinawa propolis (OP) inhibits the PAK1-dependent growth of A549 lung cancer cells with IC_{50} around 12 $\mu\text{g/mL}$, while it blocks PAK1 in the same cell culture with the apparent IC_{50} around 6 $\mu\text{g/mL}$ as judged by "Macaroni-Western" ATP-Glo kinase assay (7). Generally speaking, when a compound blocks PAK1 by inhibiting an upstream activator of PAK1 such as RAC, instead of directly inhibiting PAK1, the apparent anti-PAK IC_{50} value is usually 3-4 times higher than the anti-cancer IC_{50} value (11). Since the outcome with OP is clearly opposite, the possibility rose that OP might directly inhibit PAK1. Here we have confirmed this notion. As shown in Figure 2, OP directly inhibited the recombinant PAK1 *in vitro* with IC_{50} around 10 $\mu\text{g/mL}$.

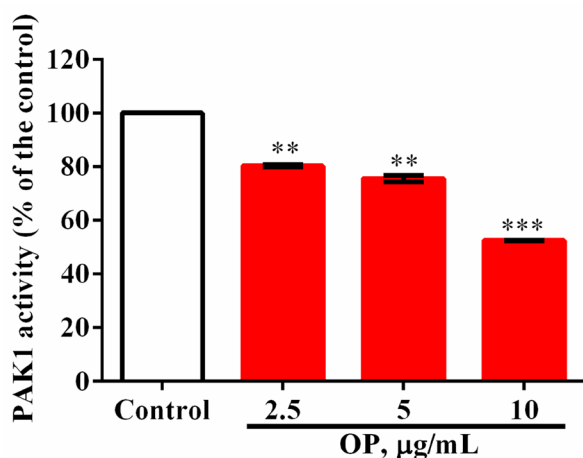


Figure 2. Okinawa propolis (OP) directly inhibits PAK1 *in vitro*. Recombinant PAK1 from SignalChem was treated with OP at the indicated concentrations *in vitro*. The experiments are conducted with twice, and the results are mean \pm SE. IC_{50} of OP against PAK1 is around 10 $\mu\text{g/mL}$. Asterisks on each bar indicate significant differences between treatment and control. * $0.01 \leq p \leq 0.05$, ** $p \leq 0.01$, *** $p \leq 0.001$.

3.1.2. Anti-cancer activity of nymphaeols A and C from OP

The major anti-cancer ingredients in OP are geranylated flavonoids called nymphaeols A-C (5), and at least nymphaeol A has been shown to inhibit the PAK1-dependent angiogenesis *in ovo* (fertilized eggs) (4), suggesting that it could block PAK1 somehow. Here, we have tested the anti-cancer activity of nymphaeols A and C. As shown in Figure 3, nymphaeols A and C inhibit the growth of A549 cancer cells with the IC_{50} = 4 μM and 7 μM , respectively.

3.1.3. Anti-PAK1 activity of nymphaeols A and C *in vitro*

The next, we have tested the anti-PAK1 activity *in vitro*. As shown in Figure 4, like OP, both nymphaeols A and C directly inhibited PAK1 with IC_{50} around 10 μM .

3.1.4. Kinase specificity of nymphaeols

In order to determine how selective the direct action of

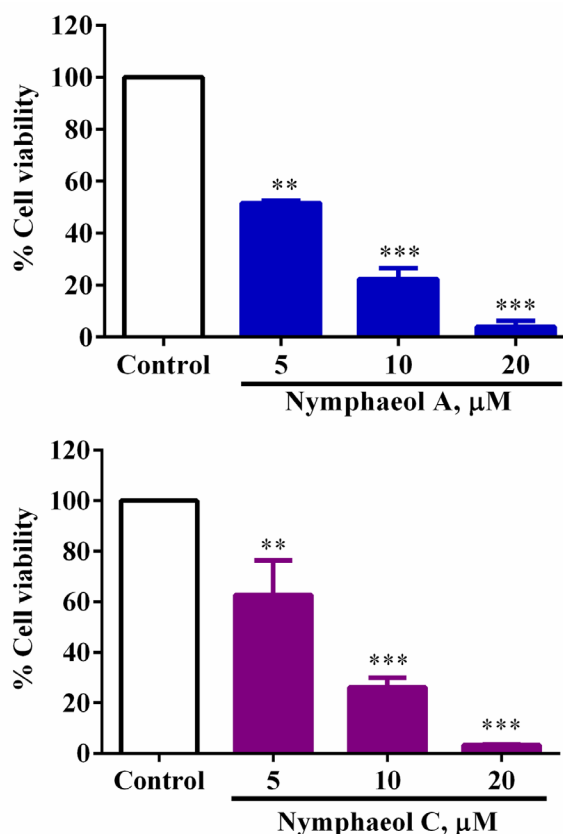


Figure 3. Anti-cancer activity of nymphaeols against the growth of A549 lung cancer cells. A549 cells were treated with either nymphaeols A (left) or C (right) at the indicated concentrations for 72 h, and the number of the viable cells was counted by Trypan blue staining. The results are mean \pm SE of two independent experiments. IC_{50} of nymphaeols A and C are around 4 and 7 μM , respectively. Asterisks on each bar indicate significant differences between treatment and control. * $0.01 \leq p \leq 0.05$, ** $p \leq 0.01$, *** $p \leq 0.001$.

nymphaeols towards PAK1 is, we have tested their anti-LIM kinase (LIMK) and anti-AKT activity *in vitro* as well. As summarized in Table 1, both nymphaeols A and C inhibited LIMK and AKT, but with the far higher IC₅₀ (160 μM and 170 μM against LIMK, and 42 μM and 74 μM against AKT, respectively), confirming their specificity towards PAK1.

3.2. Anti-PAK1 activity of frondoside A (FRA)

Extracts of several distinct sea cucumbers have been

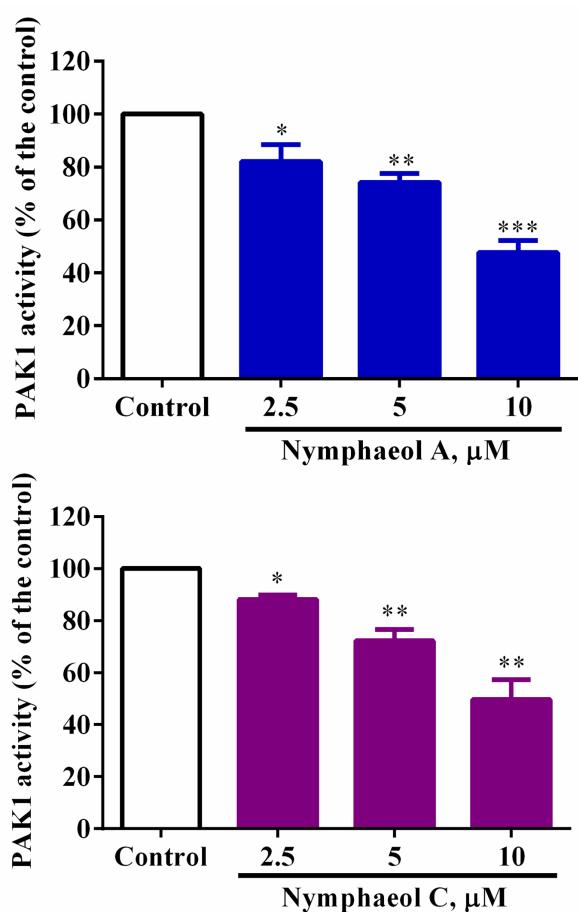


Figure 4. Nymphaeols directly inhibit PAK1 *in vitro*. PAK1 was treated *in vitro* with either nymphaeol A (left) or C (right) at the indicated concentrations. IC₅₀ of both nymphaeols A and C is around 10 μM. Asterisks on each bar indicate significant differences between treatment and control. * 0.01 ≤ p ≤ 0.05, ** p ≤ 0.01, *** p ≤ 0.001.

shown to suppress the growth of cancer cells including A549 lung cancer and pancreatic cancer cell lines which carry the oncogenic Ki-RAS mutant (8,9). In most cases, anti-cancer ingredients derived from sea cucumbers belong to sulfated saponins. Among these saponins, frondoside A (FRA) from *Cucumaria frondosa* is the most potent so far, inhibiting the PAK1-dependent growth of A549 cancer cells with IC₅₀ around 2.5 μM for 24 h (9), but under our own culture conditions (72 h), the IC₅₀ against A549 is around 0.6 μM (see Table 1). However, the precise molecular mechanism underlying its anti-cancer action still remains to be clarified.

A few previous observations raised the possibility that FRA might inhibit PAK1 directly (or indirectly): (i) FRA inhibits the PAK1-dependent growth of A549 cancer cells, (ii) FRA up-regulates p21 (CDK inhibitor) whose expression is suppressed by PAK1 (8-10), and (iii) nymphaeols from OP directly inhibits PAK1 in a selective manner (see Figure 4 and Table 1). Thus, we were prompted to test *in vitro* if FRA could inhibit PAK1 and a few other kinases as well. As shown in Figure 5, FRA directly inhibits PAK1 *in vitro* with IC₅₀ around 1 μM, but both LIMK and AKT with IC₅₀

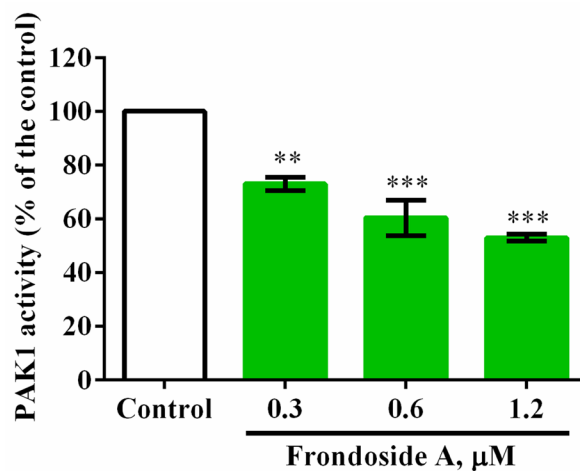


Figure 5. Frondoside A (FRA) directly inhibits PAK1 *in vitro*. PAK1 was treated *in vitro* with FRA at the indicated concentrations. The IC₅₀ of FRA against PAK1 is around 1 μM. Asterisks on each bar indicate significant differences between treatment and control. * 0.01 ≤ p ≤ 0.05, ** p ≤ 0.01, *** p ≤ 0.001.

Table 1. Anti-cancer activity and anti-kinase specificity of frondoside A and Okinawa propolis (OP) ingredients (nymphaeols)

Items	Anti-cancer (IC ₅₀)	Anti-PAK1 (IC ₅₀)	Anti-LIMK (IC ₅₀)	Anti-AKT (IC ₅₀)
Frondoside A	0.6	1.2	60	59
Okinawa propolis	12	10	39	30
Nymphaeol A	3.6	9.6	161	42
Nymphaeol C	6.5	9.8	171	74
Curcumin	23	16	30	44

IC₅₀ value is in μM, except for Okinawa propolis (OP) in μg/mL.

around 60 μ M (see Table 1), clearly indicating that FRA is indeed a potent PAK1-inhibitor, and its PAK1-specificity is even far more profound than that of nymphaeols.

To the best of our knowledge, OP is the very first propolis that has been proven to directly inhibit PAK1. All other propolis products in market such as ARC-based GP and CAPE-based Bio 30 block PAK1 only indirectly (by down-regulating RAC or other activators of PAK1).

Back in 2003, we found a rare potent marine poison called ST-2001, a 3-OH derivative of Staurosporine (ST), which directly inhibits PAK1, PKC and several other kinases with IC_{50} around 1 nM (13), but its anti-kinase mode of action is clearly "non-specific". Thus, to the best of our knowledge, FRA is the very first PAK1-specific inhibitor of marine origin. Currently, we are testing if FRA also could extend the healthy lifespan of *C. elegans*, as does OP (7).

Regarding the structure-function relationship of nymphaeols (see Figure 1 for chemical structures), either the position of geranyl side chain in nymphaeols or an extra short side chain in nymphaeol C does not seem to affect either their anti-PAK1 activity or kinase-specificity. In an attempt to determine the specific role of geranyl side chains in either anti-cancer/cell-permeability or anti-PAK1 activity/kinase specificity if any, we are planning to study the potential anti-cancer and anti-PAK1 activity of far simpler flavonoids such as naringenin and sakuranetin which contain no geranyl side chain.

Acknowledgements

We are very grateful to Mr. Md Shahinozzaman for his technical assistance to confirm the IC_{50} of Frondoside A against A549 cancer cell growth. This study was supported in part by the fishing company "Jinsho", Japan.

References

- Demestre M, Messerli SM, Celli N, Shahhossini M, Kluwe L, Mautner V, Maruta H. CAPE (caffeic acid phenethyl ester)-based propolis extract (Bio 30) suppresses the growth of human neurofibromatosis (NF) tumor xenografts in mice. *Phytother Res.* 2009; 23:226-230.
- Messerli SM, Ahn MR, Kunimasa K, Yanagihara M, Tatefuji T, Hashimoto K, Mautner V, Uto Y, Hori H, Kumazawa S, Kaji K, Ohta T, Maruta H. Artepillin C (ARC) in Brazilian green propolis selectively blocks oncogenic PAK1 signaling and suppresses the growth of NF tumors in mice. *Phytother Res.* 2009; 23:423-427.
- Maruta H. Herbal therapeutics that block the oncogenic kinase PAK1: A practical approach towards PAK1-dependent diseases and longevity. *Phytother Res.* 2014; 28:656-672.
- Tsuchiya I, Hosoya T, Ushida M, Kunimasa K, Ohta T, Kumazawa S. Nymphaeol-A isolated from Okinawan propolis suppresses angiogenesis and induces caspase-dependent apoptosis via inactivation of survival signals. *Evid Based Complement Alternat Med.* 2013; 2013:826245.
- Kumazawa S, Murase M, Momose N, Fukumoto S. Analysis of antioxidant prenylflavonoids in different parts of *Macaranga tanarius*, the plant origin of Okinawan propolis. *Asian Pac J Trop Med.* 2014; 7:16-20.
- Inui S, Hosoya T, Kumazawa S. Hawaiian propolis: comparative analysis and botanical origin. *Nat Prod Commun.* 2014; 9:165-166.
- Taira N, Nguyen BCQ, Be Tu PT, Tawata S. Effect of Okinawa Propolis on PAK1 activity, *Caenorhabditis elegans* longevity, melanogenesis, and growth of cancer cells. *J Agric Food Chem.* 2016; 64:5484-5489.
- Li X, Roginsky AB, Ding XZ, Woodward C, Collin P, Newman RA, Bell RH Jr, Adrian TE. Review of the apoptosis pathways in pancreatic cancer and the anti-apoptotic effects of the novel sea cucumber compound, Frondoside A. *Ann N Y Acad Sci.* 2008; 1138:181-198.
- Attoub S, Arafat K, Gélaude A, Al Sultan MA, Bracke M, Collin P, Takahashi T, Adrian TE, De Wever O. Frondoside a suppressive effects on lung cancer survival, tumor growth, angiogenesis, invasion, and metastasis. *PLoS One.* 2013; 8:e53087.
- Nheu T, He H, Hirokawa Y, Walker F, Wood J, Maruta H. PAK is essential for RAS-induced upregulation of cyclin D1 during the G1 to S transition. *Cell Cycle.* 2004; 3:71-74.
- Nguyen BCQ, Be Tu PT, Tawata S, Maruta H. Combination of immunoprecipitation (IP)-ATP_Glo kinase assay and melanogenesis for the assessment of potent and safe PAK1-blockers in cell culture. *Drug Discov Ther.* 2015; 9:289-295.
- Mezna M, Wong AC, Ainger M, Scott RW, Hammonds T, Olson MF. Development of a high-throughput screening method for LIM kinase 1 using a luciferase-based assay of ATP consumption. *J Biomol Screen.* 2012; 17:460-468.
- Nheu TV, He H, Hirokawa Y, Tamaki K, Florin L, Schmitz ML, Suzuki-Takahashi I, Jorissen RN, Burgess AW, Nishimura S, Wood J, Maruta H. The K252a derivatives, inhibitors for the PAK/MLK kinase family selectively block the growth of RAS transformants. *Cancer J.* 2002; 8:328-336.

(Received February 13, 2017; Revised April 6, 2017; Accepted April 9, 2017)

Levetiracetam and topiramate poisoning: Two overdoses on those drugs with no lasting effects

Moaziz Sarfaraz^{1,*}, Syeda Rana Hasan²

¹Emergency Department, Fujairah Hospital, Fujairah, United Arab Emirates;

²Emergency Department, Masafi Hospital, Masafi, Fujairah, United Arab Emirates.

Summary Levetiracetam and topiramate are newer anticonvulsants, which is why international data on overdoses of these drugs are lacking. Only a few mild adverse reactions have been noted. These anticonvulsants have been the drug of choice for neurologists. Despite their wide usage, there is a dearth of literature on symptoms and signs of their toxicity. Presented here is the case of a 21-year-old female who overdosed twice on levetiracetam and topiramate. The woman was admitted and discharged after the first overdose. Ten days later, she took multiple tablets of both drugs and was seen again. Amazingly, the woman went home after the incident with no complications at all.

Keywords: Anticonvulsants, toxicity, seizures, gastrointestinal decontamination, activated charcoal

1. Introduction

Levetiracetam entered the market in 2000 when it was approved by the US Food and Drug Administration (FDA) (1). Levetiracetam is currently being used for partial seizures and as an adjunctive therapy for generalized tonic-clonic convulsions (1-3). The mechanism of action of levetiracetam involves its effect on the intraneuronal concentration of calcium and amelioration of the inhibition of gamma-aminobutyric acid (GABA) and glycine channels. Additionally, levetiracetam has a favorable pharmacokinetic profile with quick absorption through oral intake, superb bioavailability, rapid attainment of steady-state concentrations, linear kinetics, and minimal plasma protein binding (2). Levetiracetam is not metabolized by the cytochrome P450 system but by the enzymatic degradation of its acetamide group (1,2). If it is administered orally, its absorption is not affected by food material. Less than 10% of levetiracetam binds to plasma proteins and levetiracetam has a bioavailability of 95%. Its half-life is 6-8 hours. The recommended

adult dose is 1 g/day and can be increased to 3 g/day at 2 weeks (2).

Topiramate, a sulfamate-substituted monosaccharide, is a relatively new anticonvulsant agent. It is indicated as a monotherapy or adjunctive therapy to alleviate partial seizures, generalized tonic-clonic seizures, and Lennox-Gastaut syndrome. Topiramate is also being used in the treatment of migraines, cluster headaches, essential tremors, binge eating disorders, acute mania, Tourette's syndrome, neuropathic pain, bipolar disorder, alcohol dependence, excess body weight, and smoking (4,5). Structurally, topiramate is unrelated to other anticonvulsants and acts by multiple neurostabilizing processes (6,7). The recommended adult dosage ranges from 200-400 mg/day. Topiramate peaks 2-3 hours after oral administration and its plasma elimination half-life is 18-24 hours (6,8). Its excretion is primarily (55-66%) via the kidneys (7).

2. Case Report

A young woman 21 years of age who was thin and lean (43.7 kg) and who had been an epileptic since the age of 5 was brought to the ER following ingestion of 40 tablets of levetiracetam 1 g and 60 tablets of topiramate 25 mg nearly 1.5 hours prior. This means she took 60 g of levetiracetam (20 times the maximum dose) and 1.5 g of topiramate (4 times the maximum dose). Her epilepsy was partially controlled and her last seizure

Released online in J-STAGE as advance publication March 19, 2017.

*Address correspondence to:

Dr. Moaziz Sarfaraz, Emergency Department, Fujairah Hospital, Fujairah, United Arab Emirates.

E-mail: m4moaziz@yahoo.com

occurred nearly a year prior. She was fully active and conscious in the ER. No drowsiness or difficulty breathing was observed. There were no complaints of any abdominal discomfort, nausea, or vomiting. Results of a general physical examination were normal. Gastrointestinal decontamination was done with 50 g of activated charcoal. The patient began vomiting and vomitus showed streaks of white material along with tiny fragments of tablets. A complete blood count (CBC), urea levels, creatinine levels, urinary calcium excretion (UCE), amylase levels, results of a liver function test (LFT), and an electrolyte and coagulation profile were all normal. An electrocardiogram (EKG) showed normal sinus rhythm. An examination of levetiracetam and topiramate levels in the blood was not possible at this facility. The woman was admitted to the general ward and closely monitored and observed. The next day, she was behaving normally and there were no complaints. She ate a full meal and her status was completely normal, so was discharged after 24 hours.

Ten days later the woman was seen again after she took multiple tablets of the same drugs 1 hour prior. At the time, she had taken 30 tablets of levetiracetam 1 g and 7 tablets of topiramate 25 mg. As in the previous incident, she was hemodynamically stable, fully active, and conscious. She had no gastrointestinal complaints. No drowsiness or lethargy was observed. She started vomiting after ingesting activated charcoal. Small pieces of tablets and white streaks were found in vomitus. Levels of the 2 drugs in blood could not be measured, but baseline values for the CBC, UCE, LFT, amylase, the electrolyte and coagulation profile, and arterial blood gases revealed no abnormalities. The patient was kept under close observation in the general ward. The next day, she was completely normal, eating, chatting, and roaming around normally. She was discharged 24 hours after admission in healthy condition.

3. Discussion

Topiramate is a newer anti-epileptic and is used as a monotherapy or in combination with other agents (8). It is also indicated in the treatment of psychiatric illnesses. Several cases of an accidental overdose in children or an intentional or suicidal overdose in older individuals have been reported (6,9). At therapeutic levels, topiramate is benign, and the most prevalent adverse reactions are dizziness, somnolence, and ataxia. However, acute psychosis, hepatic failure accompanied by encephalopathy, hyperthermia, hyperchloremic metabolic acidosis, nephrolithiasis, and parasthesia have also been reported (5,8,10,11). Beer *et al.* reported a death following an overdose of topiramate and other drugs (6). A retrospective study of anticonvulsant overdoses by Wills *et al.* indicated

that 43% of patients had no symptoms and 34% had mild symptoms, while only 20 patients (4%) were severely affected (10). The patient reported by Lynch *et al.* was brought in unresponsive after intoxication (8). However, the current patient was brought in fully conscious and remained conscious on both occasions. Ozer and Altunkaya noted high anion gap metabolic acidosis 7 days after a topiramate overdose (11). Three of the 6 patients reported by Wisniewski *et al.* had metabolic acidosis after a topiramate overdose (5). In the current case, however, a metabolic imbalance was not noted when the patient was brought in the second time. Christian *et al.* and Anand *et al.* reported seizures after a topiramate overdose (4,9), but the current patient remained absolutely normal.

Levetiracetam has recently been approved and is used as adjunctive therapy for the treatment of adult patients with partial seizures with or without secondary generalization that are refractory to other antiepileptic drugs (12). A multicenter, double-blind, and randomized trial clearly indicated that levetiracetam significantly reduces the frequency of partial seizures. A study by Harden *et al.* found it well-tolerated and without risks (13). According to Wills *et al.*, patients only had some gastrointestinal (GI) problems and levetiracetam appeared to have the lowest toxicity (10). This may be due to the fact that levetiracetam is mostly excreted as-is in urine, although 24% is hydrolyzed to an inactive metabolite in the blood (2). The patients reported by Vellinga *et al.* and Barrueto *et al.* experienced respiratory distress after intoxication and needed endotracheal intubation, though they did recover in 24 hours (2,14). In contrast, the current patient overdosed twice within a short period of time but her condition remained completely normal throughout observation and she was discharged safely and in healthy condition.

4. Conclusion

To the extent known, there are no reported cases of overdoses involving both topiramate and levetiracetam. The striking feature of the current case is that the patient heavily overdosed twice with these two antiepileptic agents in a short span of time. Amazingly, the patient had no lasting effects and her condition returned to normal after both incidents. She experienced no psychological or biochemical complications, but a few cases of respiratory distress that ultimately required definitive airway protection have been reported. The bottom line is that strict vigilance is mandatory several hours after overdoses involving both topiramate and levetiracetam.

References

1. Larkin TM, Cohen-Oram AN, Catalano G, Catalano MC. Overdose with levetiracetam: A case report and review of

- the literature. *J Clin Pharm Ther.* 2013; 38:68-70.
2. Vellinga SE, Jagt M, Hunfeld NGM. Coma after levetiracetam overdose. *Neth J Crit Care.* 2015; 20:29-32.
 3. Chayasirisobhon S, Chayasirisobhon WV, Tsay C. Acute levetiracetam overdose presented with mild adverse events. *Acta Neurol Taiwan.* 2010; 19:292-295.
 4. Anand JS, Chodorowsk Z, Wisniewski M. Seizures induced by topiramate overdose. *Clin Toxicol (Phila).* 2007; 45:197.
 5. Wisniewski M, Lukasik-Glebocka M, Anand JS. Acute topiramate overdose – Clinical manifestations. *Clin Toxicol (Phila).* 2009; 47:317-320.
 6. Beer B, Libiseller K, Oberacher H, Pavlic M. A fatal intoxication case involving topiramate. *Forensic Sci Int.* 2010; 202:e9-11.
 7. Shank RP, Maryanoff BE. Molecular pharmacodynamics, clinical therapeutics and pharmacokinetics of topiramate. *CNS Neurosci Ther.* 2008; 14:120-142.
 8. Lynch MJ, Pizon AF, Siam MG, Krasowski MD. Clinical effects and toxicokinetic evaluation following massive topiramate ingestion. *J Med Toxicol.* 2010; 6:135-138.
 9. Brandt C, Elsner H, Furatsch N, Hoppe M, Nieder E, Rambeck B, Ebner A, May TW. Topiramate overdose: A case report of a patient with extremely high topiramate concentrations and nonconvulsive status epilepticus. *Epilepsia.* 2010; 51:1090-1093.
 10. Wills B, Reynolds P, Chu E, Murphy C, Cumpston K, Stromber P, Rose R. Clinical outcome in newer anticonvulsant overdose: A poison centre observational study. *J Med Toxicol.* 2014; 10:254-260.
 11. Ozer Y, Altunkaya H. Topiramate induced metabolic acidosis. *Anaesthesia.* 2004; 59:830.
 12. Patsalos PN. Clinical pharmacokinetics of levetiracetam. *Clin Pharmacokinet.* 2004; 43:707-724.
 13. Harden C. Safety profile of levetiracetam. *Epilepsia.* 2001; 42:36-39.
 14. Barrueto F Jr, Williams K, Howland MA, Hoffman RS, Nelson LS. A case of levetiracetam (Keppra) poisoning with clinical and toxicokinetic data. *J Toxicol Clin Toxicol.* 2002; 40:881-884.
- (Received December 19, 2016; Revised February 4, 2017; Re-revised February 10, 2017; Accepted February 12, 2017)*

Guide for Authors

1. Scope of Articles

Drug Discoveries & Therapeutics welcomes contributions in all fields of pharmaceutical and therapeutic research such as medicinal chemistry, pharmacology, pharmaceutical analysis, pharmaceuticals, pharmaceutical administration, and experimental and clinical studies of effects, mechanisms, or uses of various treatments. Studies in drug-related fields such as biology, biochemistry, physiology, microbiology, and immunology are also within the scope of this journal.

2. Submission Types

Original Articles should be well-documented, novel, and significant to the field as a whole. An Original Article should be arranged into the following sections: Title page, Abstract, Introduction, Materials and Methods, Results, Discussion, Acknowledgments, and References. Original articles should not exceed 5,000 words in length (excluding references) and should be limited to a maximum of 50 references. Articles may contain a maximum of 10 figures and/or tables.

Brief Reports definitively documenting either experimental results or informative clinical observations will be considered for publication in this category. Brief Reports are not intended for publication of incomplete or preliminary findings. Brief Reports should not exceed 3,000 words in length (excluding references) and should be limited to a maximum of 4 figures and/or tables and 30 references. A Brief Report contains the same sections as an Original Article, but the Results and Discussion sections should be combined.

Reviews should present a full and up-to-date account of recent developments within an area of research. Normally, reviews should not exceed 8,000 words in length (excluding references) and should be limited to a maximum of 100 references. Mini reviews are also accepted.

Policy Forum articles discuss research and policy issues in areas related to life science such as public health, the medical care system, and social science and may address governmental issues at district, national, and international levels of discourse. Policy Forum articles should not exceed 2,000 words in length (excluding references).

Case Reports should be detailed reports of the symptoms, signs, diagnosis, treatment, and follow-up of an individual patient. Case reports may contain a demographic profile of the patient but usually describe an unusual or novel occurrence. Unreported or unusual side effects or adverse interactions involving medications will also be considered. Case

Reports should not exceed 3,000 words in length (excluding references).

News articles should report the latest events in health sciences and medical research from around the world. News should not exceed 500 words in length.

Letters should present considered opinions in response to articles published in Drug Discoveries & Therapeutics in the last 6 months or issues of general interest. Letters should not exceed 800 words in length and may contain a maximum of 10 references.

3. Editorial Policies

Ethics: Drug Discoveries & Therapeutics requires that authors of reports of investigations in humans or animals indicate that those studies were formally approved by a relevant ethics committee or review board.

Conflict of Interest: All authors are required to disclose any actual or potential conflict of interest including financial interests or relationships with other people or organizations that might raise questions of bias in the work reported. If no conflict of interest exists for each author, please state "There is no conflict of interest to disclose".

Submission Declaration: When a manuscript is considered for submission to Drug Discoveries & Therapeutics, the authors should confirm that 1) no part of this manuscript is currently under consideration for publication elsewhere; 2) this manuscript does not contain the same information in whole or in part as manuscripts that have been published, accepted, or are under review elsewhere, except in the form of an abstract, a letter to the editor, or part of a published lecture or academic thesis; 3) authorization for publication has been obtained from the authors' employer or institution; and 4) all contributing authors have agreed to submit this manuscript.

Cover Letter: The manuscript must be accompanied by a cover letter signed by the corresponding author on behalf of all authors. The letter should indicate the basic findings of the work and their significance. The letter should also include a statement affirming that all authors concur with the submission and that the material submitted for publication has not been published previously or is not under consideration for publication elsewhere. The cover letter should be submitted in PDF format. For example of Cover Letter, please visit <http://www.ddtjournal.com/downloadcentre.php> (Download Centre).

Copyright: A signed JOURNAL PUBLISHING AGREEMENT (JPA) must be provided by post, fax, or as a scanned file before acceptance of the article. Only forms with a hand-written signature are accepted. This copyright will ensure the widest possible dissemination of information. A form facilitating transfer of copyright can be downloaded by clicking the appropriate link and can be returned to the e-mail address or fax number noted on the form (Please visit

Download Centre). Please note that your manuscript will not proceed to the next step in publication until the JPA form is received. In addition, if excerpts from other copyrighted works are included, the author(s) must obtain written permission from the copyright owners and credit the source(s) in the article.

Suggested Reviewers: A list of up to 3 reviewers who are qualified to assess the scientific merit of the study is welcomed. Reviewer information including names, affiliations, addresses, and e-mail should be provided at the same time the manuscript is submitted online. Please do not suggest reviewers with known conflicts of interest, including participants or anyone with a stake in the proposed research; anyone from the same institution; former students, advisors, or research collaborators (within the last three years); or close personal contacts. Please note that the Editor-in-Chief may accept one or more of the proposed reviewers or may request a review by other qualified persons.

Language Editing: Manuscripts prepared by authors whose native language is not English should have their work proofread by a native English speaker before submission. If not, this might delay the publication of your manuscript in Drug Discoveries & Therapeutics.

The Editing Support Organization can provide English proofreading, Japanese-English translation, and Chinese-English translation services to authors who want to publish in Drug Discoveries & Therapeutics and need assistance before submitting a manuscript. Authors can visit this organization directly at <http://www.iacmhr.com/iac-eso/support.php?lang=en>. IAC-ESO was established to facilitate manuscript preparation by researchers whose native language is not English and to help edit works intended for international academic journals.

4. Manuscript Preparation

Manuscripts should be written in clear, grammatically correct English and submitted as a Microsoft Word file in a single-column format. Manuscripts must be paginated and typed in 12-point Times New Roman font with 24-point line spacing. Please do not embed figures in the text. Abbreviations should be used as little as possible and should be explained at first mention unless the term is a well-known abbreviation (*e.g.* DNA). Single words should not be abbreviated.

Title page: The title page must include 1) the title of the paper (Please note the title should be short, informative, and contain the major key words); 2) full name(s) and affiliation(s) of the author(s); 3) abbreviated names of the author(s); 4) full name, mailing address, telephone/fax numbers, and e-mail address of the corresponding author; and 5) conflicts of interest (if you have an actual or potential conflict of interest to disclose, it must be included as a footnote on the title page of the manuscript; if no conflict of interest exists for each author, please state "There is no conflict of interest to disclose"). Please visit [Download Centre](#) and refer to the title page of the manuscript sample.

Abstract: The abstract should briefly state the purpose of the study, methods, main findings, and conclusions. For article types including Original Article, Brief Report, Review, Policy Forum, and Case Report, a one-paragraph abstract consisting of no more than 250 words must be included in the manuscript. For News and Letters, a brief summary of main content in 150 words or fewer should be included in the manuscript. Abbreviations must be kept to a minimum and non-standard abbreviations explained in brackets at first mention. References should be avoided in the abstract. Key words or phrases that do not occur in the title should be included in the Abstract page.

Introduction: The introduction should be a concise statement of the basis for the study and its scientific context.

Materials and Methods: The description should be brief but with sufficient detail to enable others to reproduce the experiments. Procedures that have been published previously should not be described in detail but appropriate references should simply be cited. Only new and significant modifications of previously published procedures require complete description. Names of products and manufacturers with their locations (city and state/country) should be given and sources of animals and cell lines should always be indicated. All clinical investigations must have been conducted in accordance with Declaration of Helsinki principles. All human and animal studies must have been approved by the appropriate institutional review board(s) and a specific declaration of approval must be made within this section.

Results: The description of the experimental results should be succinct but in sufficient detail to allow the experiments to be analyzed and interpreted by an independent reader. If necessary, subheadings may be used for an orderly presentation. All figures and tables must be referred to in the text.

Discussion: The data should be interpreted concisely without repeating material already presented in the Results section. Speculation is permissible, but it must be well-founded, and discussion of the wider implications of the findings is encouraged. Conclusions derived from the study should be included in this section.

Acknowledgments: All funding sources should be credited in the Acknowledgments section. In addition, people who contributed to the work but who do not meet the criteria for authors should be listed along with their contributions.

References: References should be numbered in the order in which they appear in the text. Citing of unpublished results, personal communications, conference abstracts, and theses in the reference list is not recommended but these sources may be mentioned in the text. In the reference list, cite the names of all authors when there are fifteen or fewer authors; if there are sixteen or more authors, list the first three followed by *et al.* Names of journals should

be abbreviated in the style used in PubMed. Authors are responsible for the accuracy of the references. Examples are given below:

Example 1 (Sample journal reference):
Nakata M, Tang W. Japan-China Joint Medical Workshop on Drug Discoveries and Therapeutics 2008: The need of Asian pharmaceutical researchers' cooperation. *Drug Discov Ther.* 2008; 2:262-263.

Example 2 (Sample journal reference with more than 15 authors):
Darby S, Hill D, Auvinen A, *et al.* Radon in homes and risk of lung cancer: Collaborative analysis of individual data from 13 European case-control studies. *BMJ.* 2005; 330:223.

Example 3 (Sample book reference):
Shalev AY. Post-traumatic stress disorder: Diagnosis, history and life course. In: *Post-traumatic Stress Disorder, Diagnosis, Management and Treatment* (Nutt DJ, Davidson JR, Zohar J, eds.). Martin Dunitz, London, UK, 2000; pp. 1-15.

Example 4 (Sample web page reference):
World Health Organization. The World Health Report 2008 – primary health care: Now more than ever. http://www.who.int/whr/2008/whr08_en.pdf (accessed September 23, 2010).

Tables: All tables should be prepared in Microsoft Word or Excel and should be arranged at the end of the manuscript after the References section. Please note that tables should not in image format. All tables should have a concise title and should be numbered consecutively with Arabic numerals. If necessary, additional information should be given below the table.

Figure Legend: The figure legend should be typed on a separate page of the main manuscript and should include a short title and explanation. The legend should be concise but comprehensive and should be understood without referring to the text. Symbols used in figures must be explained.

Figure Preparation: All figures should be clear and cited in numerical order in the text. Figures must fit a one- or two-column format on the journal page: 8.3 cm (3.3 in.) wide for a single column, 17.3 cm (6.8 in.) wide for a double column; maximum height: 24.0 cm (9.5 in.). Please make sure that artwork files are in an acceptable format (TIFF or JPEG) at minimum resolution (600 dpi for illustrations, graphs, and annotated artwork, and 300 dpi for micrographs and photographs). Please provide all figures as separate files. Please note that low-resolution images are one of the leading causes of article resubmission and schedule delays. All color figures will be reproduced in full color in the online edition of the journal at no cost to authors.

Units and Symbols: Units and symbols conforming to the International System of Units (SI) should be used for physicochemical quantities. Solidus notation (*e.g.* mg/kg, mg/mL, mol/mm²/min) should be used. Please refer to the SI Guide www.bipm.org/en/si/ for standard units.

Supplemental data: Supplemental data might be useful for supporting and enhancing your scientific research and Drug Discoveries & Therapeutics accepts the submission of these materials which will be only published online alongside the electronic version of your article. Supplemental files (figures, tables, and other text materials) should be prepared according to the above guidelines, numbered in Arabic numerals (*e.g.*, Figure S1, Figure S2, and Table S1, Table S2) and referred to in the text. All figures and tables should have titles and legends. All figure legends, tables and supplemental text materials should be placed at the end of the paper. Please note all of these supplemental data should be provided at the time of initial submission and note that the editors reserve the right to limit the size and length of Supplemental Data.

5. Submission Checklist

The Submission Checklist will be useful during the final checking of a manuscript prior to sending it to Drug Discoveries & Therapeutics for review. Please visit [Download Centre](#) and download the Submission Checklist file.

6. Online submission

Manuscripts should be submitted to Drug Discoveries & Therapeutics online at <http://www.ddtjournal.com>. The manuscript file should be smaller than 5 MB in size. If for any reason you are unable to submit a file online, please contact the Editorial Office by e-mail at office@ddtjournal.com

7. Accepted manuscripts

Proofs: Galley proofs in PDF format will be sent to the corresponding author *via* e-mail. Corrections must be returned to the editor (proof-editing@ddtjournal.com) within 3 working days.

Offprints: Authors will be provided with electronic offprints of their article. Paper offprints can be ordered at prices quoted on the order form that accompanies the proofs.

Page Charge: A page charge of \$140 will be assessed for each printed page of an accepted manuscript. The charge for printing color figures is \$340 for each page. Under exceptional circumstances, the author(s) may apply to the editorial office for a waiver of the publication charges at the time of submission.

(Revised February 2013)

Editorial and Head Office:

Pearl City Koishikawa 603
2-4-5 Kasuga, Bunkyo-ku
Tokyo 112-0003
Japan
Tel: +81-3-5840-9697
Fax: +81-3-5840-9698
E-mail: office@ddtjournal.com

JOURNAL PUBLISHING AGREEMENT (JPA)

Manuscript No.:

Title:

Corresponding author:

The International Advancement Center for Medicine & Health Research Co., Ltd. (IACMHR Co., Ltd.) is pleased to accept the above article for publication in Drug Discoveries & Therapeutics. The International Research and Cooperation Association for Bio & Socio-Sciences Advancement (IRCA-BSSA) reserves all rights to the published article. Your written acceptance of this JOURNAL PUBLISHING AGREEMENT is required before the article can be published. Please read this form carefully and sign it if you agree to its terms. The signed JOURNAL PUBLISHING AGREEMENT should be sent to the Drug Discoveries & Therapeutics office (Pearl City Koishikawa 603, 2-4-5 Kasuga, Bunkyo-ku, Tokyo 112-0003, Japan; E-mail: office@ddtjournal.com; Tel: +81-3-5840-9697; Fax: +81-3-5840-9698).

1. Authorship Criteria

As the corresponding author, I certify on behalf of all of the authors that:

- 1) The article is an original work and does not involve fraud, fabrication, or plagiarism.
- 2) The article has not been published previously and is not currently under consideration for publication elsewhere. If accepted by Drug Discoveries & Therapeutics, the article will not be submitted for publication to any other journal.
- 3) The article contains no libelous or other unlawful statements and does not contain any materials that infringes upon individual privacy or proprietary rights or any statutory copyright.
- 4) I have obtained written permission from copyright owners for any excerpts from copyrighted works that are included and have credited the sources in my article.
- 5) All authors have made significant contributions to the study including the conception and design of this work, the analysis of the data, and the writing of the manuscript.
- 6) All authors have reviewed this manuscript and take responsibility for its content and approve its publication.
- 7) I have informed all of the authors of the terms of this publishing agreement and I am signing on their behalf as their agent.

2. Copyright Transfer Agreement

I hereby assign and transfer to IACMHR Co., Ltd. all exclusive rights of copyright ownership to the above work in the journal Drug Discoveries & Therapeutics, including but not limited to the right 1) to publish, republish, derivate, distribute, transmit, sell, and otherwise use the work and other related material worldwide, in whole or in part, in all languages, in electronic, printed, or any other forms of media now known or hereafter developed and the right 2) to authorize or license third parties to do any of the above.

I understand that these exclusive rights will become the property of IACMHR Co., Ltd., from the date the article is accepted for publication in the journal Drug Discoveries & Therapeutics. I also understand that IACMHR Co., Ltd. as a copyright owner has sole authority to license and permit reproductions of the article.

I understand that except for copyright, other proprietary rights related to the Work (e.g. patent or other rights to any process or procedure) shall be retained by the authors. To reproduce any text, figures, tables, or illustrations from this Work in future works of their own, the authors must obtain written permission from IACMHR Co., Ltd.; such permission cannot be unreasonably withheld by IACMHR Co., Ltd.

3. Conflict of Interest Disclosure

I confirm that all funding sources supporting the work and all institutions or people who contributed to the work but who do not meet the criteria for authors are acknowledged. I also confirm that all commercial affiliations, stock ownership, equity interests, or patent-licensing arrangements that could be considered to pose a financial conflict of interest in connection with the article have been disclosed.

Corresponding Author's Name (Signature):

Date:

